Soluble Factor Mediated Manipulation of Mesenchymal Stem Cell Mechanics for Improved Function of Cell-based Therapeutics

A Thesis
Presented to
The Academic Faculty

by

Deepraj Ghosh

In Partial Fulfillment
of the Requirements for the Degree
Doctor of Philosophy in the
School of Chemical and Biomolecular Engineering

Georgia Institute of Technology
August 2014

Soluble Factor Mediated Manipulation of Mesenchymal Stem Cell Mechanics for Improved Function of Cell-based Therapeutics

Approved by:

Dr. Michelle R. Dawson, Advisor
School of Chemical and Biomolecular Engineering
Georgia Institute of Technology

Dr. Hang Lu
School of Chemical and Biomolecular Engineering
Georgia Institute of Technology

Dr. John F. McDonald
School of Biology
Georgia Institute of Technology

Dr. Edward A. Botchwey
School of Biomedical Engineering
Georgia Institute of Technology

Dr. Lakeshia Taite
School of Chemical and Biomolecular Engineering
Georgia Institute of Technology

Date Approved: [June 25, 2014]

ACKNOWLEDGEMENTS

I would like to express my deepest and sincerest gratitude to my advisor Dr. Michelle Dawson for her support, encouragement and guidance throughout my work. Her valuable opinions and insights, allowed me to expand my ideas and move in the right direction. I would also like to thank my present and past committee members, Dr. John McDonald, Dr. Lakeshia Taite, Dr. Hang Lu, Dr. Edward A. Botchwey, Dr. Athanassios Sambanis and Dr. Barbara Boyan for their valuable comments and insights.

I am very thankful to my present colleagues and past members in the Dawson group whom I have worked very closely to complete this thesis: Daniel McGrail, Kate McAndrews, Kevin Rodriguez, Russell Jampol. I hope success to all of your future endeavors, and that we can continue our friendship for years to come. I would also like to thank the members of Dr. McDonald's group for their extensive help during our collaboration.

I wish to thank my parents, my brother and my whole family for their support during my time here and beyond. Last but not least, I would like to acknowledge my friends who helped me to adapt and mature as a person. I am highly appreciative of all the friendships that got me through my 5 years stay in Atlanta: Marcos, Jose, Souvik, Nitesh, Carine, Frank, Wilmarie, Joaquin, Alejandra, Andac, Christine, Sandeep, Aritra, Dwaipayan, Nagesh, Fabian, Siladitya, Avisek, Rajdeep, Atanu, Messi and many more friends.

TABLE OF CONTENTS

LIST OF TABLES

Page

LIST OF FIGURES

Page

LIST OF SYMBOLS AND ABBREVIATIONS

a	Particle radius
D	Diffusion coefficient
E	Young's modulus
G^*	Frequency-dependent complex shear modulus
G’	Elastic modulus
G’’	Viscous modulus
k_B	Boltzmann’s constant
T	Temperature
δ	Phase angle
η	Viscosity of the fluid
ABPs	Actin-binding proteins
ALK	Activin like receptor
Ang-2	Angiopoietin 2
bFGF/FGF-2	Basic fibroblast growth factor
CAFs	Carcinoma associated fibroblasts
CAMs	Cell adhesion molecules
CCL2/MCP-1	Monocyte chemotactic protein 1
CD11b	α_M integrin
CD29	β_1 integrin
CD45	Protein tyrosine phosphatase
CD51	α_v integrin
CD54/ICAM1	Intracellular adhesion molecule-1
CD61	β_3 integrin
CD106/VCAM1	Vascular cell adhesion molecule-1
ECM	Extracellular matrix
FA	Focal adhesion
FAK	Focal adhesion kinase
HGF	Hepatocyte growth factor
MFI	Mean fluorescence intensity
MPT/MPTM	Multiple particle tracking microrheology
MSCs	Mesenchymal stem cells
MSD	Mean square displacement
PBS	Phosphate buffered solution
PCR	Polymerase chain reaction
PDGF	Platelet derived growth factor
PPC	Percent positive population

RT-PCR	Reverse transcription polymerase chain reaction
Sca1	Stem cell antigen-1
SDF-1α	Stromal derived factor-1α
α-SMA	α-smooth muscle actin
TCM	Tumor cell conditioned media
TGF-β1	Transforming growth factor β1
VEGF	Vascular endothelial growth factor

SUMMARY

Mesenchymal stem cells (MSCs) are bone marrow derived multipotent cells with the ability to self-renew and differentiate into multiple connective cell lineages. *In vivo*, MSCs travel from the bone-marrow to the inflammatory sites and actively participate in remodeling and regeneration process under the influence of soluble growth factors. Due to these inherent properties, MSCs have emerged as an ideal candidate for diverse regenerative therapeutic applications. The development of MSC-based therapies requires *in vitro* expansion of MSCs; however, MSC expansion results in phenotypical changes that have limited its efficacy upon reintroduction *in vivo*. In order to increase the efficacy of MSC-based therapeutics, it is critical for us to improve the current understanding of MSC interactions with its niche specific factors and explore new methods to enhance MSC function *in vivo*.

We used tumor conditioned media, which contains soluble factors secreted by tumor cells in culture (TCM), and inflammatory niche-specific soluble factors, such as platelet derived growth factor (PDGF) and transforming growth factor-β1 (TGF-β1), to characterize the mechanical response of MSCs. The intracellular mechanical properties of MSCs were dramatically altered in response to soluble factors and MSCs displayed cytosolic stiffening in response to TCM and TGF-β1. Although PDGF treated cells did not elicit any mechanical response, blocking PDGF signaling with a small molecule inhibitor reversed the stiffening response in TGF-β1 treated cells, indicating crosstalk between these two pathways is essential in TGF-β1 mediated cell stiffening. Furthermore,

a genome-wide microarray analysis revealed TGF-β1 dependent regulation of cytoskeletal actin-binding protein (ABP) genes. Actin crosslinking and bundling protein genes, which regulate cytosolic rheology through changes in semiflexible actin polymer meshworks, were upregulated with TGF-β1 treatment.

Since TGF-β1 treatment profoundly altered the MSC phenotype after relatively short exposure times, we sought to understand if pretreated cells could sustain these enhanced characteristics leading to higher efficacy *in vivo*. We found that MSCs pretreated with TGF-β1 displayed enhanced adhesive properties while maintaining the expression profile of surface adhesion molecules even after removal of stimulus. Additionally, pretreated MSCs exposed to lineage specific induction media, demonstrated superior differentiation potential along multiple lineages. Based on the large number of sustained changes, TGF-β1 pretreated cells were used to treat full thickness skin wounds for *in vivo* wound healing model to determine their therapeutic efficacy. TGF-β1 pretreated MSCs increased wound closure rate and displayed enhanced migration of MSCs towards the center of the wound compared to the control cells.

In conclusion, MSCs with altered mechanical properties after soluble factor pretreatment display significantly improved cell functions leading to highly efficient tissue regeneration *in vivo*. Mechanical priming of MSCs with niche specific factors prior to transplantation can become a viable strategy to maximize their therapeutic potential.

CHAPTER 1: INTRODUCTION

Current strategies for healing damaged tissues rely heavily on native cell recruitment [1]. Biomaterials are often used to create scaffolds that mimic *in vivo* tissue niches. Bioactive factors found in these niches can then be incorporated in these scaffolds or used directly to promote native cell recruitment [2,3]. Acellular scaffolds and bioactive factors have been used successfully in tissue engineering and regenerative medicine applications; however, these strategies are difficult to apply in acute conditions or chronic diseases when native cell recruitment is more limited. Also, these treatment strategies are not useful in gene therapy where cells must first be engineered to correct gene defects. Alternatively, stem cell based therapy has been proposed to improve upon the current techniques and provide an exciting new platform for tissue engineering, regenerative medicine, and gene therapy [4-6]. Stem cells possess the ability to self-renew and differentiate into multiple cell lineages that play a central role in the regeneration process. Mesenchymal stem cells (MSCs) which differentiate into connective tissue cells are very attractive candidates for cell therapy in part to their natural ability to home to damaged tissues without eliciting an immune response [7]. The methods of delivering MSCs are diverse; they can be infused systemically in blood or transplanted topically and they can also be embedded in a scaffold, which is used to guide their migration and differentiation [8]. Scaffolds can be designed to mimic the native tissue structure by providing chemical and mechanical cues that support cell engraftment and differentiation along specific mesodermal lineages. In fact environmental cues present in the regenerating tissues

determine the fate of transplanted cells; manipulating *in vivo* tissue environments to control cell fate provides a major obstacle in the use of stem cells expanded *ex vivo* [9].

In vivo, MSCs are actively recruited to sites of inflammation where they can be exposed to a diverse range of niche specific factors. MSCs can successfully adapt to environments with mechanically stringent characteristics such as cyclic stress and strain in damaged cartilage, coordinated contraction and relaxation of cardiac muscle in the heart, extremely rigid bone tissue, as well as chemically enriched networks of fibrotic tissues and tumors. Cells can generate force and balance intracellular tension caused by external forces and other biophysical stimuli in these tissue niches [10]. The mechanical response of a cell to chemical or physical stimuli is critical for a multitude of cellular processes including cell adhesion and motility, cell growth and differentiation, protein and DNA synthesis, and apoptosis [11,12]. A more dynamic understanding of how mechanical stress regulates cell function requires increased knowledge of the microscopic mechanical properties of cells and their extracellular environments. The intracellular mechanical properties of live cells are determined by the complex organization of cytoskeletal filamentous proteins including actin, microtubules and intermediate filaments, extending from the cell cortex (just below the plasma membrane) to the cell nucleus [13]. Chemical and physical stimuli alter cell shape and cytoskeletal organization by activating cytoskeletal mediators, including small Rho GTPases RhoA, Rac1, and Cdc42 and actin-binding proteins (ABPs), which regulate actin filament length through capping, branching, and severing processes. The cytoskeletal network responds dynamically to soluble or mechanical cues provided by the extracellular matrix (ECM)

and is directly connected to canonical signal transduction pathways important in tissue regeneration and cancer [14,15].

Biological tissues consist of a multitude of cells organized in a scaffold of extracellular matrix (ECM) proteins to form specific structures important for normal physiology. Cells communicate in these complex tissue environments through direct cell contacts and paracrine signaling to maintain the balance of cell proliferation and cell death required for normal tissue homeostasis [16]. Although multiple studies have provided mechanistic insight into both microscale cell mechanics and macroscale tissue properties individually, the correlation between the two is far more complex and has yet to be elucidated [17,18]. Nonetheless, it is well established that physiological behavior of tissue is very much dependent upon its cellular components. Cells can mechanically respond to the chemical and mechanical cues present in ECM and reciprocate the interaction by actively remodeling the surrounding ECM.

1.1. THESIS OVERVIEW

The development of stem cell based therapeutics that engraft and incorporate into biological tissues may expand the current limits of regenerative medicine. Although MSCs hold great promise as cell-based therapies, the results from clinical studies have been inconsistent [19-21]. In order to increase the efficacy of MSC-based therapeutics, it is critical for us to improve the current understanding of MSC interactions with tissue niche related factors and explore new methods to enhance MSC function *in vivo*.

In Chapter 2, the key concepts that are essential to review the studies are briefly discussed. First, the properties of mesenchymal stem cells and the role of soluble factors in recruiting them to tissue niches are described followed by the discussion of the

relevant signaling pathways important in regulating MSC behavior. The intracellular cytoskeletal machinery that controls cell mechanics is next outlined. Finally, we conclude with the theory of Brownian motion and the technique of multiple particle tracking (MPT), which was used for the mechanical characterization of MSCs.

In chapters 3-4, we detailed our studies on the effects of specific soluble factors on cytoskeletal mechanics of murine bone marrow derived mesenchymal stem cells. In chapter 3, tumor conditioned media, a cocktail of growth factors representing the chemical cues in the inflammatory tumor niche, was utilized to characterize the mechanical response of MSCs in comparison to fibroblasts. In chapter 4, we describe the effects of individual factors platelet derived growth factor (PDGF) and transforming growth factor-β1 (TGF-β1) on microrheology of MSCs. Although, the presence of these two factors in inflammatory niches and their crosstalk in cells of mesenchymal origin has been well-documented, their effects on the mechanical properties of individual cells remained poorly understood. Here, the role of the crosstalk between these two signaling pathways in regulating MSC behavior was elucidated.

In chapter 5, the effects of TGF-β1 and PDGF on MSC migration and adhesion were examined. Cell adhesion and migration play key roles during embryonic development, inflammation, and tissue regeneration. These studies were essential to understand the role of soluble factors in regulating the interaction between MSCs and the ECM.

In chapter 6, we provide a detailed genome wide microarray analysis to understand the effects of TGF-β1 and PDGF on transcriptional profile of MSCs. This

study helped us to identify key networks and molecular pathways that regulate MSC functions.

In chapter 7, the sustained effects of TGF-β1 pretreatment on MSC functions, including, adhesion, migration, and differentiation, were examined. An *in vivo* punch biopsy full thickness skin wound model was used to determine the effects of MSC pretreatment on wound healing. Finally, the important findings and future directions of this project were summarized in Chapter 8.

1.2. REFERENCES

1. Ko IK, SJ Lee, A Atala and JJ Yoo. (2013). In situ tissue regeneration through host stem cell recruitment. Experimental & molecular medicine 45:e57.

2. (2012). Advances in Wound Healing: A Review of Current Wound Healing Products. Plastic Surgery International 2012.

3. Boateng JS, KH Matthews, HNE Stevens and GM Eccleston. (2008). Wound healing dressings and drug delivery systems: A review. Journal of Pharmaceutical Sciences 97:2892-2923.

4. Daley GQ and DT Scadden. (2008). Prospects for stem cell-based therapy. Cell 132:544-548.

5. Robinton DA and GQ Daley. (2012). The promise of induced pluripotent stem cells in research and therapy. Nature 481:295-305.

6. Daley GQ. (2012). The promise and perils of stem cell therapeutics. Cell stem cell 10:740-749.

7. Satija NK, VK Singh, YK Verma, P Gupta, S Sharma, F Afrin, M Sharma, P Sharma, R Tripathi and G Gurudutta. (2009). Mesenchymal stem cell-based therapy: a new paradigm in regenerative medicine. Journal of cellular and molecular medicine 13:4385-4402.

8. Caplan AI. (2007). Adult mesenchymal stem cells for tissue engineering versus regenerative medicine. Journal of cellular physiology 213:341-347.

9. Tamama K, H Kawasaki and A Wells. (2010). Epidermal growth factor (EGF) treatment on multipotential stromal cells (MSCs). Possible enhancement of therapeutic potential of MSC. Journal of Biomedicine and Biotechnology 2010.

10. Discher DE, DJ Mooney and PW Zandstra. (2009). Growth factors, matrices, and forces combine and control stem cells. Science 324:1673-1677.

11. Discher DE, P Janmey and Y-l Wang. (2005). Tissue cells feel and respond to the stiffness of their substrate. Science 310:1139-1143.

12. Janmey PA and CA McCulloch. (2007). Cell mechanics: integrating cell responses to mechanical stimuli. Annual Review of Biomedical Engineering 9:1-34.

13. Fletcher DA and RD Mullins. (2010). Cell mechanics and the cytoskeleton. Nature 463:485-492.

14. Schmidt A and MN Hall. (1998). Signaling to the Actin Cytoskeleton. Annual Review of Cell and Developmental Biology 14:305-338.

15. Olson EN and A Nordheim. (2010). Linking actin dynamics and gene transcription to drive cellular motile functions. Nature reviews Molecular cell biology 11:353-365.

16. Joyce JA and JW Pollard. (2009). Microenvironmental regulation of metastasis. Nature Reviews Cancer 9:239-252.

17. Verdier C. (2003). Review Article: Rheological Properties of Living Materials. From Cells to Tissues. Journal of Theoretical Medicine 5:67-91.

18. Lecuit T and P-F Lenne. (2007). Cell surface mechanics and the control of cell shape, tissue patterns and morphogenesis. Nature Reviews Molecular Cell Biology 8:633-644.

19. Rennert RC, M Sorkin, RK Garg and GC Gurtner. (2012). Stem cell recruitment after injury: lessons for regenerative medicine. Regenerative medicine 7:833-850.

20. Malliaras K, M Kreke and E Marban. (2011). The stuttering progress of cell therapy for heart disease. Clinical Pharmacology & Therapeutics 90:532-541.

21. Ankrum J and JM Karp. (2010). Mesenchymal stem cell therapy: Two steps forward, one step back. Trends in molecular medicine 16:203-209.

CHAPTER 2: BACKGROUND

Mesenchymal stem cells (MSCs) are multipotent progenitor cells which can be isolated from bone marrow (BM), expanded rapidly, and genetically modified for stable production of therapeutic proteins. MSCs spontaneously home to sites of inflammation including wounds, tumors, and regenerating tissues and subsequently integrate themselves in those tissue niches. Pro-inflammatory molecules secreted by tumors and wounds regulate the fate of MSCs incorporated in the tissues; however, their effects on the mechanical properties of MSCs have not been fully investigated. The studies presented in this thesis were focused on determining the effects of tumor conditioned media, which contains soluble factors secreted by tumor cells in culture, and inflammatory niche-specific soluble factors, such as platelet derived growth factor (PDGF) and transforming growth factor-β1 (TGF-β1), on the mechanical, adhesive and transcriptional properties of MSCs. The remainder of this chapter is devoted to outlining the key concepts that have been used recurrently in this thesis.

2.1. MESENCHYMAL STEM CELLS

Mesenchymal stem cells (MSCs) were initially isolated from bone marrow and characterized as a clonal population of spindle-shaped stromal cells that were adherent to plastic and had a propensity to differentiate toward osteogenic lineages [1,2]. MSCs reside in the bone marrow and other tissues and can differentiate into connective tissue cells, including adipocytes, osteoblasts, chondrocytes, and smooth muscle cells (Figure 2-1), required for tissue maintenance and repair [3,4]. MSCs have been isolated from

different tissue sources, including bone marrow [3], fat [5], umbilical cord [6], skin [7], cartilage [8], and dental pulp [9], and expanded *in vitro* and thus represent a population of multipotent stem cells available in high numbers for therapeutic use. Although MSC potency is more limited than embryonic stem (ES) cells, which differentiate along all cell lineages, MSCs are safer as a cell source, since they do not spontaneously form teratomas like ES cells [10,11]. MSCs have been genetically engineered to express a wide array of therapeutic proteins without inducing malignant transformation [12-15]. Additionally, MSCs secrete soluble factors important in autocrine and paracrine signaling and extracellular matrix proteins important in tissue remodeling [16]. In summary, due to their regenerative ability, immunosuppressive nature, and capacity to secrete chemotactic factors and extracellular matrix proteins, MSCs have been used as therapeutics in numerous applications, including myocardial infarction, diabetes, sepsis, lung disease and wound healing [17-21]. Currently, 407 clinical trials involving MSCs are in progress worldwide (*https://clinicaltrials.gov/).* Since soluble factors are used as modulators of cell function in this study, we next discuss the role of soluble factors in mediating cell signaling pathways involved in MSC recruitment and behavior.

2.2. SOLUBLE GROWTH FACTORS

Soluble growth factors are hormone like molecules which can interact with cells at both local and distal sites *in vivo*. Therefore, these factors play a prominent role in recruiting cells and influencing the cell fate in both normal and pathological conditions. Soluble growth factors, like vascular endothelial growth factor (VEGF), platelet derived growth factor (PDGF), basic fibroblast growth factor (b-FGF), and stromal derived factor-1α

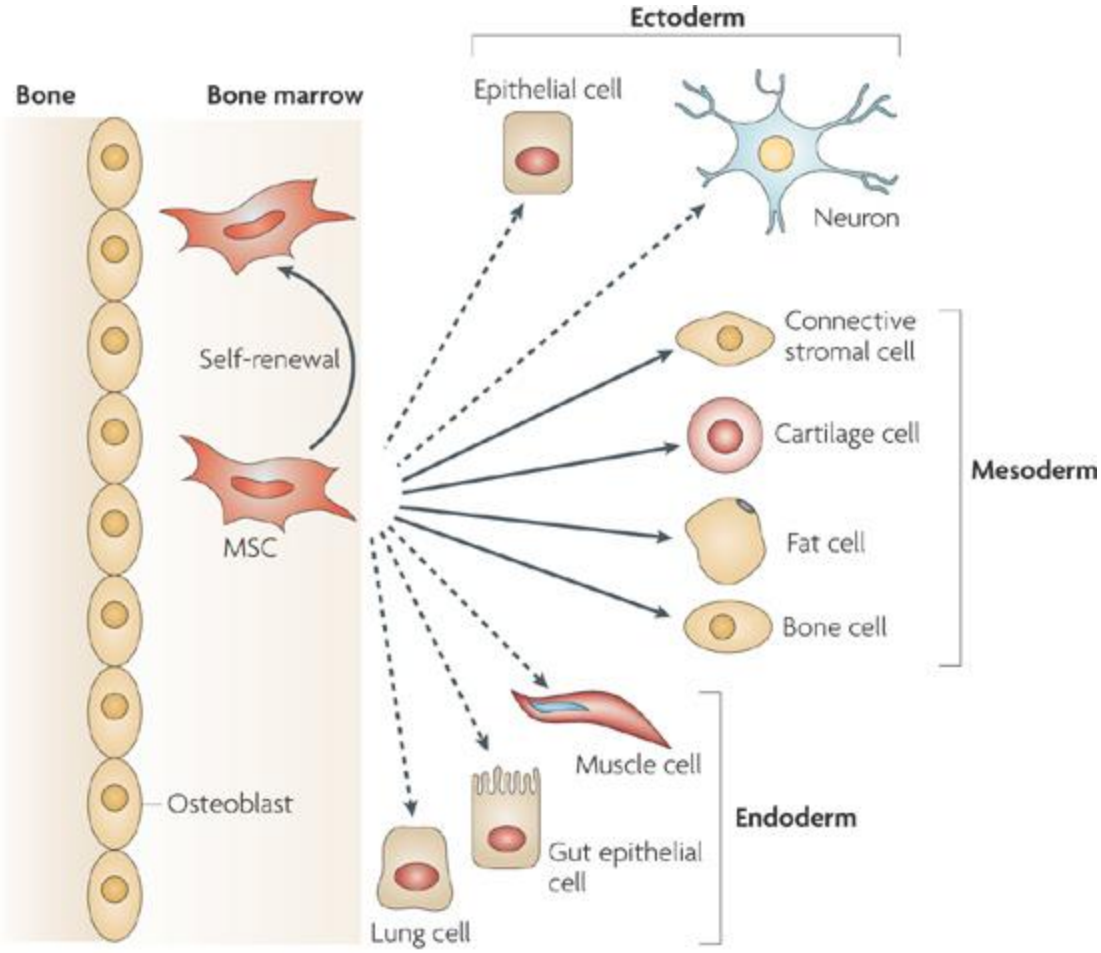

Figure 2-1. *Multipotent potential of mesenchymal stem cells.* Mesenchymal stem cells can self-renew and differentiate into multiple lineages including osteoblasts, chondrocytes, adipocytes. Transdifferentiaiton into controversial lineages are shown by dashed arrows. Adapted by permission from Macmillan Publishers Ltd: Nature Reviews Immunology (8.9: 726-736) by Uccelli et al., Copyright © 2008, Rights Managed by Nature Publishing Group (2008) [22].

(SDF-1α), secreted by cells in the tumor microenvironment mediate the recruitment of cells directly from the bone marrow, including myeloid derived progenitors which establish a chronic state of inflammation in the tumor [23]. Subsequent, recruitment of MSCs to the tumor microenvironment is a key step in tumor growth and progression to metastatic disease that requires the formation of new blood vessels (angiogenesis), which supply nutrients to the tumor and provide potential routes for cancer cell dissemination.

Platelets in wound sites and tumor cells in inflammatory niches release factors such as, transforming growth factor-β1 (TGF-β1) and platelet derived growth factor-BB (PDGF-BB) that have been recognized to play an important role in remodeling cell microenvironments in the tumor and the wound bed by promoting fibroblast activation, angiogenesis, differentiation and immunomodulation [24,25]. Here we briefly discuss the PDGF and TGF-β1signaling pathways before elaborating their role in controlling MSC behavior.

2.2.1. TRANSFORMING GROWTH FACTOR B1 (TGF- B1)

Transforming growth factor-β1, a secreted protein of the TGF-β superfamily, plays a critical role in embryonic development and tissue homeostasis by regulating cell proliferation, differentiation, adhesion, migration and apoptosis [26, 27]. TGF-β1 binds with high affinity to TGF-β receptor type II where it recruits TGF-β receptor type I (ALK5) to form a tetrameric signaling complex [28]. Upon activation, TGF-β1 signaling pathways influence a myriad of cell processes through SMAD-dependent or independent pathways (Figure 2-2) [28]. The receptor activated SMAD protein complexes travel through the cytoplasm and translocate to the nucleus, where they bind to DNA and

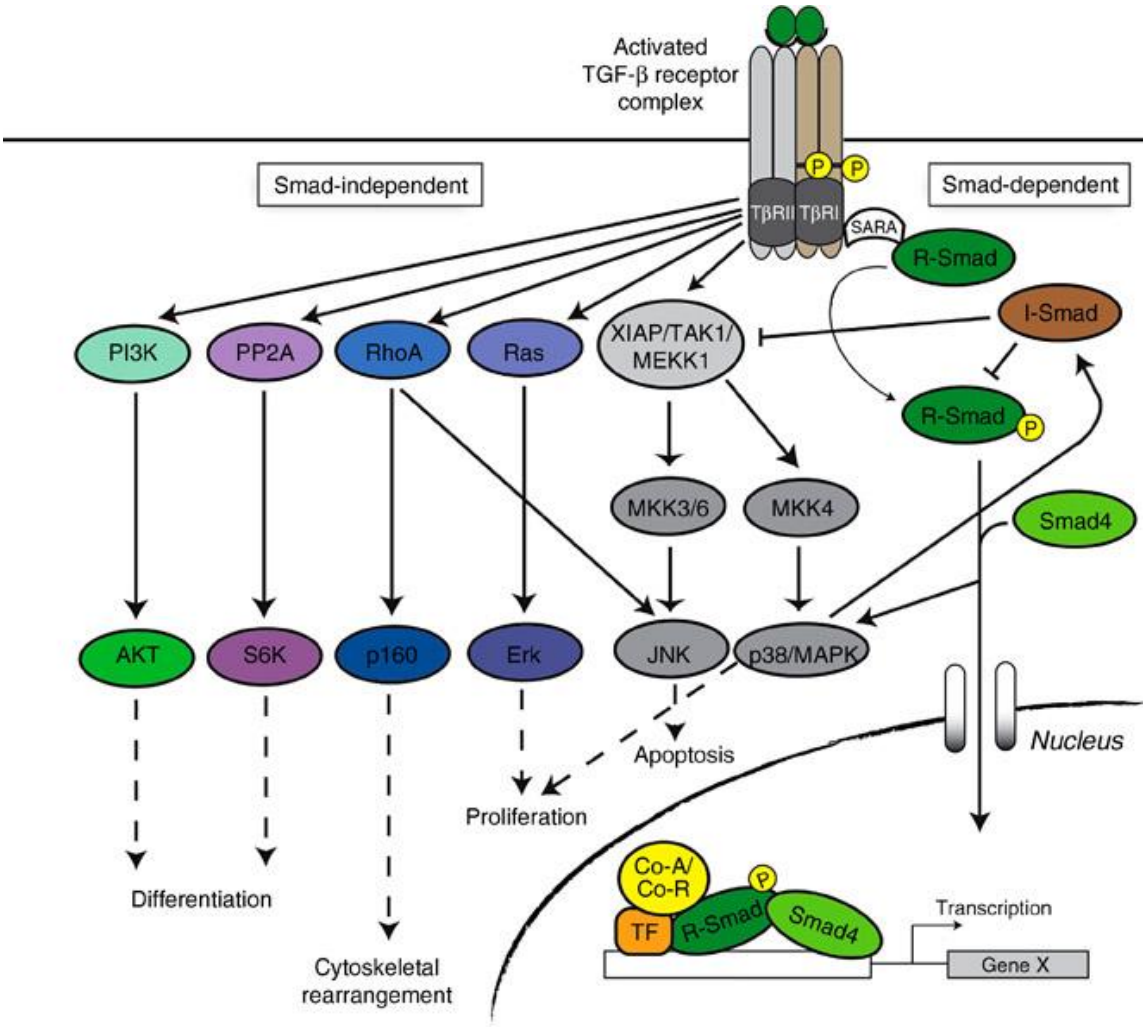

Figure 2-2. *TGF-β signaling pathway.* TGF-β ligand bind to its surface affinity receptors to induce SMAD-dependent and independent signaling cascades. Adapted by permission from Springer Science and Business Media, Pancreatic Cancer (pp 419-439) by Norris et al., Copyright © 2010, Springer Science and Business Media, LLC (2010) [29].

regulate the transcriptional response. Additionally, the activated TGF-β receptor complex on the cell surface can regulate a diverse array of signaling pathways (example: Rho GTPases ERK/MAPK, PI3K/AKT) by phosphorylation or direct interaction with the mediator proteins in a SMAD-independent manner.

Abnormalities in TGF-β signaling contribute to tumor formation, cancer progression, inflammation, hypertrophic scar formation, and fibrosis [27, 30, 31]. The function of TGF-β1 on a cellular level is dependent on the developmental cell lineage, context of the interaction, and concentration [32]. The variation in TGF-β1-induced responses is easily illustrated in the context of cancer where TGF-β1 suppresses early tumor growth but promotes tumor progression and metastasis at later stages [33]. Inhibition of TGF-β1signaling has been investigated as a treatment for immune disorders [34], fibrosis, and metastatic cancer [35]. TGF-β1 can profoundly influence MSC differentiation into specific tumor-associated stromal cells, such as carcinoma associated fibroblasts (CAFs) [36, 37, 38], pericyte progenitor cells [39], or myofibroblasts [37, 40].

2.2.2. PLATELET DERIVED GROWTH FACTOR-BB (PDGF-BB)

PDGF is a key regulator of cell growth, proliferation, survival, and chemotaxis [41, 42]. PDGF interacts with PDGFR alpha (α) and beta (β) tyrosine kinase receptors that dimerize for activation of intracellular signaling (Figure 2-3). The PDGF-B ligand interacts with both PDGFR α and β but PDGF-A has a higher affinity for PDGFR-α [43]. The PDGF-A/PDGFRα signaling axis is vital for proliferation and lineage-commitment of mesenchymal progenitor cells during embryogenesis and organogenesis [44]. In addition to these paracrine signaling processes, autocrine signaling is also

important in the tumor environment where it has been implicated in epithelial to mesenchymal transition of carcinoma cells [45]. MSCs primarily express PDGFR-β [46] which, with its ligand PDGF-B, plays a critical role in mediating the tropism and differentiation during vascular remodeling [44]. PDGF mediated migration is essential for MSC recruitment to nascent vessels and maturation into perivascular cells for angiogenesis.

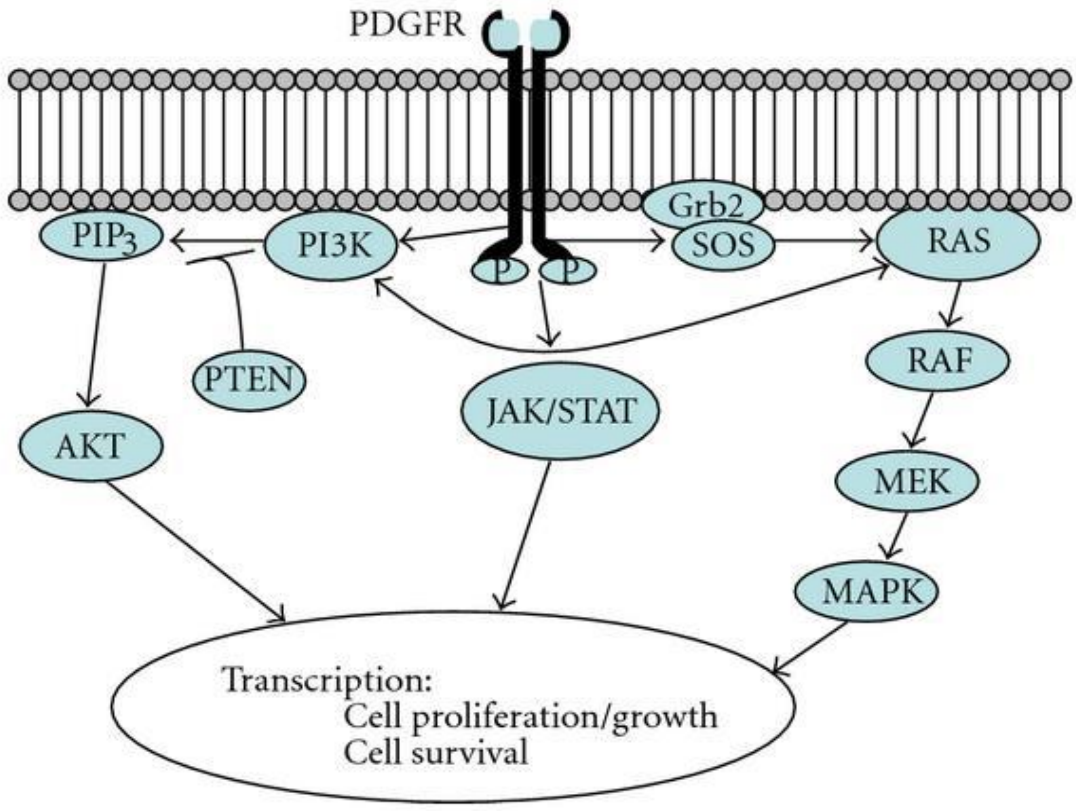

Figure 2-3. *PDGF signaling pathway.* Binding of PDGF-BB ligands to its surface receptors (PDGFR-β) lead to homodimerization of the receptors and intracellular signal transduction. PDGF signaling is important in regulating cellular processes such as proliferation, survival and migration. Adapted from Plesec TP. Pathology Research International (2011) [47].

2.3. CELL CYTOSKELETON

Cells undergo rapid changes in shape and organization during soluble factor-mediated cell division and migration. During these dynamic changes, a group of cytoplasmic polymers mechanically support the cell structure and spatially organizes the contents of the cell. This family of proteins, collectively known as cytoskeleton, consists of actin filaments, microtubules and intermediate filaments. Both microtubules and intermediate filaments contribute significantly to the organization and integrity of cells; however, actin cytoskeleton and its associated proteins enable cells to dynamically respond and adapt to the environmental cues [48]. The organization of filamentous actin, which is controlled by the rapid polymerization and depolymerization of globular actin, changes dynamically to transform cell shape and generate mechanical forces required for numerous cellular processes, including adhesion, migration, division, molecular transport, and differentiation. Small RhoGTPases and actin binding proteins control the organization of cytoskeletal actin by regulating assembly and disassembly of the filaments as well its interaction with other structural complexes like focal adhesion; whereas, myosin motor proteins interact with actin filaments to control actin myosin contractility and cell migration. The family of binding proteins consists of several classes of regulatory proteins such as polymerizing factors (example: twinfilin, profilin), which promote actin filament growth, nucleation and branch forming proteins (example: Arp2/3), which initiate new filament formation; capping proteins (example: formin, capZ), which abrogate filament growth; depolymerizing (example: ADF/cofilin) and severing factors (example: gelsolin), which dissociate the monomers from filaments; and bundlers(example: α-actinin, fascin), crosslinkers (example: filamin) and stabilizing

proteins (example: tropomyosin, calponin), which give rise to higher-order network structures like stress fibers (Figure 2-4) [49].

The actin cytoskeleton is linked to the extracellular matrix or other cells via cell adhesion molecules (CAMs), including integrins [50] and cadherins [51]. Integrins are membrane-spanning cell surface receptors that play a major role in cell-matrix interactions. The extracellular portion of integrin glycoproteins interacts with matrix proteins, including fibronectin and collagen, and the intracellular domain is bound to integrin-actin linker protein complex (focal adhesion), formed by talin, vinculin, and α-actinin [50]. These groups of linker proteins are very dynamic to reciprocate the force between cell and its niche, thus playing key role during mechanotransduction [52].

2.4. CELL RHEOLOGY

The study of rheology is used to describe the flow and deformation of materials under applied force. Cells are considered soft biomaterials that behave as complex fluids [53, 54]. They are viscoelastic in nature since they resist deformation at small time scales like an elastic solid and deform at larger time scales like a viscous fluid. The intracellular rheological properties of the cell are determined by the organization of cytoskeletal actin, which forms a mesh-like structure in the cell cytoplasm [53, 55]. Parallel bundles of actin filaments provide tensile strength and strong contractile activity; whereas, cross-linked bundles of actin filaments increase intracellular elasticity. Due to inherent heterogeneity in actin architecture, local rheological properties can vary drastically throughout the cell [56, 57]. Characterization of this heterogeneity during a biochemical or biophysical factor mediated event can provide new insights into the cell behavior in normal and diseased microenvironments.

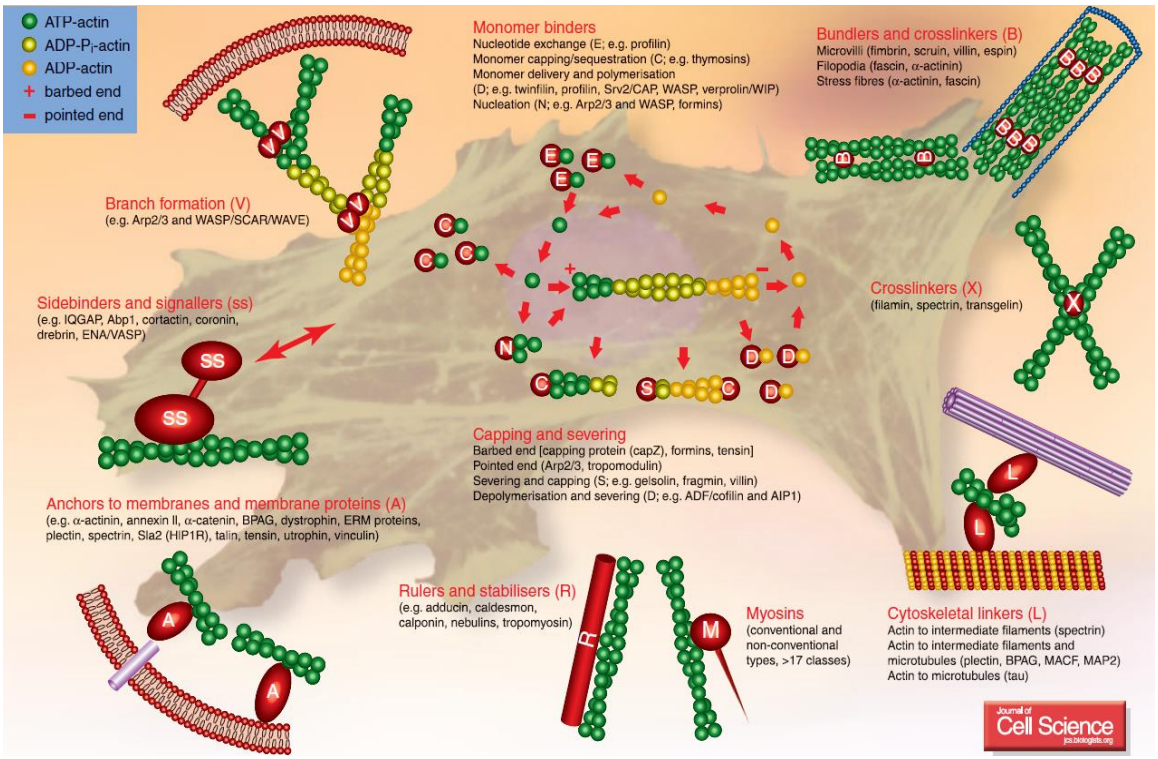

Figure 2-4. *Family of Actin-binding proteins.* Actin-binding proteins dynamically regulate growth, organization and interaction of actin with other proteins in cytoplasm and membrane. Adapted from Winder et al. Journal of cell science 118:651-654 (2005)) [49]

Among the techniques available to characterize intracellular rheology [53], multiple particle tracking microrheology (MPTM) enables direct and rapid measurements to capture the short-term or transient mechanical response in a cell [58]. MPTM has been successfully used to map the heterogeneities in local microrheological properties of cells. To elaborate, injected submicron particles are embedded in the cytosol to probe the local microenvironment (Figure 2-5). The movement of the embedded particles is heavily influenced by organization of the actin meshwork and can be used to determine the local viscoelastic properties in the following manner [58, 59].

Brownian motion describes the movement of a particle in a quiescent fluid, which is driven by the inherent thermal energy. Motion of a nanoparticle suspended in a purely viscous liquid remains unhindered and eventually the particle can move to a new location independent of the previous step. This pattern of movement resembles very well with the random walk model that can be used to describe the random motion of the embedded particle. In this scenario the particle motion is diffusive and the mean square displacement (MSD) of the particle varies linearly with time. When the particle is embedded in a viscoelastic fluid, its motion becomes more restricted ("subdiffusive") due to entrapment in the surrounding structure. In this case the MSD of the nanoparticle varies with time at slope $< < 1$. To capture the viscoelastic behavior of cells, the internal thermal energy driven Brownian motion of the embedded nanoparticles are captured at a high magnification with high speed camera for relatively short time (video duration under a minute). For 2D tracking, x-y displacements of the tracked particles are used to calculate mean square displacement using the following equation:

$$\text{MSD}=\left\langle \Delta r^2(\tau) \right\rangle = < [x(t+\tau)-x(t)]^2 + [y(t+\tau)-y(t)]^2 >$$

The mean square displacements (MSD) of the particles are correlated to the local diffusivity of the cytoskeleton, determined by:

$$D = \frac{\left\langle \Delta r^2(\tau) \right\rangle}{4\tau}$$

In a viscous liquid, diffusivity due to thermal energy driven motion can be described using Stokes-Einstein equation:

$$D = \frac{\mathrm{k_B T}}{6\ \pi\ \mathrm{a}\ \eta}$$

where D is the diffusion coefficient, k_B is Boltzmann's constant, T is temperature, a is particle radius, and η is viscosity of the fluid.

To describe viscoelastic properties of complex fluids, Mason et al derived complex shear modulus of the viscoelastic fluid using a modified Stokes-Einstein equation in the frequency domain:

$$G^*(\omega) = \frac{2\ \mathrm{k_B T}}{3\ \pi\ \mathrm{a}\ < \Delta \mathrm{r}^2(1/\omega) >\ \Gamma[1+\alpha(\omega)]}$$

where G^* is the frequency-dependent complex shear modulus, Γ is the gamma function. The in-phase component of the complex shear modulus (G*) is known as the elastic modulus (G'), and out-of-phase component is known as the viscous modulus (G'').

$$G'(\omega) = \left|G^*(\omega)\right| \cos\left(\frac{\pi\alpha(\omega)}{2}\right)$$

$$G''(\omega) = \left|G^*(\omega)\right| \sin\left(\frac{\pi\alpha(\omega)}{2}\right)$$

Cells typically behave like viscous liquid (G''>G') at lower frequencies (or higher time scales) and elastic solid (G'>G'') at large frequencies (or short time scales). The phase angle (δ, where δ= arctan (G''/G')) can be used to characterize the viscoelastic nature of the cell cytoplasm, where $\delta=90^0$ for a Newtonian viscous liquid, $\delta=0^0$ for a Hookean solid, $0^0< \delta <90^0$ for a viscoelastic material. Individual location specific particles MSDs can be used to calculate local viscoelastic properties; whereas, all MSDs from a cell can be ensemble averaged to evaluate overall viscoelastic behavior. This technique uniquely allows measuring the local rheological properties in specific regions of the cell to determine the heterogeneity, which are not measurable by bulk rheological techniques. MPTM has been successfully adapted to characterize a great range of complex biological fluids including mucus, reconstituted actin solution [60, 61].

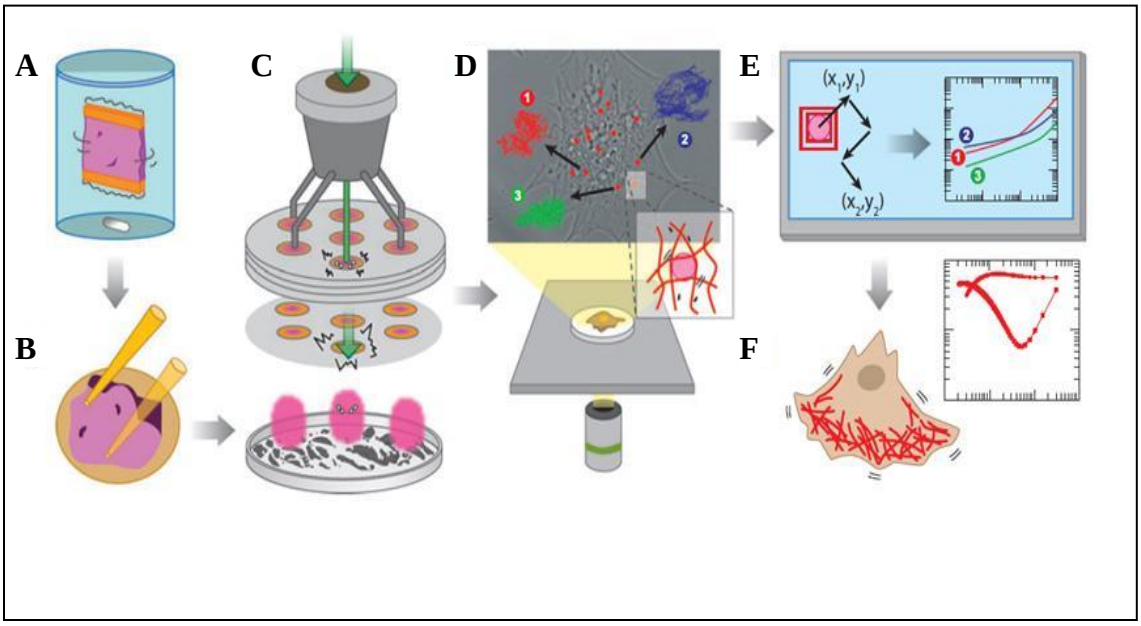

Figure 2-5: *Thematic presentation of multiple particle tracking microrheology.* (A) dialysis of nano/micro-particle; (B) Distribution of particle on micro-carrier; (C) injection of particles using a ballistic particle injector (not shown) in the cells, (D) capturing displacement of embedded nanoparticle using fluorescence microscope and high speed CCD camera; (E) and (F) calculation of micro-rheological parameters using appropriate software. Adapted from Annual review of biophysics (38: 301-326), by Wirtz, D. (2009) [58].

2.3. REFERENCES

1. Caplan AI. (1991). Mesenchymal stem cells. Journal of Orthopaedic Research 9:641-650.

2. Friedenstein AJ, KV Petrakova, AI Kurolesova and GP Frolova. (1968). Heterotopic of bone marrow. Analysis of precursor cells for osteogenic and hematopoietic tissues. Transplantation 6:230-47.

3. Pittenger MF, AM Mackay, SC Beck, RK Jaiswal, R Douglas, JD Mosca, MA Moorman, DW Simonetti, S Craig and DR Marshak. (1999). Multilineage potential of adult human mesenchymal stem cells. science 284:143-147.

4. Chamberlain G, J Fox, B Ashton and J Middleton. (2007). Concise Review: Mesenchymal Stem Cells: Their Phenotype, Differentiation Capacity, Immunological Features, and Potential for Homing. STEM CELLS 25:2739-2749.

5. Zuk PA, M Zhu, H Mizuno, J Huang, JW Futrell, AJ Katz, P Benhaim, HP Lorenz and MH Hedrick. (2001). Multilineage cells from human adipose tissue: implications for cell-based therapies. Tissue Eng 7:211-28.

6. Lee OK, TK Kuo, W-M Chen, K-D Lee, S-L Hsieh and T-H Chen. (2004). Isolation of multipotent mesenchymal stem cells from umbilical cord blood. Blood 103:1669-1675.

7. Shih DT-b, D-C Lee, S-C Chen, R-Y Tsai, C-T Huang, C-C Tsai, E-Y Shen and W-T Chiu. (2005). Isolation and Characterization of Neurogenic Mesenchymal Stem Cells in Human Scalp Tissue. STEM CELLS 23:1012-1020.

8. Hiraoka K, S Grogan, T Olee and M Lotz. (2006). Mesenchymal progenitor cells in adult human articular cartilage. Biorheology 43:447-54.

9. Perry BC, D Zhou, X Wu, FC Yang, MA Byers, TM Chu, JJ Hockema, EJ Woods and WS Goebel. (2008). Collection, cryopreservation, and characterization of human dental pulp-derived mesenchymal stem cells for banking and clinical use. Tissue Eng Part C Methods 14:149-56.

10. Gerecht-Nir S and J Itskovitz-Eldor. (2004). The promise of human embryonic stem cells. Best Practice & Research Clinical Obstetrics & Gynaecology 18:843-852.

11. Nishikawa S-i, RA Goldstein and CR Nierras. (2008). The promise of human induced pluripotent stem cells for research and therapy. Nature Reviews Molecular Cell Biology 9:725-729.

12. Studeny M, FC Marini, JL Dembinski, C Zompetta, M Cabreira-Hansen, BN Bekele, RE Champlin and M Andreeff. (2004). Mesenchymal Stem Cells: Potential Precursors for Tumor Stroma and Targeted-Delivery Vehicles for Anticancer Agents. Journal of the National Cancer Institute 96:1593-1603.

13. Hamada H, M Kobune, K Nakamura, Y Kawano, K Kato, O Honmou, K Houkin, T Matsunaga and Y Niitsu. (2005). Mesenchymal stem cells (MSC) as therapeutic cytoreagents for gene therapy. Cancer Science 96:149-156.

14. Ren C, S Kumar, D Chanda, J Chen, JD Mountz and S Ponnazhagan. (2008). Therapeutic Potential of Mesenchymal Stem Cells Producing Interferon-α in a Mouse Melanoma Lung Metastasis Model. STEM CELLS 26:2332-2338.

15. Loebinger MR, A Eddaoudi, D Davies and SM Janes. (2009). Mesenchymal Stem Cell Delivery of TRAIL Can Eliminate Metastatic Cancer. Cancer Research 69:4134-4142.

16. Hocking AM and NS Gibran. (2010). Mesenchymal stem cells: paracrine signaling and differentiation during cutaneous wound repair. Experimental cell research 316:2213-2219.

17. Caplan AI. (2007). Adult mesenchymal stem cells for tissue engineering versus regenerative medicine. Journal of Cellular Physiology 213:341-347.

18. da Silva Meirelles L, AM Fontes, DT Covas and AI Caplan. (2009). Mechanisms involved in the therapeutic properties of mesenchymal stem cells. Cytokine & growth factor reviews 20:419-427.

19. Caplan AI and SP Bruder. (2001). Mesenchymal stem cells: building blocks for molecular medicine in the 21st century. Trends in molecular medicine 7:259-264.

20. Trounson A, RG Thakar, G Lomax and D Gibbons. (2011). Clinical trials for stem cell therapies. BMC medicine 9:52.

21. Joyce JA and JW Pollard. (2009). Microenvironmental regulation of metastasis. Nat Rev Cancer 9:239-252.

22. Tocci A and L Forte. (2013). Mesenchymal stem cell: use and perspectives. The Hematology Journal 4:92-96.

23. Uccelli A, L Moretta and V Pistoia. (2008). Mesenchymal stem cells in health and disease. Nature Reviews Immunology 8:726-736.

24. Margadant C and A Sonnenberg. (2010). Integrin–TGF-β crosstalk in fibrosis, cancer and wound healing. EMBO reports 11:97-105.

25. Epstein FH, GC Blobe, WP Schiemann and HF Lodish. (2000). Role of transforming growth factor β in human disease. New England Journal of Medicine 342:1350-1358.

26. Derynck R and K Miyazono. *The TGF-[beta] family*. (2008). Cold Spring Harbor Laboratory Press.

27. Massagué J. (1998). TGF-β signal transduction. Annual review of biochemistry 67:753-791.

28. Derynck R and YE Zhang. (2003). Smad-dependent and Smad-independent pathways in TGF-β family signalling. Nature 425:577-584.

29. Norris A and M Korc. (2010). Smad4/TGF-β Signaling Pathways in Pancreatic Cancer Pathogenesis. In: *Pancreatic Cancer*. Springer. pp 419-439.

30. Crowe MJ, T Doetschman and DG Greenhalgh. (2000). Delayed wound healing in immunodeficient TGF-beta 1 knockout mice. J Invest Dermatol 115:3-11.

31. Hanahan D and RA Weinberg. (2000). The hallmarks of cancer. cell 100:57-70.

32. Moustakas A, K Pardali, A Gaal and CH Heldin. (2002). Mechanisms of TGF-beta signaling in regulation of cell growth and differentiation. Immunol Lett 82:85-91.

33. Leight JL, MA Wozniak, S Chen, ML Lynch and CS Chen. (2012). Matrix rigidity regulates a switch between TGF-beta1-induced apoptosis and epithelial-mesenchymal transition. Mol Biol Cell 23:781-91.

34. Chen W and SM Wahl. (1999). Manipulation of TGF-beta to control autoimmune and chronic inflammatory diseases. Microbes Infect 1:1367-80.

35. Yingling JM, KL Blanchard and JS Sawyer. (2004). Development of TGF-β signalling inhibitors for cancer therapy. Nature Reviews Drug Discovery 3:1011-1022.

36. Orimo A and RA Weinberg. (2006). Stromal fibroblasts in cancer: a novel tumor-promoting cell type. Cell Cycle 5:1597-601.

37. Kojima Y, A Acar, EN Eaton, KT Mellody, C Scheel, I Ben-Porath, TT Onder, ZC Wang, AL Richardson, RA Weinberg and A Orimo. (2010). Autocrine TGF-β and stromal cell-derived factor-1 (SDF-1) signaling drives the evolution of tumor-promoting mammary stromal myofibroblasts. Proceedings of the National Academy of Sciences 107:20009-20014.

38. Stagg J. (2008). Mesenchymal stem cells in cancer. Stem Cell Rev 4:119-24.

39. Song S, AJ Ewald, W Stallcup, Z Werb and G Bergers. (2005). PDGFRbeta+ perivascular progenitor cells in tumours regulate pericyte differentiation and vascular survival. Nat Cell Biol 7:870-9.

40. Hanahan D and RA Weinberg. (2011). Hallmarks of cancer: the next generation. Cell 144:646-74.

41. Ponte AL, E Marais, N Gallay, A Langonne, B Delorme, O Herault, P Charbord and J Domenech. (2007). The in vitro migration capacity of human bone marrow mesenchymal stem cells: comparison of chemokine and growth factor chemotactic activities. Stem cells 25:1737-1745.

42. Fiedler J, G Röderer, KP Günther and RE Brenner. (2002). BMP-2, BMP-4, and PDGF-bb stimulate chemotactic migration of primary human mesenchymal progenitor cells. Journal of cellular biochemistry 87:305-312.

43. Betsholtz C, L Karlsson and P Lindahl. (2001). Developmental roles of platelet-derived growth factors. BioEssays 23:494-507.

44. Betsholtz C. (2004). Insight into the physiological functions of PDGF through genetic studies in mice. Cytokine & Growth Factor Reviews 15:215-228.

45. Jechlinger M, A Sommer, R Moriggl, P Seither, N Kraut, P Capodiecci, M Donovan, C Cordon-Cardo, H Beug and S Grünert. (2006). Autocrine PDGFR signaling promotes mammary cancer metastasis. The Journal of Clinical Investigation 116:1561-1570.

46. Ball SG, CA Shuttleworth and CM Kielty. (2007). Platelet-derived growth factor receptor-[alpha] is a key determinant of smooth muscle [alpha]-actin filaments in bone marrow-derived mesenchymal stem cells. The International Journal of Biochemistry & Cell Biology 39:379-391.

47. Plesec TP. (2011). Gastrointestinal Mesenchymal Neoplasms other than Gastrointestinal Stromal Tumors: Focusing on Their Molecular Aspects. Pathology Research International 2011.

48. Stricker J, T Falzone and ML Gardel. (2010). Mechanics of the F-actin cytoskeleton. Journal of biomechanics 43:9-14.

49. Winder SJ and KR Ayscough. (2005). Actin-binding proteins. Journal of cell science 118:651-654.

50. Vicente-Manzanares M, CK Choi and AR Horwitz. (2009). Integrins in cell migration--the actin connection. J Cell Sci 122:199-206.

51. Aberle H, H Schwartz and R Kemler. (1996). Cadherin-catenin complex: protein interactions and their implications for cadherin function. J Cell Biochem 61:514-23.

52. Ross TD, BG Coon, S Yun, N Baeyens, K Tanaka, M Ouyang and MA Schwartz. (2013). Integrins in mechanotransduction. Current opinion in cell biology 25:613-618.

53. Kollmannsberger P and B Fabry. (2011). Linear and nonlinear rheology of living cells. Annual Review of Materials Research 41:75-97.

54. Verdier C. (2003). Review Article: Rheological Properties of Living Materials. From Cells to Tissues. Journal of Theoretical Medicine 5:67-91.

55. Verdier C, J Etienne, A Duperray and L Preziosi. (2009). Review: Rheological properties of biological materials. Comptes Rendus Physique 10:790-811.

56. Tseng Y, TP Kole and D Wirtz. (2002). Micromechanical mapping of live cells by multiple-particle-tracking microrheology. Biophys J 83:3162-76.

57. Kole TP, Y Tseng and D Wirtz. (2004). Intracellular microrheology as a tool for the measurement of the local mechanical properties of live cells. Methods Cell Biol 78:45-64.

58. Wirtz D. (2009). Particle-tracking microrheology of living cells: principles and applications. Annual review of biophysics 38:301-326.

59. Panorchan P, JS Lee, BR Daniels, TP Kole, Y Tseng and D Wirtz. (2007). Probing cellular mechanical responses to stimuli using ballistic intracellular nanorheology. Methods in cell biology 83:113-140.

60. Tseng Y and D Wirtz. (2001). Mechanics and Multiple-Particle Tracking Microheterogeneity of α-Actinin-Cross-Linked Actin Filament Networks. Biophysical journal 81:1643-1656.

61. Suh J, M Dawson and J Hanes. (2005). Real-time multiple-particle tracking: applications to drug and gene delivery. Advanced drug delivery reviews 57:63-78.

CHAPTER 3: DIFFERENTIAL MECHANICAL RESPONSE OF MESENCHYMAL STEM CELLS TO TUMOR-CONDITIONED MEDIA

The progression of neoplastic malignancies is a complex process resulting not only from the accumulation of mutations within tumor cells, but also modulation of the tumor microenvironment. Recent advances have shown that the recruitment and subsequent heterotypic interactions between cancer cells and stromal cells including fibroblasts and bone marrow-derived mesenchymal stem cells (MSCs) are crucial for carcinogenesis. Though extensive work has been done analyzing the signals that recruit these cells, the governing mechanical properties have not been fully investigated. Here, we reported that despite their initial similarities, MSCs not only responded faster but also more dramatically to pro-migratory tumor-secreted soluble factors. Utilizing multiple particle tracking microrheology to probe the cytoskeletal mechanical properties, we showed that MSCs stiffen completely within one hour, three times faster than fibroblasts. In addition, unlike fibroblasts, MSCs exposed to tumor-secreted soluble factors displayed a functionally different phenotype characterized by morphological elongation, decreased actin stress fiber density, and decreased adhesion. These findings demonstrated a fundamental difference in the recruitment of fibroblasts and MSCs, knowledge necessary for the understanding of tumor development. Furthermore, this native homing ability of MSCs makes them ideal vectors for delivery of therapeutic genes directly to the tumor.

3.1. INTRODUCTION

The microenvironment in a solid tumor develops under the constant influence of inflammatory mediators [1]. These molecules, which include a milieu of cytokines, chemokines, and growth factors, are important targets for recruitment of a variety of cells such as leukocytes, macrophages, monocytes, fibroblasts and mesenchymal stem cells (MSCs) [2]. Previous literature on the MSCs and fibroblasts suggests functional similarity as indicated both by global gene expression [3] as well as immunosuppression in allogeneic transplantation[4]. In the tumor stroma both can also form activated cancer associated fibroblasts (CAFs) or myofibroblasts [2,5], though MSCs can additionally differentiate into pericyte progenitor cells (PPCs) [6]. Increased numbers of myofibroblasts in the wound bed and in other sites of chronic inflammation have also been associated with MSC progenitors [2]. Notably, both cell types also aid in tumor growth and metastasis via autocrine and paracrine signaling [7,8]. In light of this, recent studies have begun to investigate these cells not only as alternative targets for anti-cancer therapy [9], but also for use as targeted gene-delivery vehicles [10].

For the latter approach, MSCs have shown greater promise than fibroblasts [11]. This may be in part because fibroblasts are recruited locally to form activated CAFs [12], whereas MSCs derived from the bone marrow must natively home through circulation to distal tumor sites. Consequentially, the therapeutic use of systemically infused MSCs to tumors has been investigated in breast [13], colon [14], ovarian carcinomas [15], gliomas [16], and Kaposi's sarcomas [17]. Despite this potential, extended *ex vivo* culture reduces homing capacity of MSCs [18] and the majority of systemically infused MSCs become trapped in the lungs [5,19,20]. To overcome this, breast cancer cell-conditioned media

[7], hypoxic preconditioning [21,22], and treatment with individual chemokines or growth factors [23,24] have all been investigated to increase MSC mobility; however, the effects of inflammatory mediators on the microscopic mechanical properties of MSCs have not been fully elucidated.

This study sought to understand the underlying mechanical differences in MSCs and fibroblasts as they migrate toward tumors. In order to best simulate the signals migrating cells would receive *in vivo*, we utilized 4T1 breast tumor cell conditioned media (TCM) to stimulate the cells *in vitro*. We found that after treatment with TCM, MSCs underwent an exaggerated response as compared to fibroblasts, and that this response could potentially be explained by altered gene expression of Rho GTPases Cdc42 and RhoA. We further demonstrate that even one hour incubation with TCM increases cell motility, indicating a novel 'mechanical priming' achieved by short-term TCM preconditioning.

3.2. MATERIALS AND METHODS

Materials: Cellgro IMDM, RPMI 1640, DMEM, L-glutamine, sodium bicarbonate, PBS, and penicillin-streptomycin were purchased from Mediatech. FBS was purchased from Atlanta Biologicals and Type I, II collagenase from Worthington Biochemicals. Rat anti-mouse PE-Sca1, PerCP-CD45, PE-CD29, and APC-CD11b, and red blood cell lysis buffer were purchased from Biolegend. Rhodamine-Phalloidin, rabbit vinculin monoclonal antibody, Alexa Fluor 488 anti-rabbit IgG, FITC-conjugated mouse anti-alpha tubulin, and Fluospheres carboxylate-modified 100 nm particles (F8801) were purchased from Invitrogen. Cy3-SMA was purchased from Sigma. PDS-1000 Biolistic Helium Particle Injection, 1800 psi rupture discs, and macrocarriers were purchased from

BioRad. Primers for gene analysis were obtained from IDT. All other reagents were purchased from VWR or Sigma-Alrich unless otherwise specified.

Cell Culture: Swiss 3T3 fibroblasts and 4T1 mammary carcinoma cells were purchased from American Type Cell Culture and cultured according to manufacturer's protocol. MSCs were isolated from murine bone marrow and cultured in MSC growth media (IMDM supplemented with 20% FBS, 2 mM L-glutamine, 100 U/ml penicillin, and 100 U/ml streptomycin). Bone marrow was extracted from the femurs and tibias of 8–10 week old Balb/C mice (Charles River Laboratories, Wilmington, MA) by crushing the bones in FBS solution (1 mg/ml Type I collagenase in 30% FBS and 70% PBS), filtering the cell suspension using a 70-µm cell strainer, and centrifuging at 2000× g for 10 minutes. The bone marrow cells were resuspended in MSC growth media and seeded at 3×10^6 cells/cm^2. After 24 hours, non-adherent cells were removed, and cells were cultured in MSC growth media (replaced 3 times per week). Differentiation was induced with either adipogenic or osteogenic media per standard protocols. All animal studies were approved by the Institutional Animal Care and Use Committee at Georgia Institute of Technology.

Flow Cytometry: To determine cell phenotype, cells were analyzed with a LSR-II flow cytometer. Briefly, cells were detached, centrifuged, and separated into 100 µl aliquots then labeled with either 2% PerCP-CD45, PE-Sca1, and APC-CD11b antibodies or PE-CD61, FITC-CD29, and APC-VCAM1. A negative control for each cell type was used to determine positive populations. All studies were performed in triplicate with n = 100,000 events per sample.

Conditioned Media Collection: Murine mammary carcinoma 4T1 cells were cultured to confluency in 10 cm dishes with standard growth media, then washed in PBS, and incubated in 8 mL unsupplemented DMEM for 24 hours. Cell-free TCM was obtained by centrifugation and filtration. TCM was prepared in a single batch, aliquoted and frozen at −80°C for future use. For all assays with TCM, control media was unsupplemented DMEM.

Microrheological Characterization: Intracellular mechanical properties of living cells were determined by multiple particle tracking microrheology (MPTM), as previously described [25]. Briefly, 100 nm probe particles were injected into the cytosol of MSCs using PDS-1000 Biolistic Helium Particle Injection System (Biorad). The thermal motion of these probes is directly related directly to local rheological properties via the Stokes-Einstein equation [26]. High spatiotemporal resolution videos of injected cells were collected with a Nikon CFI Apochromat TIRF 100X oil-immersion lens (NA=1.49) on a Nikon Eclipse Ti inverted epifluorescent microscope maintained at 37° C and 5% carbon dioxide. A custom MPT routine incorporated in the MetaMorph software (Molecular Devices; Downington, PA) was then used to simultaneously monitor the coordinates of 5-20 particles per video. For each condition, particles were tracked in a minimum of 10 cells per condition. Time-dependent individual particle mean square displacements (MSDs) were ensemble-averaged and used to determine the average frequency dependent elastic moduli (G'), viscous moduli (G'') and phase angle (δ), which were reported in this study.

Immunoflourescence Assays: For visualization of cytoskeletal proteins, cells cultured on glass cover slips were briefly extracted in a buffer containing 80 mM PIPES (pH 6.8),

1 mM $MgCl_2$, 5 mM EDTA, and 0.5% Triton X-100 before fixation with 0.5% glutaraldehyde in PBS. The reaction was quenched with 1 mg/mL sodium borohydride, before permeabilization with Triton X-100 and blocking with FBS. Cells were stained for one hour at room temperature with either 1:50 FITC-conjugated anti-tubulin, 1:200 Rhodamine Phalloidin , or 1 µg/mL rabbit anti-vinculin followed by 1:1000 goat anti-rabbit Alexa Flour 488 before sealing with Vectashield (Vector Labs) containing DAPI. For morphological visualization, cells were stained with crystal violet then rinsed extensively. All cells were visualized using either an inverted Nikon Eclipse Ti or Zeiss LSM 510 UV confocal microscope.

Quantitative Image Analysis: Quantitative image analysis was performed by a series of custom written MATLAB algorithms. For cell elongation, borders were manually drawn around cells before segmentation to extract cell major and minor axis. After normalization for background, stress fibers were segmented by a Laplacian filter, and then normalized to cell area extracted from a built-in MATLAB thresholding algorithm. Nuclei were analyzed using a semi-automated MATLAB algorithm that visualized each image before quantification to ensure only single nuclei were measured. Similarly, for actin and vinculin quantification, images were normalized then segmented for quantification.

Gene Expression Analysis: Total RNA was isolated using TRIzol reagent (Invitrogen) per manufacturer's protocol before reverse transcription using the iScript cDNA synthesis kit (BioRad). DNA concentration and quality were verified by spectroscopy. To verify differentiation, PCR was run per previous literature. For qRT-PCR on the small Rho GTPases, Cdc42, RhoA, and Rac1, as well as an endogenous GAPDH control, the real-

time PCR reaction was run using SsoAdvanced SYBR Green Supermix (BioRad) in an AB Step One Plus thermocycler (n = 5). Primer sequences are reported in Appendix 1 (Table A-1). Values are reported as fold change in expression over fibroblasts in CM ± S.E.M. after normalization to respective endogenous GAPDH control.

Statistics: All studies were performed in triplicate (unless otherwise indicated). Statistical analysis was carried out using a student's t-test for comparison between two groups or analysis of variance (ANOVA) to compare effects between cell types, considering $p<0.05$ to be significant (***$p<0.001$,**$p<0.01$,*$p<0.05$). Data were reported as the mean ± s.e.m.

3.3. RESULTS

Characterization of Bone Marrow Derived MSCs: To verify the phenotype of MSCs, cells were assayed for both cell surface marker expression and differentiation capacity. After purification by adherence to plastic, MSCs were negative for myeloid and hematopoietic stem cell markers CD11b and CD45 and positive for Sca1, CD29, CD61, and VCAM1 (Figure 3-1). Fibroblast expression is provided for comparison (Figure 1A, Right). Osteogenesis and adipogenesis were induced in passage 4 MSCs using standard protocols [27]. After 4 weeks incubation in adipogenic and osteogenic media, MSCs differentiated into adipocytes (Figure 3-2A) and osteoblasts (Figure 3-2B) respectively, as verified by histological staining.

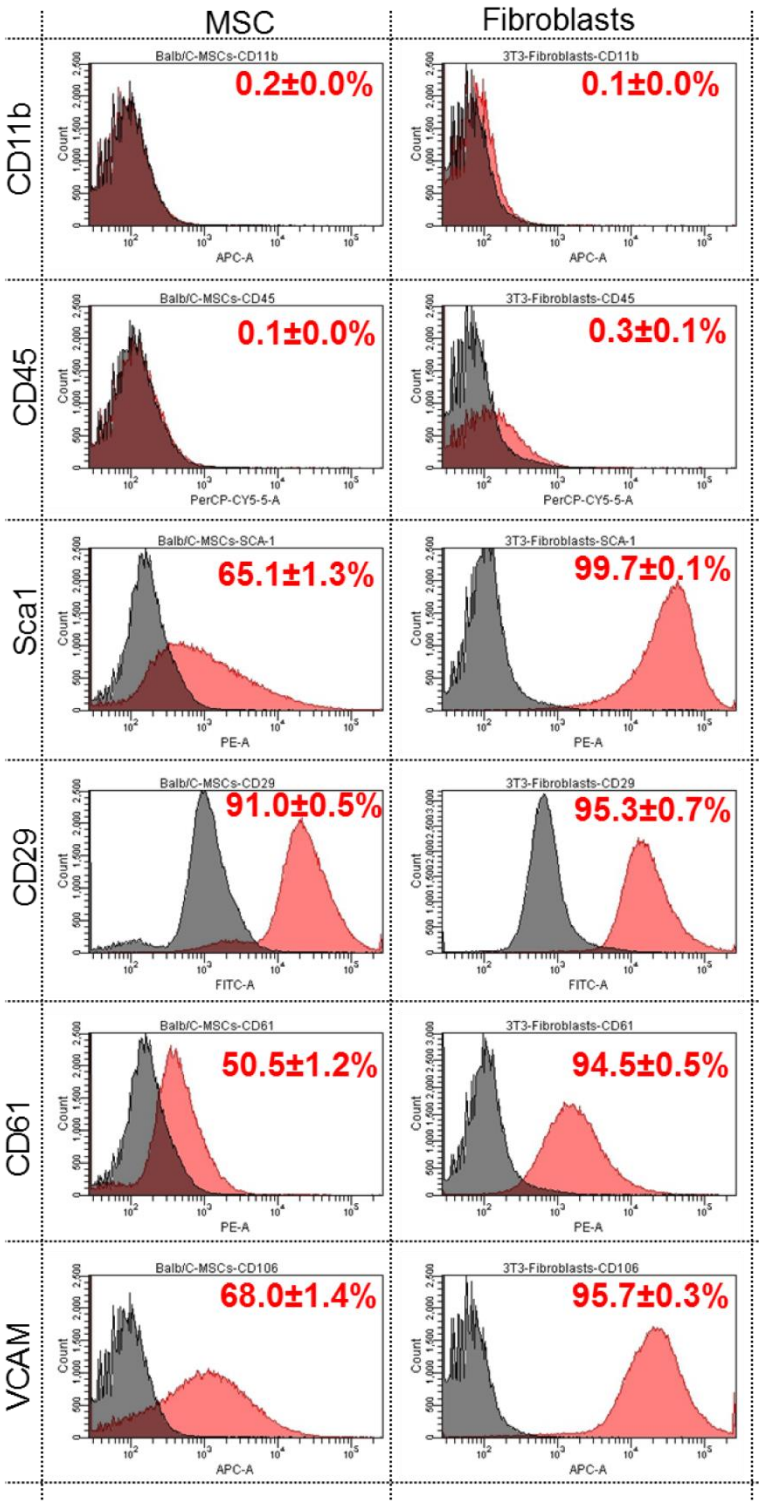

Figure 3-1. *Characterization of bone marrow isolated MSCs and fibroblasts.* Phenotypic analysis was performed by flow cytometry on adherent bone marrow cells and Swiss 3T3 fibroblasts with positive populations in red given with S.E.M.

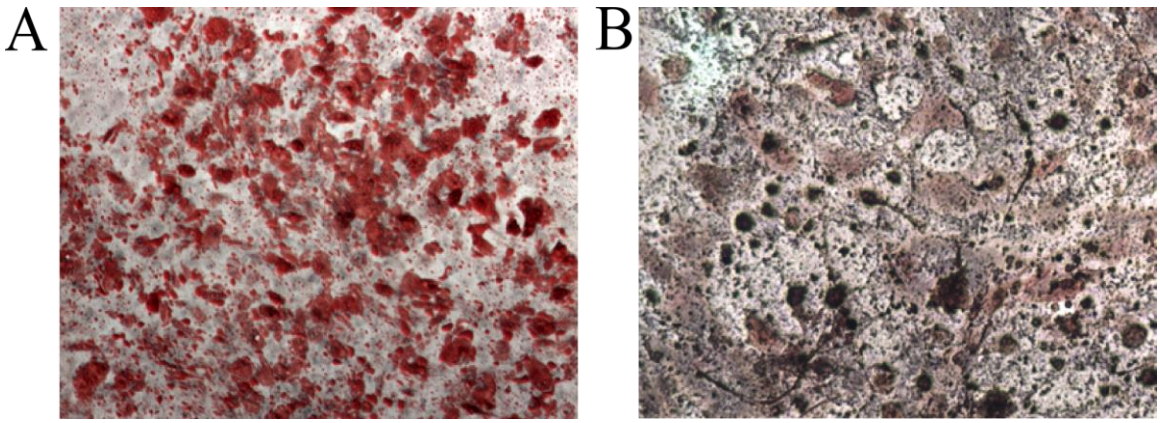

Figure 3-2. *Multilineage differentiation potential of MSCs*. Purified MSCs differentiated into adipocytes (A) and osteoblasts (B) within 3 weeks in lineage-specific differentiation media as shown by staining. Adipocytes and osteoblasts were stained with oil red o and von kossa respectively. (scale bar = 100μm).

Morphological Changes after Incubation with Tumor Cell-Secreted Soluble Factors:

To investigate the response of MSCs to tumor cell-conditioned media (TCM), cells were incubated in serum-free TCM or control media (CM) for 24 hours. MSCs underwent a morphological change from a cobblestone appearance to an elongated phenotype (Figure 3-3A-B). In comparison, Swiss 3T3 fibroblasts (Figure 3-3C-D) and primary isolated kidney fibroblasts (Figure 3-3E-F) had similar initial morphologies, but did not undergo a morphological change upon treatment with TCM.

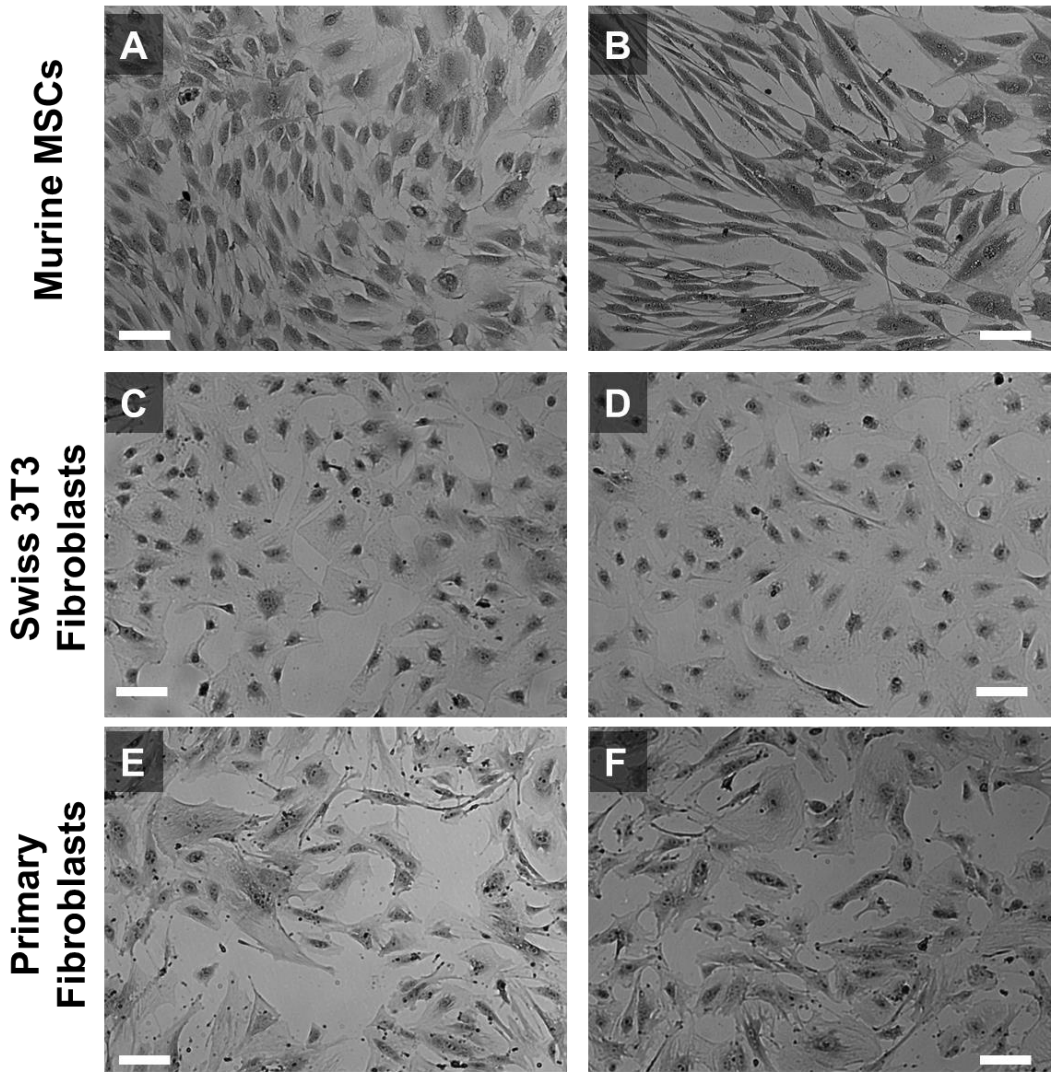

Figure 3-3. *Tumor-secreted soluble factors alter MSC morphology.* Brightfield images of (A-B) primary fibroblasts (isolated from Balb/C mouse kidney), (C-D) Swiss 3T3 fibroblasts, and (E-F) murine MSCs (isolated from Balb/C mouse bone marrow) incubated for 24 hours in control media (CM, top) or tumor cell-conditioned media (TCM, bottom), then fixed in methanol, and stained with crystal violet. MSCs elongated dramatically in response to TCM (E-F); whereas, primary (A-B) and immortalized (C-D) fibroblasts did not respond to TCM treatment. (Scale bar = 100 μm)

Cytoskeletal Changes after TCM Treatment: We next examined the changes in cytoskeletal arrangement necessary to produce the elongated phenotype. To accomplish this, CM and TCM treated cells were fixed and stained for filamentous actin, microtubules, and nuclei (Figure 3-4). Cytoskeletal parameters were quantified from maximum intensity projections of confocal image stacks (3 images per stack) using a custom-written MATLAB algorithm. First, the cell elongation factor was quantified using a ratio of the minor to major cell axis (Figure 3-5A). For control MSCs and 3T3 fibroblasts, the cell shape factors were near unity, indicating similarity in their native cell shape. In the presence of TCM, MSCs elongated by ~30% after 12 hours ($p<0.05$) and ~75% after 24 hours ($p<0.001$); whereas, the elongation factor of 3T3 fibroblasts remained near unity. We then quantified the stress fiber factor, which is the density of stress fibers normalized to cell area (Figure 3-5B). The stress fiber factor of TCM-treated 3T3 fibroblasts remained constant; whereas, the stress fiber factor of MSCs was reduced more than 25% within 12 hours. Though this could in part be due to control cells being flatter than TCM treated cells, the use of maximum intensity projections minimizes this possibility, suggesting the changes are in fact due to decreases in actin stress fiber density. Upon stimulation with TCM, the nuclei of MSCs elongated dramatically (Figure 3-4). A nuclear shape factor was used to characterize nuclear elongation (Figure 3-5C), with a value of one indicating the nucleus is perfectly round. Initially, MSCs and 3T3 fibroblasts had nuclear shape factors of approximately 0.75; however, upon incubation with TCM for 12 hours, MSC nuclei were elongated by approximately 13% (Figure 3-5C). Nuclear elongation was never seen in 3T3 fibroblasts and no further elongation was observed in MSCs from 12–24 hours (Figure 3-5C).

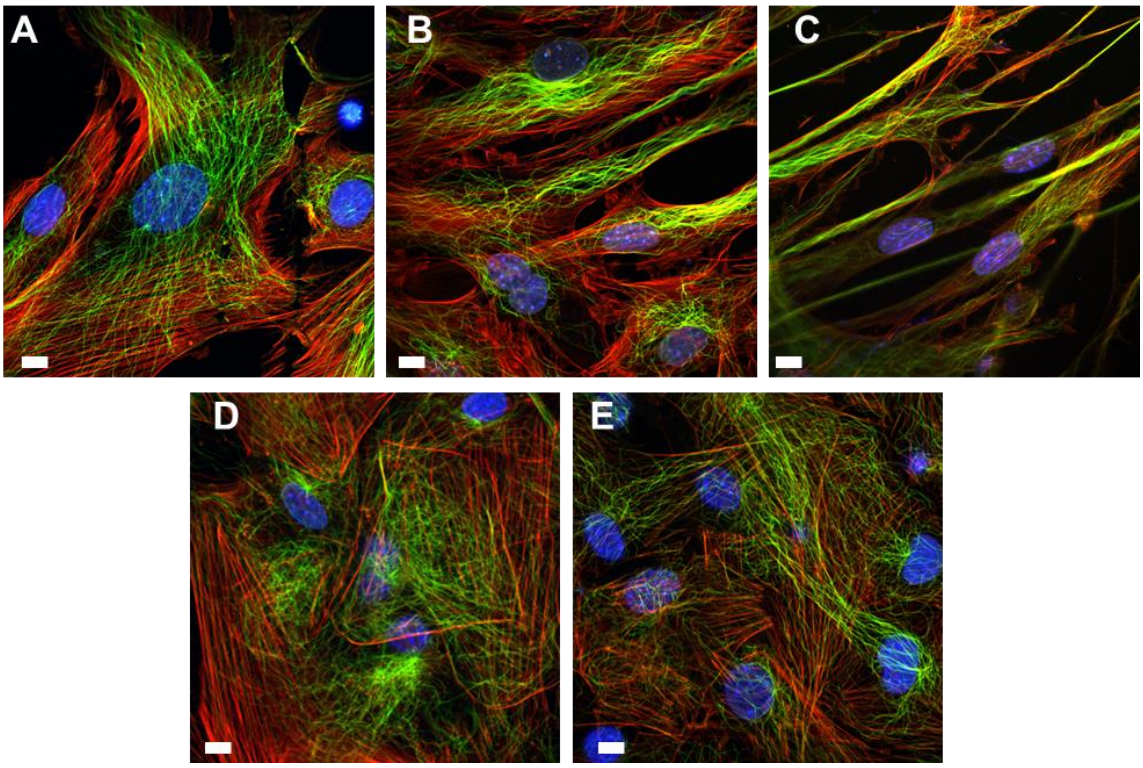

Figure 3-4. *MSCs reorganize their cytoskeleton in response to tumor-secreted soluble factors.* Confocal images of CM and TCM-treated MSCs (A-C) and 3T3 fibroblasts (D-E) stained with Phalloidin (F-actin, red), anti-α-tubulin (microtubules, green), and DAPI (nucleus, blue). The shape and cytoskeletal organization of CM-treated MSCs (A) and CM- (D) and TCM- (E) treated Swiss 3T3 fibroblasts were similar (24 hours after CM or TCM addition); whereas, TCM-treated MSCs were elongated with extended cytoskeletal filaments (B-C). MSC elongation increased between 12- (B) and 24- (C) hours, indicating that cytoskeletal changes may be progressive. (scale bars = 10μm)

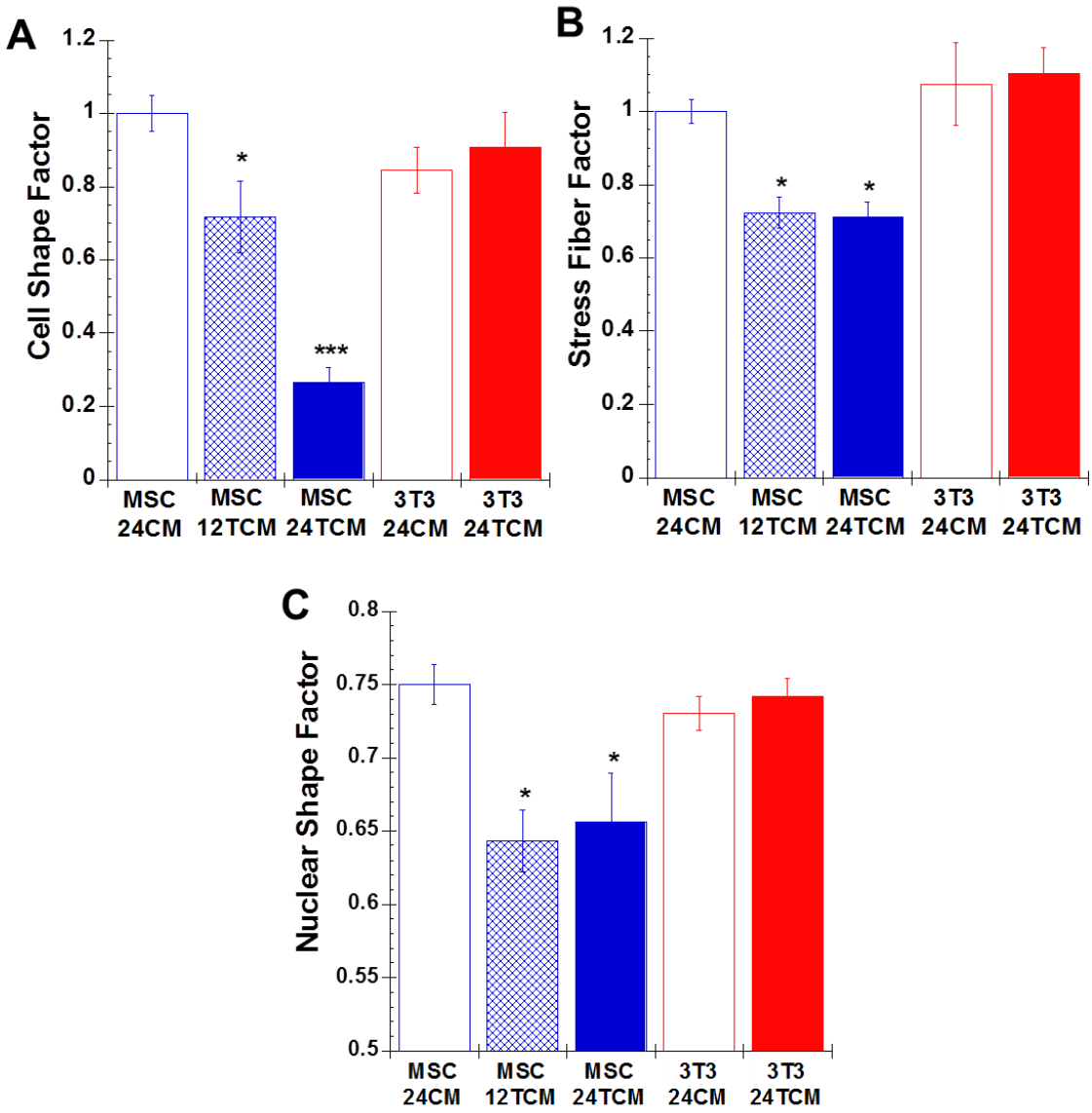

Figure 3-5. *Cytoskeletal parameters were determined by analysis of confocal images with a custom MATLAB routine.* The cell (A) and nuclear (C) shape factors were used to characterize the circularity of an elliptical outline of the cell or nucleus, respectively, with a shape factor of 1 indicating a perfect circle. The stress fiber factor (B) was used to characterize the density of actin stress fibers per cell area. Cytoskeletal changes observed in TCM-treated MSCs (Figure 3-4B-C) were confirmed using the cytoskeletal parameters (A-C), which indicated dramatic reductions in cell and nuclear shape factors and stress fiber densities.

TCM Alters the Distribution and Strength of MSC Focal Adhesions: The cytoskeleton is linked to the extracellular environment via focal adhesion complexes, which are important regulators of cell motility. To determine the effects of TCM on cell adhesion, control and TCM-treated MSCs and 3T3 fibroblasts (treated for 24 hours) were fixed and stained with FITC anti-vinculin, a focal adhesion marker, and Rhodamine-Phalloidin, which stains filamentous actin (Figure 3-6, Figure 3-7). TCM treatment dramatically affected the overall number and morphology of focal adhesions on MSCs (Figure 3-6, Figure 3-7); however, it had no apparent effect on 3T3 fibroblast focal adhesions (Figure 3-6). For MSCs, the ratio of vinculin to actin was quantified from confocal images using a MATLAB routine (Figure 3-7B). Twenty-four hours after TCM addition the vinculin to actin ratio was reduced by 50% (Figure 3-7B) and focal adhesions no longer displayed their characteristic brush-like pattern (Figure 3-6) but were instead localized at the tips of elongated cells (Figure 3-6, Figure 3-7).

Cytoskeletal Stiffening in Response to TCM: MPT was used to characterize the immediate effects of TCM (30 minutes to 3 hours) on the intracellular mechanical properties of MSCs (Figure 3-8A, Figure 3-9A–E) and 3T3 fibroblasts (Figure 3-8B, Figure 3-9F–J). Corresponding morphological changes were not seen in immunostained fixed MSCs until 12–24 hours after TCM treatment and were never seen in 3T3 fibroblasts (Figure 3-4). For MPT studies, 100 nm probe particles, with diameters more than 100-fold smaller than the cells, were injected into the cytoplasm (Figure 3-8C), and their mobility, characterized by the $<<\Delta r^2(\Delta t)>>$ (Figure 3-8A–B), was used to determine intracellular rheology. Initially, the amplitude and logarithmic slope of the $<<\Delta r^2(\Delta t)>>$ for MSCs and 3T3 fibroblasts were comparable, indicating similarity in

their microscopic mechanical properties (Figure 3-9A,F). Within 30 minutes, TCM treatment reduced the $<<\Delta r^2(\Delta t)>>$ for MSCs up to 20-fold; however, similar changes were not seen in 3T3 fibroblasts until 2–3 hours after TCM treatment.

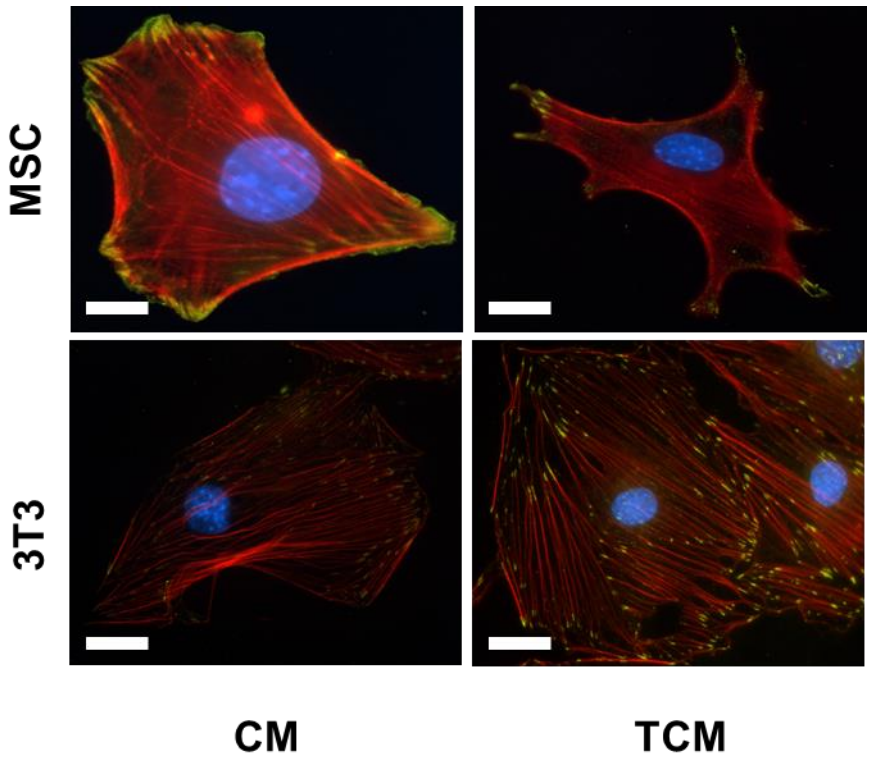

Figure 3-6. *Epifluorescent microscopy was used to further investigate the effect of TCM on focal adhesion distribution in MSCs and 3T3 fibroblasts.* CM-treated MSCs displayed a brush-like pattern of focal adhesions; whereas, focal adhesion on TCM-treated cells appeared as points at the end of cytoskeletal extensions.TCM-treatment had no effect on the pattern of focal adhesions on 3T3 cells. (scale bars = 10μm)

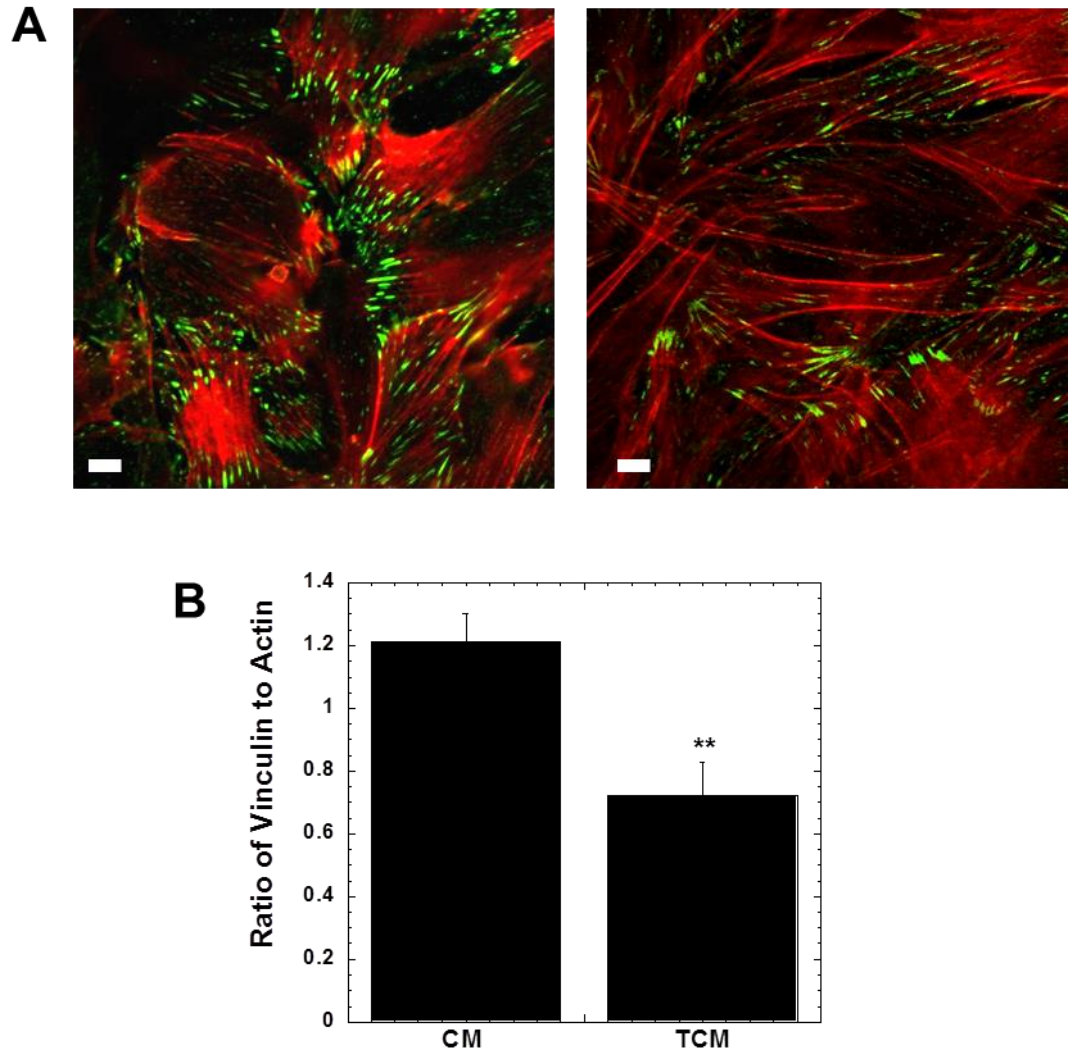

Figure 3-7. *Changes in the distribution of focal adhesions.* (A) Confocal micrographs of 24-hour CM- (left) and TCM- (right) treated MSCs stained with Phalloidin (F-actin, red), and anti-vinculin (green). (B) The vinculin to actin ratios quantified from confocal images demonstrated a reduced concentration of focal adhesion proteins in TCM-treated MSCs. (scale bars = 10μm)

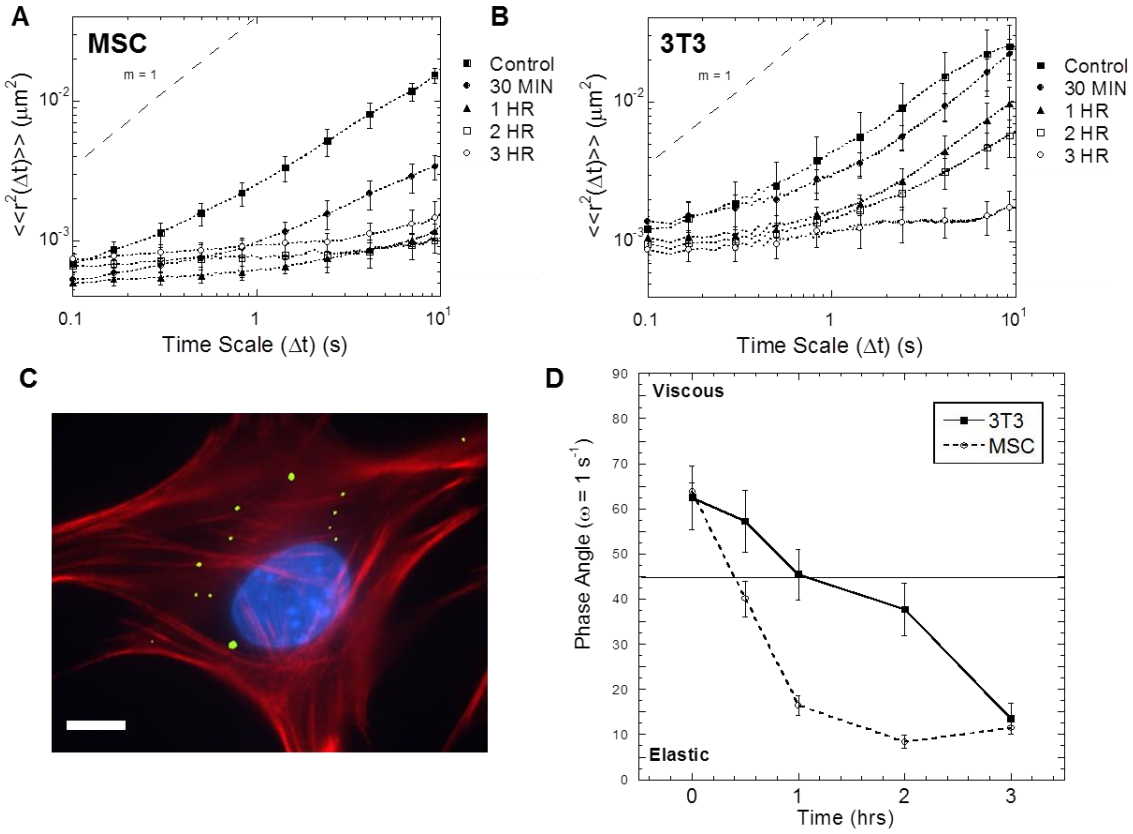

Figure 3-8. *Multiple particle tracking microrheology.* The ensemble averaged mean squared displacements ($<<r^2(\Delta t)>>$) of 100 nm particles embedded in the cytoplasm of TCM-treated MSCs (A) and 3T3 fibroblasts (B) were evaluated from 0-3 hours. For both cell lines, treatment with TCM reduced the rate of cytoplasmic particle transport in a time-dependent manner. Fluorescent image of 100 nm particles (green) in the cytoplasm of a MSC, which was fixed and stained with phalloidin (red) and DAPI (blue) (C). The phase angle, $\delta = \arctan(G''(\omega))/ G'(\omega))$, was used to characterize the viscoelastic nature of the cytoplasm over the course of the experiment (D). The viscoelastic nature of MSCs and 3T3 fibroblasts were similar initially and 3 hours after TCM-treatment; however, MSCs responded much more rapidly to TCM with a 4-fold reduction in δ within 60 minutes. (scale bar = 10μm)

The ratio of viscous to elastic character, or phase angle (δ), of control cells was $55° < \delta < 70°$, indicating that initially the cytoplasm behaved more like a viscous liquid than an elastic solid. One hour after TCM treatment, the cytoplasm of MSCs had dramatically stiffened with $10° < \delta < 15°$. This effect was not seen in 3T3 fibroblasts until 3 hours after TCM treatment. MPTM was also used to quantify the rheological properties of the cytoplasm, which is highly viscoelastic in part to its crowded nature. The frequency-dependent viscoelasticity of MSCs changed dramatically after TCM treatment (Figure 3-9A–E). In fact, the cytoplasm became highly elastic with $G' \sim 400$ dyn/cm^2 (Figure 3-9B–E).

TCM Rapidly Increases *In vitro* Cell Migration: Previous studies documented increased MSC migration toward chemotactic factors after 18-24 hours [23,24,28]. Our multiple particle tracking studies revealed dramatic changes in intracellular mechanics within 1 hour. To determine if these mechanical changes were correlated with increased mobility, the migration of control and treated cells toward CM or TCM was measured hourly for 3 hours using transwell inserts with 3μm (Figure 3-10A) or 8μm (Figure 3-10B) pores. Without chemotactic factors present, few MSCs and 3T3 fibroblasts migrated through 3μm pores; however, when TCM was added, there was a significant increase in MSC migration within 3 hours ($p < 0.01$, Figure 3-10A). MSC migration through 8μm pores was almost always significantly greater than 3T3 fibroblast migration (Figure 3-10B-C)).

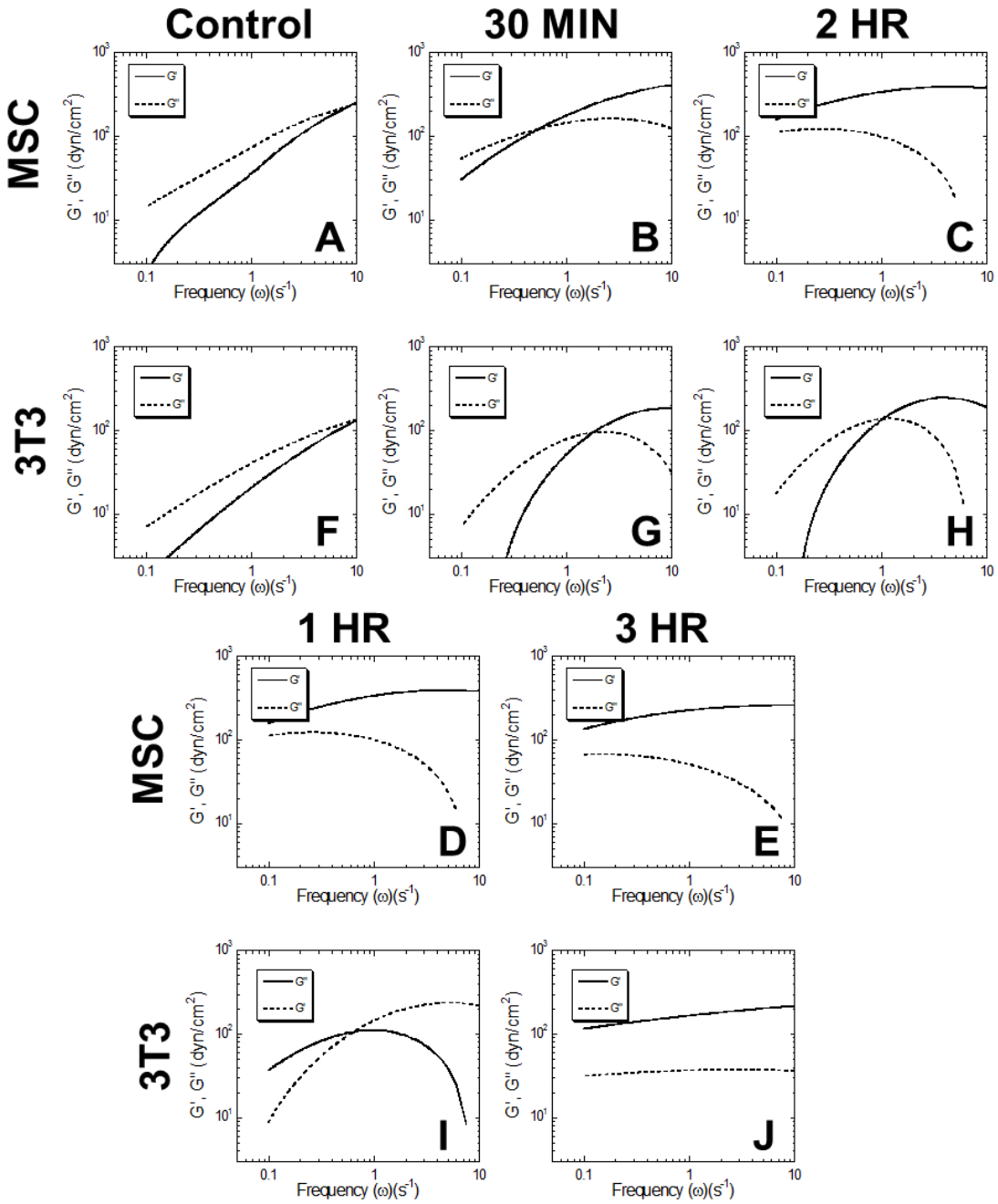

Figure 3-9. *TCM alters cytoplasmic rheology.* The time-dependent ensemble averaged MSDs of 100 nm particles embedded in the cytoplasm of MSCs and 3T3 fibroblasts were converted to frequency-dependent elastic (G', solid lines) and visous (G", dashed lines) moduli using a custom algorithm written for Matlab software. The ensemble-averaged frequency-dependent viscoelasticities of MSCs (A-E, left) and 3T3 fibroblasts (F-J, right) prior to (A,F) and 30 minutes (B,G), 1 hour (C,H), 2 hours (D,I), or 3 hours (E,J) after treatment with TCM. The cytoplasm of MSCs became predominantly elastic within 60 minutes; whereas, 3T3 fibroblasts required 3 hours to undergo a similar change.

MSCs also responded more rapidly to TCM, with increased MSC migration within 2 hours ($p<0.001$) and increased 3T3 fibroblast migration within 3 hours ($p<0.01$). To determine if mechanical changes exhibited by MSCs in the first hour were indicative of a more migratory phenotype, we pre-treated both cell types for one hour with TCM before seeding in 8μm transwell inserts. Pre-treatment with TCM increased MSC and 3T3 fibroblast migration toward CM and TCM, though more significantly toward TCM (Figure 3-10C). Statistical analysis also revealed synergistic effects of TCM pre-treatment and migration toward TCM for both cell types, suggesting that not only does pre-treatment increase motility but also causes a preferential migration towards chemotactic gradients.

Changes in Gene Expression Associated with Altered Mechanical Response: To understand genotypic changes resulting in altered mechanical responses, we performed qRT-PCR to investigate the expression of the Rho GTPases RhoA, Rac1, and Cdc42 that modulate the actin cytoskeleton (Figure 3-11A). We found that after TCM treatment, both cell types express significantly more Rac1 ($p<0.05$) as compared to their respective controls. Furthermore, ANOVA revealed that MSCs expressed significantly more RhoA overall ($p<0.0001$). Moreover, it showed a significant interaction effect between cell type and TCM treatment for Cdc42 ($p<0.005$), suggesting that this molecule is largely responsible for the altered mechanical response.

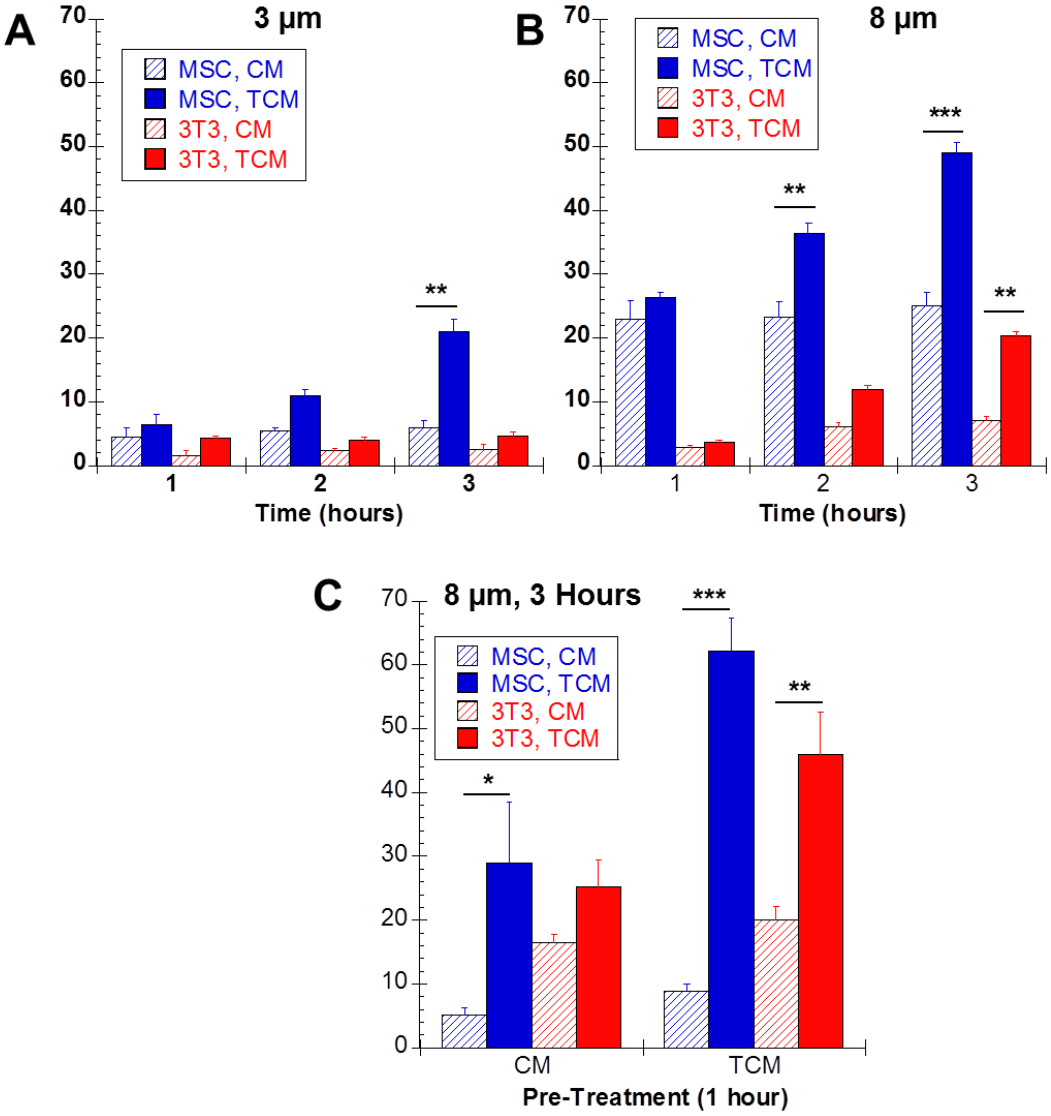

Figure 3-10. *Effect of TCM on Cell Migration.* Tranwell assays were used to measure the migration of MSCs and 3T3 fibroblasts through 3 µm- (A) and 8 µm- (B) pore transwell inserts toward CM or TCM. The average number of cells per image (n=9), collected with a 10x-objective, was reported. TCM significantly increased MSC migration, compared to CM, through 3 µm pores within 3 hours and 8 µm pores within 2 hours; however, fibroblast migration was only increased through 8 µm pores within 3 hours. MSCs and 3T3 fibroblasts were then treated with CM or TCM for 1 hour and allowed to migrate through 8 µm-pore transwell inserts toward CM or TCM for 3 hours (C). Pre-treatment with TCM resulted in synergistic effects on chemotactic migration for both cell types.

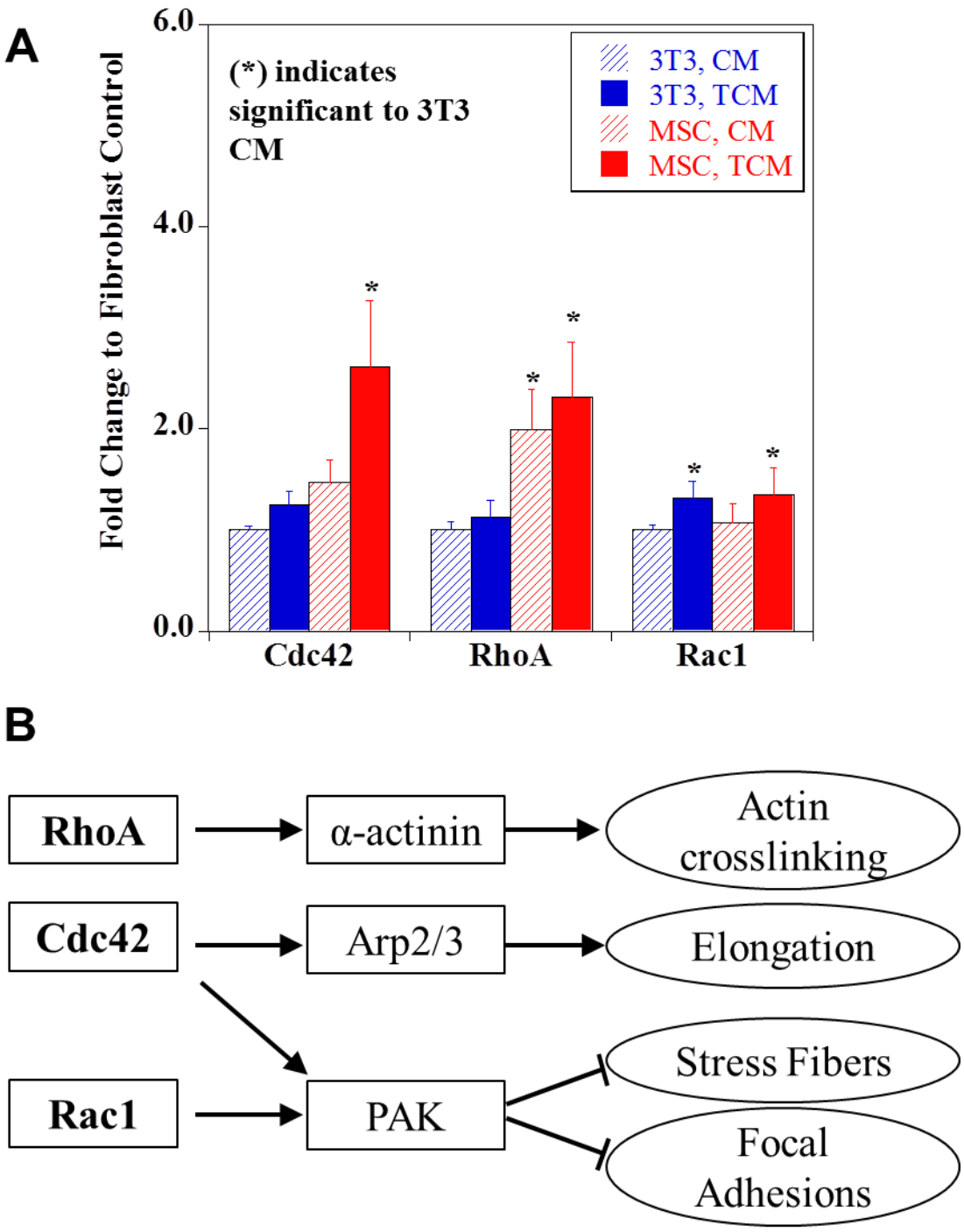

Figure 3-11. *Alterations in Gene Expression.* (A) Changes in expression of small Rho GTPases RhoA, Rac1, and Cdc42 before and after prolonged treatment with TCM. (B) After 24 hour exposure to TCM, alterations in morphology and adhesion can be explained by differential gene expression in MSCs and fibroblasts.

3.4. DISCUSSION

In this study, TCM isolated from 4T1 metastatic breast cancer cells was used to mimic the chemotactic factors released by tumors. Previous studies have demonstrated that TCM is a potent pro-migratory cocktail of growth factors and chemokines [28,29]. Literature on 4T1 tumor cell conditioned media shows that it contains soluble growth factors including platelet-derived growth factor (PDGF), transforming growth factor (TGF-β1), and vascular endothelial growth factor (VEGF) [30], as well as cytokines, chemokines, acute phase proteins and preoteases. In two separate studies [31,32], researchers examined the gene expression profile of 4T1 tumor cells in comparison to less metastatic cell lines, finding a variety of up-regulated pro-migratory soluble factors including: (a) growth factors angiopoietin 2, VEGF-C, insulin-like growth factor 2, (b) chemokines CCL5, CCL7, CXCL1, CXCL16, CSF2, CSF3, (c) interleukins 1α and 23, and (d) matrix metalloproteases 13,3,9. It is noted this list is not comprehensive, as the complexity of TCM continues to yield novel pro-migratory soluble factors [29] in addition to unique miRNA secretomes [33].

Some of these growth factors, such as PDGF, TGF- β1, and VEGF, have been shown to directly induce mechanical and migratory changes in MSCs and fibroblasts [23,24,28,34-36]. However, the effects of other soluble factors present in TCM are often much more difficult to determine. Menon et al found that MSC exposure to tumor cell conditioned media up-regulates mRNA levels of 104 genes, including genes for stromal cell-derived factor 1 (SDF-1/CXCL12), monocyte chemotactic protein 1 (MCP-1/CCL2), and growth-regulated protein β (Gro-β/CXCL2), which are all potent chemokines that act in an autocrine fashion to further stimulate MSC migration [28]. In the same study,

Menon et al also found that TCM altered the organization of cytoskeletal actin, resulting in increased polarity and directional migration [28]. In another study, soluble factors (identified as extracellular matrix peptides) in LLC1 tumor cell conditioned media induced bone marrow derived cell secretion of pro-inflammatory cytokines, including IL-1β, IL-6, and tumor necrosis factor α (TNF-α); whereas, serum-free media and 3T3 conditioned media had no effect on cytokine production [37]. In contrast, tumor cells exchange paracrine signals with normal fibroblasts, which have been shown to promote matrix remodeling and tumor cell invasiveness [34]. One way this occurs is through tumor cell secretion of IL-1, basic fibroblast growth factor (bFGF/ FGF-2), PDGF, and/or TGF-β, which induce hepatocyte growth factor (HGF) secretion from fibroblasts. HGF then binds with its cognate receptor, c-MET, which is expressed by normal and cancer stem cells [38]. The HGF/c-MET signaling pathway triggers cell growth and angiogenesis, which are important mechanisms of cancer development, normal growth, and wound healing [34].

We hypothesize that several of the growth factors and chemokines in TCM, such as VEGF, PDGF, TGF- β1, directly stimulate changes in MSCs and fibroblasts; however, other factors in TCM, such as IL-1β, colony-stimulating factor (CSF), and TNF-α are more potent mediators of changes in MSCs due to autocrine signaling pathways including SDF-1, MCP-1, and Gro-β, which they activate rapidly. Interestingly, a more detailed analysis of MSC migration to individual growth factors and chemokines found that TNF-α stimulation was necessary for MSC migration towards all chemokines tested, but had little effect on the migration of MSCs toward growth factors. Due to the complicated nature of the autocrine and paracrine signaling pathways involved in the recruitment of

cells to tumors, we focused our study on characterizing the effects of a cocktail of these factors in TCM on MSC and fibroblast behavior.

The molecular response of MSCs to various soluble factors has been well characterized, but the mechanical properties that govern their migration are yet to be fully investigated. MPTM was used to analyze the real-time changes in live-cell mechanics. Previous MPT studies have demonstrated that fibroblasts stiffen both during migration and in response to activation of RhoA, Cdc42, or Rac1, with the largest response to RhoA [35,39]. This technique revealed cytoskeletal stiffening after TCM treatment larger than previously documented, completely changing the intracellular mechanical phenotype, three-fold faster in MSCs (Figure 3-8, 9).

Analysis of expression of RhoA in untreated MSCs and fibroblasts reveals two-fold higher expression in MSCs (Figure 3-11A), which could account for more rapid cytoskeletal stiffening of MSCs. RhoA can act by Rho Kinase (ROCK) to induce stress fiber formation and focal adhesions or to crosslink actin filaments via its downstream effector α-actinin [40]. In MSCs, inhibition of ROCK has been shown to increase cell motility, an effect which is increased in presence of the RhoA activator lysophosphatidic acid (LPA) [41]. In fibroblasts, equivalent stiffening to that induced by TCM was found by inhibition of ROCK before RhoA activation [39]. Moreover, this increase in elastic character is in good agreement with *in vitro* experiments analyzing actin polymerization and crosslinking dynamics [42]. A simplified schematic of this process can be seen in Figure 3-12.

Transwell migration assays further illustrated how crucial this stiffening was for chemotaxis, as significant migration to TCM over control media was not achieved until

the time point after cells had transitioned to a primarily elastic phenotype (Figure 3-10B). Additionally, *in vitro* migration assays show that even a one hour exposure to TCM increases MSC migration. Since soluble factors mediate cell migration by interacting with cell surface receptors that require much longer synthesis and transport times [43], these results suggest a novel 'mechanical priming' achieved by short-term TCM preconditioning.

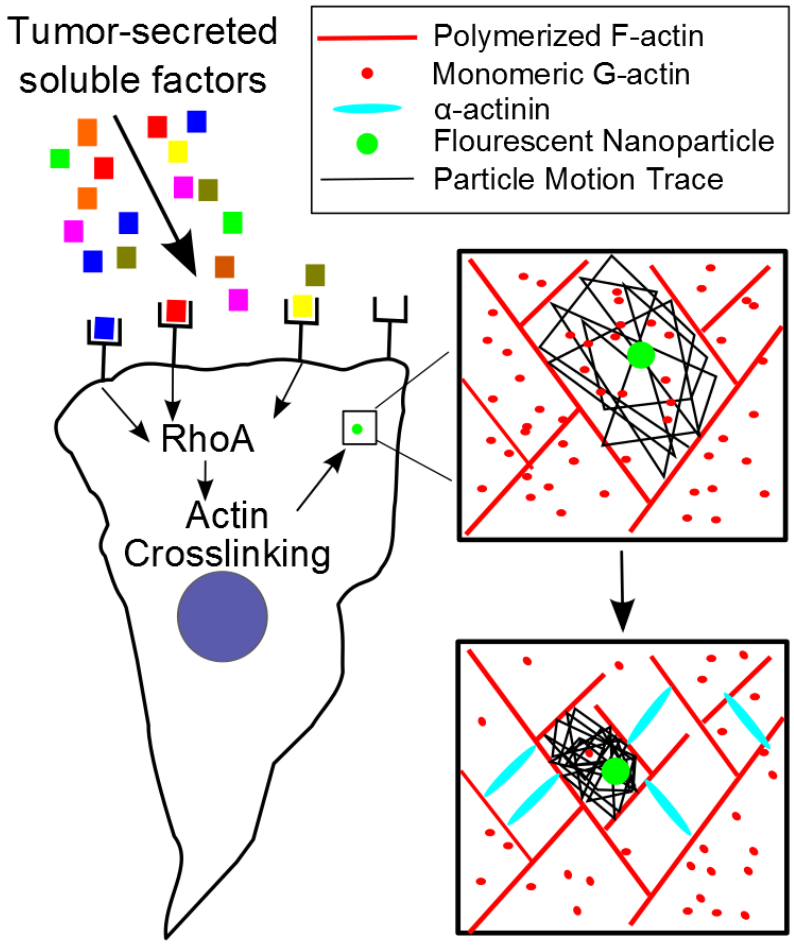

Figure 3-12. *A simplified diagram of short-term response of cells to treatment with TCM by actin polymerization and crosslinking.*

Initially, the morphology of fibroblasts and MSCs was similar; however, after prolonged TCM treatment, MSCs acquired an elongated spindle-shape morphology, and 3T3 and primary fibroblasts maintained their original shape (Figure 3-3C–F). This morphological change in MSCs coincided with the extension of linear actin filaments and microtubules (Figure 3-4). These changes further support the importance of RhoA, as activation of Rho effector mDia1 induces cell elongation coupled with parallel alignment of linear actin and microtubules [44].

The prolonged exposure of MSCs to TCM also resulted in visible loss of stress fibers (Figure 3-5B) and focal adhesions (Figure 3-6, Figure 3-7). These changes correlate with increased expression of Cdc42, which can block Rho-induced focal adhesions and stress fibers [45]. Furthermore, Cdc42 is crucial in cell elongation processes, such as neurite outgrowth [46]. ANOVA revealed that only Cdc42 shows a significant interaction effect between cell type and treatment, suggesting it is a primary contributor to the long-term differences.

Two unique obstacles in MSC homing as compared to fibroblasts include extravasation from the bone marrow to enter circulation and intravasation into the site of inflammation [47]. The differential cellular elongation could aid as cells squeeze through the basement membrane. Since undifferentiated MSCs have a more deformable nucleus, they are better suited for this task [48]. Our results indicate that MSC nuclei elongate in response to TCM (Figure 3-5C). The up-regulation of Cdc42 may also prove beneficial in this process, as it is critical for nuclear translocation [49].

These results elucidate a fundamental difference in the recruitment of fibroblasts and MSCs to tumors by utilizing a unique set of mechanical changes to overcome their

extensive physiological barriers. Furthermore, this new knowledge may be used in the development of novel therapeutics. Understanding the mechanisms of MSC homing can be used for more successful tumor targeting. Further studies can be focused on discovering the complex interactions of Rho GTPases and their effectors which modulate these cell-specific mechanical changes.

3.5. CONCLUSIONS

Tumor cells recruit both MSCs and fibroblasts to the tumor microenvironment by secreting pro-migratory soluble factors. Both these cell types have been investigated as a drug delivery vehicle to transport anti-cancer therapeutics to the tumor milieu. This study indicates that MSCs are more rapidly responsive to tumor secreted soluble factors leading dramatic changes in cell shape and rheology, and increased directed migration. This study suggests that MSCs may be more efficient tool for cell based cancer therapeutics compared to fibroblasts.

3.6. REFERENCES

1. Balkwill F and A Mantovani. (2001). Inflammation and cancer: back to Virchow? Lancet 357:539-545.

2. Hanahan D and RA Weinberg. (2011). Hallmarks of cancer: the next generation. Cell 144:646-74.

3. Covas DT, RA Panepucci, AM Fontes, WA Silva Jr, MD Orellana, MCC Freitas, L Neder, ARD Santos, LC Peres, MC Jamur and MA Zago. (2008). Multipotent mesenchymal stromal cells obtained from diverse human tissues share functional properties and gene-expression profile with CD146+ perivascular cells and fibroblasts. Exp Hematol 36:642-654.

4. Haniffa MA, X-N Wang, U Holtick, M Rae, JD Isaacs, AM Dickinson, CMU Hilkens and MP Collin. (2007). Adult Human Fibroblasts Are Potent Immunoregulatory Cells and Functionally Equivalent to Mesenchymal Stem Cells. The Journal of Immunology 179:1595-1604.

5. Stagg J. (2008). Mesenchymal stem cells in cancer. Stem Cell Rev 4:119-24.

6. Song S, AJ Ewald, W Stallcup, Z Werb and G Bergers. (2005). PDGFRbeta+ perivascular progenitor cells in tumours regulate pericyte differentiation and vascular survival. Nat Cell Biol 7:870-9.

7. Karnoub AE, AB Dash, AP Vo, A Sullivan, MW Brooks, GW Bell, AL Richardson, K Polyak, R Tubo and RA Weinberg. (2007). Mesenchymal stem cells within tumour stroma promote breast cancer metastasis. Nature 449:557-63.

8. Orimo A, PB Gupta, DC Sgroi, F Arenzana-Seisdedos, T Delaunay, R Naeem, VJ Carey, AL Richardson and RA Weinberg. (2005). Stromal Fibroblasts Present in Invasive Human Breast Carcinomas Promote Tumor Growth and Angiogenesis through Elevated SDF-1/CXCL12 Secretion. Cell 121:335-348.

9. Micke P and A tman. (2004). Tumour-stroma interaction: cancer-associated fibroblasts as novel targets in anti-cancer therapy? Lung Cancer 45, Supplement 2:S163-S175.

10. Hall B, M Andreeff and F Marini. (2007). The Participation of Mesenchymal Stem Cells in Tumor Stroma Formation and Their Application as Targeted-Gene Delivery Vehicles. In: *Bone Marrow-Derived Progenitors*. Kauser K and A-M Zeiher eds. Springer Berlin Heidelberg. pp 263-283.

11. Kucerova L, V Altanerova, M Matuskova, S Tyciakova and C Altaner. (2007). Adipose Tissue–Derived Human Mesenchymal Stem Cells Mediated Prodrug Cancer Gene Therapy. Cancer Research 67:6304-6313.

12. Rønnov-Jessen L, OW Petersen, VE Koteliansky and MJ Bissell. (1995). The origin of the myofibroblasts in breast cancer. Recapitulation of tumor environment in culture unravels diversity and implicates converted fibroblasts and recruited smooth muscle cells. The Journal of Clinical Investigation 95:859-873.

13. Studeny M, FC Marini, RE Champlin, C Zompetta, IJ Fidler and M Andreeff. (2002). Bone marrow-derived mesenchymal stem cells as vehicles for interferon-beta delivery into tumors. Cancer Res 62:3603-8.

14. Hung SC, WP Deng, WK Yang, RS Liu, CC Lee, TC Su, RJ Lin, DM Yang, CW Chang, WH Chen, HJ Wei and JG Gelovani. (2005). Mesenchymal stem cell targeting of microscopic tumors and tumor stroma development monitored by noninvasive *in vivo* positron emission tomography imaging. Clin Cancer Res 11:7749-56.

15. Komarova S, Y Kawakami, MA Stoff-Khalili, DT Curiel and L Pereboeva. (2006). Mesenchymal progenitor cells as cellular vehicles for delivery of oncolytic adenoviruses. Mol Cancer Ther 5:755-66.

16. Nakamura K, Y Ito, Y Kawano, K Kurozumi, M Kobune, H Tsuda, A Bizen, O Honmou, Y Niitsu and H Hamada. (2004). Antitumor effect of genetically engineered mesenchymal stem cells in a rat glioma model. Gene Ther 11:1155-64.

17. Khakoo AY, S Pati, SA Anderson, W Reid, MF Elshal, Rovira, II, AT Nguyen, D Malide, CA Combs, G Hall, J Zhang, M Raffeld, TB Rogers, W Stetler-Stevenson, JA Frank, M Reitz and T Finkel. (2006). Human mesenchymal stem cells exert potent antitumorigenic effects in a model of Kaposi's sarcoma. J Exp Med 203:1235-47.

18. Rombouts WJC and RE Ploemacher. (2003). Primary murine MSC show highly efficient homing to the bone marrow but lose homing ability following culture. Leukemia 17:160-170.

19. Dwyer RM, SM Potter-Beirne, KA Harrington, AJ Lowery, E Hennessy, JM Murphy, FP Barry, T O'Brien and MJ Kerin. (2007). Monocyte chemotactic protein-1 secreted by primary breast tumors stimulates migration of mesenchymal stem cells. Clin Cancer Res 13:5020-7.

20. Kumar S, TR Nagy and S Ponnazhagan. (2010). Therapeutic potential of genetically modified adult stem cells for osteopenia. Gene Ther 17:105-16.

21. Rosova I, M Dao, B Capoccia, D Link and JA Nolta. (2008). Hypoxic preconditioning results in increased motility and improved therapeutic potential of human mesenchymal stem cells. Stem cells 26:2173-82.

22. Ohnishi S, T Yasuda, S Kitamura and N Nagaya. (2007). Effect of Hypoxia on Gene Expression of Bone Marrow-Derived Mesenchymal Stem Cells and Mononuclear Cells. Stem Cells 25:1166-1177.

23. Ponte AL, E Marais, N Gallay, A Langonné, B Delorme, O Hérault, P Charbord and J Domenech. (2007). The *In vitro* Migration Capacity of Human Bone Marrow Mesenchymal Stem Cells: Comparison of Chemokine and Growth Factor Chemotactic Activities. Stem cells 25:1737-1745.

24. Ozaki Y, M Nishimura, K Sekiya, F Suehiro, M Kanawa, H Nikawa, T Hamada and Y Kato. (2007). Comprehensive Analysis of Chemotactic Factors for Bone Marrow Mesenchymal Stem Cells. Stem Cells and Development 16:119-130.

25. Tseng Y, TP Kole and D Wirtz. (2002). Micromechanical mapping of live cells by multiple-particle-tracking microrheology. Biophys J 83:3162-76.

26. Wirtz D. (2009). Particle-Tracking Microrheology of Living Cells: Principles and Applications. Annual Review of Biophysics 38:301-326.

27. Peister A, JA Mellad, BL Larson, BM Hall, LF Gibson and DJ Prockop. (2004). Adult stem cells from bone marrow (MSCs) isolated from different strains of inbred mice vary in surface epitopes, rates of proliferation, and differentiation potential. Blood 103:1662-8.

28. Menon LG, S Picinich, R Koneru, H Gao, SY Lin, M Koneru, P Mayer-Kuckuk, J Glod and D Banerjee. (2007). Differential Gene Expression Associated with Migration of Mesenchymal Stem Cells to Conditioned Medium from Tumor Cells or Bone Marrow Cells. Stem cells 25:520-528.

29. Lin S-Y, J Yang, AD Everett, CV Clevenger, M Koneru, PJ Mishra, B Kamen, D Banerjee and J Glod. (2008). The isolation of novel mesenchymal stromal cell chemotactic factors from the conditioned medium of tumor cells. Experimental Cell Research 314:3107-3117.

30. Klopp AH, EL Spaeth, JL Dembinski, WA Woodward, A Munshi, RE Meyn, JD Cox, M Andreeff and FC Marini. (2007). Tumor irradiation increases the recruitment of circulating mesenchymal stem cells into the tumor microenvironment. Cancer Res 67:11687-95.

31. Yang J, SA Mani, JL Donaher, S Ramaswamy, RA Itzykson, C Come, P Savagner, I Gitelman, A Richardson and RA Weinberg. (2004). Twist, a Master Regulator of Morphogenesis, Plays an Essential Role in Tumor Metastasis. Cell 117:927-939.

32. Tao K, M Fang, J Alroy and GG Sahagian. (2008). Imagable 4T1 model for the study of late stage breast cancer. BMC Cancer 8:228.

33. Pigati L, SCS Yaddanapudi, R Iyengar, D-J Kim, SA Hearn, D Danforth, ML Hastings and DM Duelli. (2010). Selective Release of MicroRNA Species from Normal and Malignant Mammary Epithelial Cells. PloS one 5:e13515.

34. Coussens LM and Z Werb. (2002). Inflammation and cancer. Nature 420:860-7.

35. Kole TP, Y Tseng, I Jiang, JL Katz and D Wirtz. (2005). Intracellular mechanics of migrating fibroblasts. Mol Biol Cell 16:328-38.

36. Ponte AL, E Marais, N Gallay, A Langonne, B Delorme, O Herault, P Charbord and J Domenech. (2007). The *in vitro* migration capacity of human bone marrow mesenchymal stem cells: comparison of chemokine and growth factor chemotactic activities. Stem Cells 25:1737-45.

37. Kim S, H Takahashi, WW Lin, P Descargues, S Grivennikov, Y Kim, JL Luo and M Karin. (2009). Carcinoma-produced factors activate myeloid cells through TLR2 to stimulate metastasis. Nature 457:102-6.

38. Wels J, RN Kaplan, S Rafii and D Lyden. (2008). Migratory neighbors and distant invaders: tumor-associated niche cells. Genes Dev 22:559-74.

39. Kole TP, Y Tseng, L Huang, JL Katz and D Wirtz. (2004). Rho kinase regulates the intracellular micromechanical response of adherent cells to rho activation. Mol Biol Cell 15:3475-84.

40. Maesaki R, K Ihara, T Shimizu, S Kuroda, K Kaibuchi and T Hakoshima. (1999). The Structural Basis of Rho Effector Recognition Revealed by the Crystal Structure of Human RhoA Complexed with the Effector Domain of PKN/PRK1. Molecular Cell 4:793-803.

41. Jaganathan BG, B Ruester, L Dressel, S Stein, M Grez, E Seifried and R Henschler. (2007). Rho inhibition induces migration of mesenchymal stromal cells. Stem Cells (Dayton, Ohio) 25:1966-1974.

42. Tseng Y. (2002). Microheterogeneity Controls the Rate of Gelation of Actin Filament Networks. Journal of Biological Chemistry 277:18143-18150.

43. Truskey GA, F Yuan and DF Katz. *Transport Phenomena in Biological Systems*. (2009). Pearson Educatoin, Upper Saddle River, New Jersey.

44. Ishizaki T, Y Morishima, M Okamoto, T Furuyashiki, T Kato and S Narumiya. (2001). Coordination of microtubules and the actin cytoskeleton by the Rho effector mDia1. Nat Cell Biol 3:8-14.

45. Kozma R, S Ahmed, A Best and L Lim. (1995). The Ras-related protein Cdc42Hs and bradykinin promote formation of peripheral actin microspikes and filopodia in Swiss 3T3 fibroblasts. Molecular and Cellular Biology 15:1942-52.

46. Govind S, R Kozma, M Clinton, L Lim and S Ahmed. (2001). Cdc42Hs Facilitates Cytoskeletal Reorganization and Neurite Outgrowth by Localizing the 58-kD Insulin Receptor Substrate to Filamentous Actin. The Journal of Cell Biology 152:579-594.

47. Chamberlain G, J Fox, B Ashton and J Middleton. (2007). Concise Review: Mesenchymal Stem Cells: Their Phenotype, Differentiation Capacity, Immunological Features, and Potential for Homing. Stem cells 25:2739-2749.

48. Pajerowski JD, KN Dahl, FL Zhong, PJ Sammak and DE Discher. (2007). Physical plasticity of the nucleus in stem cell differentiation. Proceedings of the National Academy of Sciences 104:15619-15624.

49. Lee JSH, MI Chang, Y Tseng and D Wirtz. (2005). Cdc42 Mediates Nucleus Movement and MTOC Polarization in Swiss 3T3 Fibroblasts under Mechanical Shear Stress. Molecular Biology of the Cell 16:871-880.

CHAPTER 4: MECHANICAL RESPONSE OF MESENCHYMAL STEM CELLS TO TRANSFORMING GROWTH FACTOR-β1 AND PLATELET DERIVED GROWTH FACTOR-BB

Mesenchymal stem cells (MSCs) play an important role in matrix remodeling, fibroblast activation, angiogenesis, and immunomodulation and are an integral part of fibrovascular networks that form in developing tissues and tumors. The engraftment and function of MSCs in tissue niches is regulated by a multitude of soluble proteins. Transforming growth factor-β1 (TGF-β1) and platelet derived growth factor-BB (PDGF-BB) have previously been recognized for their role in MSC biology; thus, we sought to investigate their function in mediating MSC mechanics. Cytoskeletal organization, characterized by cell elongation, stress fiber formation, and condensation of actin and microtubules, was dramatically affected by TGF-β1, individually and in combination with PDGF. The intracellular mechanical response to these stimuli was measured with particle tracking microrheology. MSCs stiffened in response to TGF-β1 (their elastic moduli was 9-fold higher than control cells), a result which was enhanced by the addition of PDGF (100-fold change). These findings will provide a more mechanistic insight for modeling tissue level rigidity in fibrotic tissues and tumors.

4.1. INTRODUCTION

Earlier work has shown that both murine [1] and human [2] MSCs undergo dramatic cytoskeletal stiffening in response to the cocktail of pro-migratory molecules released by tumor cells. The degree of stiffening was shown to be a key differentiating factor

between MSCs and their less migratory fibroblast counterparts [1, 3] and even predictive of decreased MSC function *in vivo* [4]. Tumor cell-conditioned media regulates MSC survival, migration, proliferation and differentiation in a paracrine fashion or by triggering the release of other soluble factors that act through autocrine signaling pathways [3, 4]. Both platelet-derived growth factor-BB (PDGF-BB) and transforming growth factor-β1 (TGF-β1) are released by tumor cells and play important roles in recruiting MSCs to target sites and influencing their growth and regenerative capacity [5-7].

This study sought to understand the mechanical and chemical response of MSCs to TGF-β1 and PDGF-BB **(referred as PDGF)**. MSCs interact with both these factors in many *in vivo* regenerative niches as well as wound tissues and tumor. *In vitro* cell mechanics studies have thus far focused on external biophysical cues [8] or combination of chemical cues to induce differentiation [9]. Examining the mechanical response of MSCs to individual factors can provide better understanding of their role as stromal cells (for example, functional role in tissue remodeling, cell recruitment) during initial stages in wound and tumor development. MSCs treated with TGF-β1 alone or in combination with PDGF exhibited dramatic elongation, condensed actin-microtubule structure and a highly elastic cytoplasm. Although this mechano-physical response was primarily in part to TGF-β1, combination of PDGF with TGF-β1 enhanced the TGF-β1 driven changes significantly.

4.2. MATERIALS AND METHODS

Materials: IMDM, DMEM, L-glutamine, penicillin-streptomycin and trypsin were purchased from Mediatech and fetal bovine serum (FBS) was purchased from Atlanta

Biologicals. Recombinant human proteins TGF-β1 and PDGF-BB and antibodies for flow cytometry experiments were purchased from Biolegend. Rhodamine-Phalloidin, FITC-conjugated mouse anti-α-tubulin, and Fluospheres carboxylate-modified 100 nm particles (F8801) were purchased from Invitrogen. All other reagents were purchased from VWR unless otherwise specified.

MSC isolation and culture: Murine MSCs were isolated from the bone marrow of 6-10 weeks old adult male Balb/C mice (Charles River Laboratories, Wilmington, MA) and cultured in normal growth media (IMDM media supplemented with 20% FBS, 2 mM L-glutamine, 100U/ml penicillin, and 100U/ml streptomycin). Briefly, tibiae and femurs of the mice were extracted and crushed in FBS. Cold PBS and collagenase I (2mg/ml) solutions were added subsequently to facilitate cell extraction from bone with minimal cell damage. Finally, the solution mixture was filtered (70 μm cell strainer) and centrifuged (1000xg for 10 minutes) to recover the bone marrow cell population in pellet form. Media was supplanted regularly to remove non-adherent BM cell populations. Once the adherent cells reached 80-90% confluency, the cell culture was expanded and subsequently purified using EasySep™ Mouse SCA1 Positive Selection Kit (StemCell Technologies). Purified MSCs between passages 2-6 were used for all studies.

Soluble factor treatment: Soluble factor dilutions were prepared in serum-free DMEM or IMDM immediately before use. Measured values of serum and plasma PDGF and TGF-β1 concentrations in mice and humans vary from 0.1-100 ng/ml [10-14], with the majority of these values being in the range of 1-10 ng/ml. This concentration range of PDGF and TGF-β1 has been used in numerous *in vitro* cell studies [15, 16]; after screening the cell response across this concentration range, 5 ng/ml of PDGF and TGF-β1

was used in our studies. All experiments were carried out with four conditions: serum-free control media, 5ng/ml PDGF, 5ng/ml TGF-β1 and combination of PDGF and TGF-β1- each 5ng/ml. MSCs were treated for 24 hours unless otherwise specified.

Morphological analysis: Cells were fixed and stained with crystal violet and imaged with stereoscope microscope and Motic camera. Cell borders were traced manually and cell shape factors, defined as $4*\pi*\text{Area}/ (\text{Perimeter})^2$, were determined using Image J.

Immunofluorescence staining: To visualize cytoskeletal proteins, MSCs were cultured and treated on glass cover-slips in 24-well plates. Twenty four hours after soluble factor treatment, cells glass cover slips were briefly extracted in a buffer containing 80 mM PIPES (pH 6.8), 1 mM MgCl2, 5 mM EDTA, and 0.5% Triton X-100 before fixation with 0.5% glutaraldehyde in PBS. The reaction was quenched with 1 mg/mL sodium borohydride, before permeabilization with Triton X-100 and blocking with normal horse serum. Cells were stained for one hour at room temperature with either 1:50 FITC-conjugated anti-tubulin, 1:200 Rhodamine Phalloidin, before sealing with Vectashield (Vector Labs) containing DAPI. Cells were imaged with an inverted Zeiss LSM 510 UV confocal microscope. Nuclear elongation factor was determined by segmenting out nuclei using Otsu's method after background subtraction, and then was defined as $4 \bullet \pi \bullet A/P^2$, where A is the area of the nucleus and P is the perimeter of the nucleus. To segment out actin stress fibers, background-subtracted images were convolved with a Laplacian of Gaussian filter to isolated fiber-like features. After segmentation, sequential image dilation and erosion using a linear structuring element with varying degrees of rotation was used to join any disconnected stress fibers and erode any small regions produced by

image noise. All image analysis was performed in custom-written MATLAB algorithms [1].

Live-Cell Microrheology: Intracellular mechanical properties of living cells were determined by multiple particle tracking microrheology (MPTM), as previously described [3,4]. Briefly, 100 nm probe particles were injected into the cytosol of MSCs using PDS-1000 Biolistic Helium Particle Injection System (Biorad). The thermal motions of these probes are directly related to the local rheological properties via the Stokes-Einstein equation. High spatiotemporal resolution videos of injected cells were collected with a Nikon CFI Apochromat TIRF 100X oil-immersion lens (NA=1.49) on a Nikon Eclipse Ti inverted epifluorescent microscope maintained at 37° C and 5% carbon dioxide. A custom MPT routine incorporated in the MetaMorph software (Molecular Devices; Downington, PA) was then used to simultaneously monitor the coordinates of 5-20 particles per video. For each condition, particles were tracked in a minimum of 10 cells per condition. Time-dependent individual particle mean square displacements (MSDs) were ensemble-averaged and used to determine the average frequency dependent elastic moduli (G'), viscous moduli (G'') and phase angle (δ), which were reported in this study.

Flow cytometry: MSCs were analyzed with a BD LSR-II flow cytometer to capture the effects of soluble factor treatment on cell surface markers. Briefly, both treated and untreated cells were detached from 10 cm dishes, centrifuged, and suspended in 100 µl cold FACS buffer (2% FBS, 1mM EDTA in PBS). Cells were then incubated with APC-CD140b/PDGFR-β (1:20). To quantify PDGFR-β expression after 1 hour, cells were primarily incubated with biotin conjugated anti-mouse CD140b and subsequently stained

with DyLight™ 488 streptavidin. All studies were performed in triplicate with at least n = 50,000 events per sample.

Inhibition studies: SB-505124 and JNJ-10198409 (Sigma, USA) were used to inhibit TGF-β1 and PDGF signaling, respectively. These chemicals bind to their corresponding cell surface receptors and block signaling pathways. Concentrations were determined from literature review and titration studies, which were used to identify maximum concentration associated with non-significant viable cell loss. These initial concentration ranges have previously been used to inhibit TGF-β1 dependent migration [17] and differentiation [18] of MSCs and PDGFR-β dependent kinase activity in NIH 3T3 [19] and proliferation in tumor cells [19, 20]. For all studies, MSCs were treated with 1uM SB-505124 and/or 50 nM JNJ-10198409 for one hour prior to soluble factor treatment.

Reverse transcription polymerase chain reaction (RT-PCR): RNA was isolated from treated cells using RiboZol RNA extraction reaction, and cDNA was synthesized by reverse transcription using the i-Script cDNA synthesis kit (BioRad). Primers were designed using NCBI primer-blast (http://www.ncbi.nlm.nih.gov/tools/primer-blast/) and PrimerBank (http://pga.mgh.harvard.edu/primerbank/). All primer sequences are listed in Appendix A (Table A-1). Polymerase chain reactions (PCR) were carried out to amplify gene sequences as per manufacturer's recommendation for Promega PCR reaction kit. Gel electrophoresis was performed with 2% (w/v) agarose gel to visualize amplified DNA. All values are normalized to endogenous control 18sRNA.

Statistics: Each experiment was performed with 3 or more replicates, and all values expressed as the mean ± s.e.m. One way Anova test with repeated measures was used to determine statistical significance of experiments involving four groups. For comparison

between groups, Tukey's HSD post-test was used. Significance was reported as * (for $p<0.05$), ** (for $p<0.005$) and *** (for $p<0.0005$).

4.3. RESULTS

MSCs respond mechanically to TGF-β1 and PDGF treatment: MPTM was used to characterize the mechanical response of MSCs to soluble factors. For these studies, the intracellular rheology was characterized from the MSDs of 100 nm probe particles embedded in the cytoplasm (Figure 4-1). In control MSCs, particle MSDs varied linearly with time (Figure 4-1A), demonstrating the viscous nature of the MSC cytoplasm [1], which corresponded with viscous moduli (G") that were higher than the elastic moduli (G') for all frequencies (Figure 4-1B). After treatment with PDGF (5ng/mL), the majority of particle MSDs still varied linearly with time, indicating that the cytosol remained primarily viscous. Furthermore, the average viscous and elastic moduli of PDGF-treated cells were similar to control, although a small population of particles (approximately 5%) encountered a more elastic cytoplasm. Treatment with an equivalent amount of TGF-β1 resulted in a homogeneous particle transport response, with 100% of the embedded particles encountering a more elastic cytoplasm as evident by particle MSDs independent of time and corresponding elastic moduli higher than the viscous moduli for all frequencies. This homogeneous stiffening response was also seen in cells treated with PDGF and TGF-β1; however, combination treatment resulted in 6-fold lower MSDs compared to TGF-β1 at τ = 1s ($p<0.05$). At the corresponding frequency, the average elastic moduli of MSCs treated for 24 hours with TGF-β1 and the combination of PDGF and TGF-β1 was 9-fold and 100-fold greater than control ($p<0.05$), respectively. Further comparison of viscoelastic properties using phase angle (δ) indicated control and PDGF

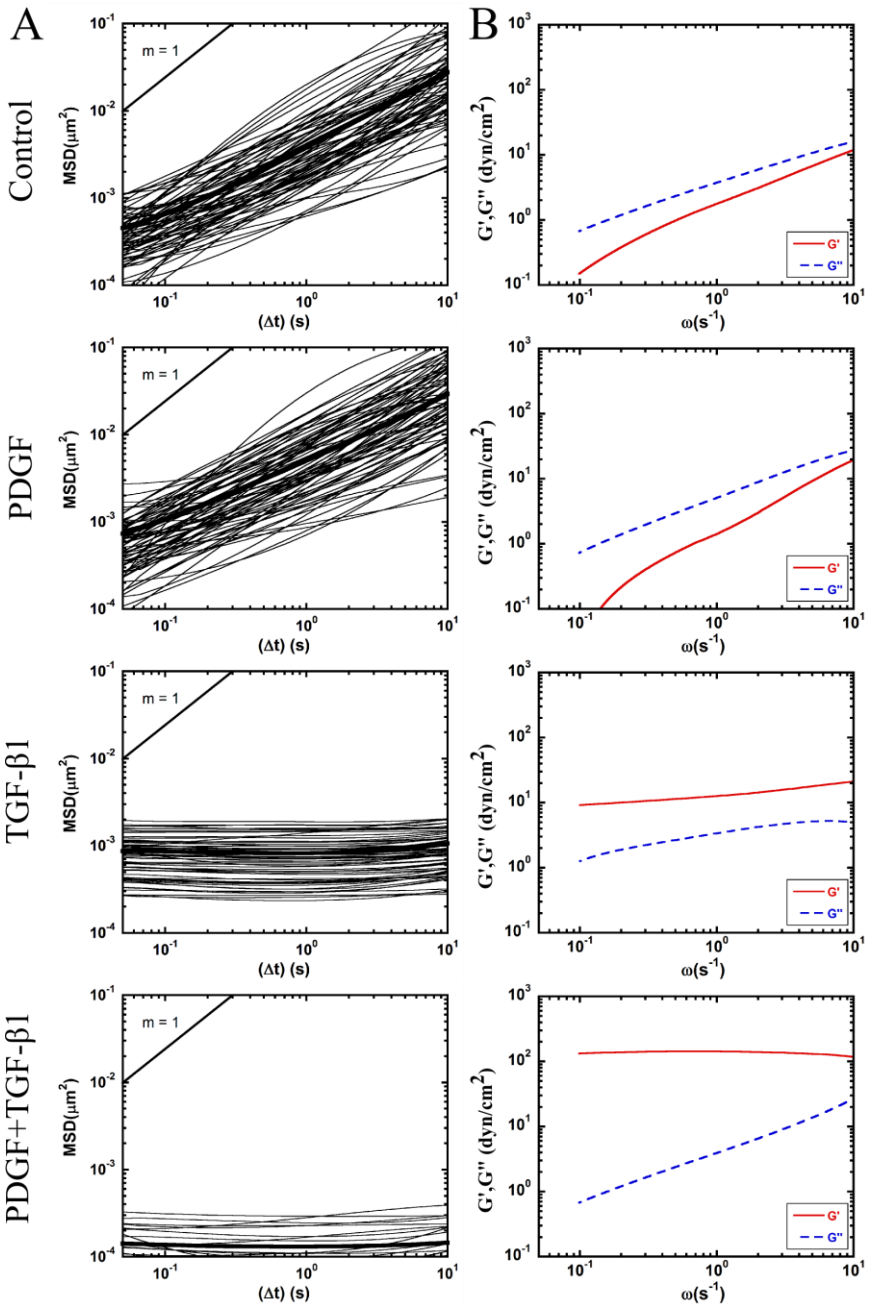

Figure 4-1. *TGF-β1 alters rheology of MSC cytosol.* (A) The ensemble averaged mean squared displacements (MSD) of 100 nm particles embedded in the cytoplasm of murine Balb/C MSCs incubated for 24 hours in control media (CM), 5ng/ml platelet derived growth factor (PDGF), 5ng/ml transforming growth factor- β1 (TGF-β1) and combination of PDGF and TGF-β1- each 5ng/ml (PDGF+TGF-β1). (B) The time-dependent ensemble averaged MSDs of 100 nm particles embedded in the cytoplasm of MSCs were converted to frequency-dependent elastic (G′) and visous (G″) moduli using a custom written algorithm for MATLAB software.

treated cells remain primarily viscous as δ remains greater than 45 degrees; whereas for TGF-β1 treated cells individually and in combination with PDGF the phase angle was well below 45 degrees, indicating the cytosol was primarily elastic (Figure 4-2).

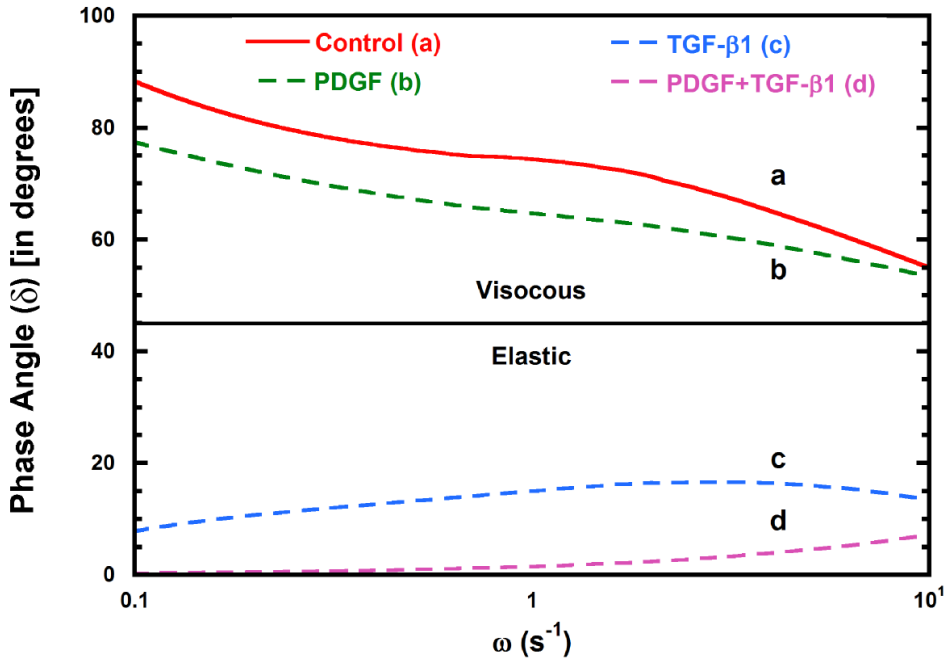

Figure 4-2. *Phase angle (δ in degrees) proportional to the ratio of viscous to elastic modulus was calculated using G' and G".* Phase angle of control and PDGF treated cells are greater than 45^0 (degrees) indicating viscous cytosol whereas for TGF-β1 treated cells individually and in combination with PDGF display phase angle well below 45^0, indicating severe cytosolic stiffening.

Effect of soluble factor treatment on MSC morphology: Since previous work has shown that MSC shape can contribute to cell stiffness [21], we stained the cells after twenty four hours with crystal violet to analyze cell morphology. In good agreement with the previous work, dramatic cell elongation was associated with TGF-β1 treatment, both individually and in combination with PDGF (Figure 4-3A). The morphological change was more quantitatively assessed using a cell shape factor (CSF) which varies from 0 for a line to 1 for a perfect circle. The CSF decreased significantly ($p<0.0005$) in response to TGF-β1 treatment alone and in combination with PDGF indicating that cells had elongated in response to these treatments (Figure 4-3B). Interestingly, PDGF alone did not alter cell morphology; however, it significantly ($p<0.0005$) enhanced the elongation effects of TGF-β1.

TGF-β1 alters cytoskeletal organization of MSCs: Next, changes in cytoskeletal organization were examined with immunofluorescence staining of microtubules (green), filamentous actin (red), and nuclei (blue) (Figure 4-4A). Confocal images revealed condensed and elongated microtubules and actin filaments in cells treated with TGF-β1 alone or in combination with PDGF. Cells treated with TGF-β1 alone were also arranged in a parallel structure, which was somewhat disrupted in combination treatment. For combination treatment condition, the nuclear shape factor (NSF), which is the nuclear equivalent of CSF, was reduced significantly ($p<0.0005$), indicating that nuclei had elongated (Figure 4-5A) which may be required for navigating narrow pores within the ECM [1]. The actin stress fiber density, which measures the density of bundled actin filaments relative to cell area, was significantly ($p<0.05$) higher in MSCs treated with TGF-β1 alone or in combination with PDGF (Figure 4-5B).

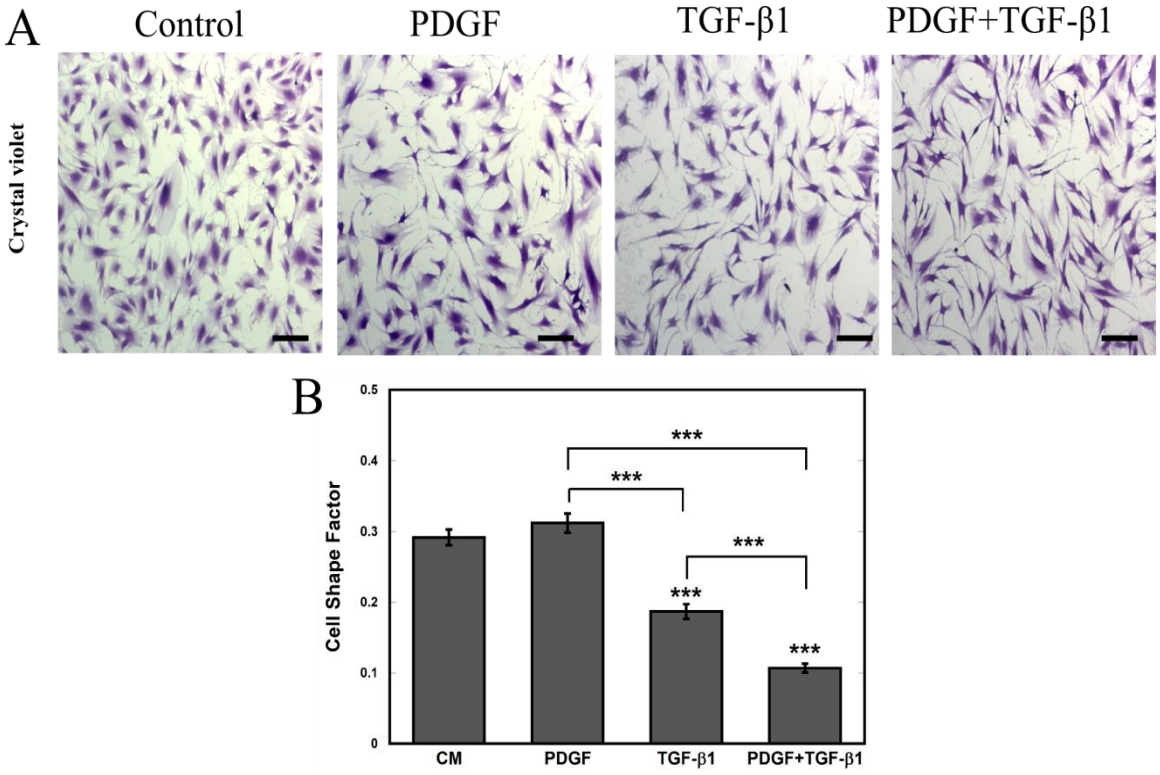

Figure 4-3. *MSCs elongate dramatically in response to TGF-β1***.** (A) Brightfield images of soluble factor-treated MSCs after 24 hours stained with crystal violet. MSCs elongated dramatically in response to TGF-β1 individually and in combination with PDGF; whereas, MSCs did not respond to PDGF treatment alone (scale bar: 100μm). (B) Cell shape factor (CSF) was determined by analysis of bright field images with image J. CSF was used to characterize the elongation of the cell, with a shape factor of 1 indicating a perfect circle and 0 indicating a straight line. Results are reported as average ± s.e.m. (n=3).

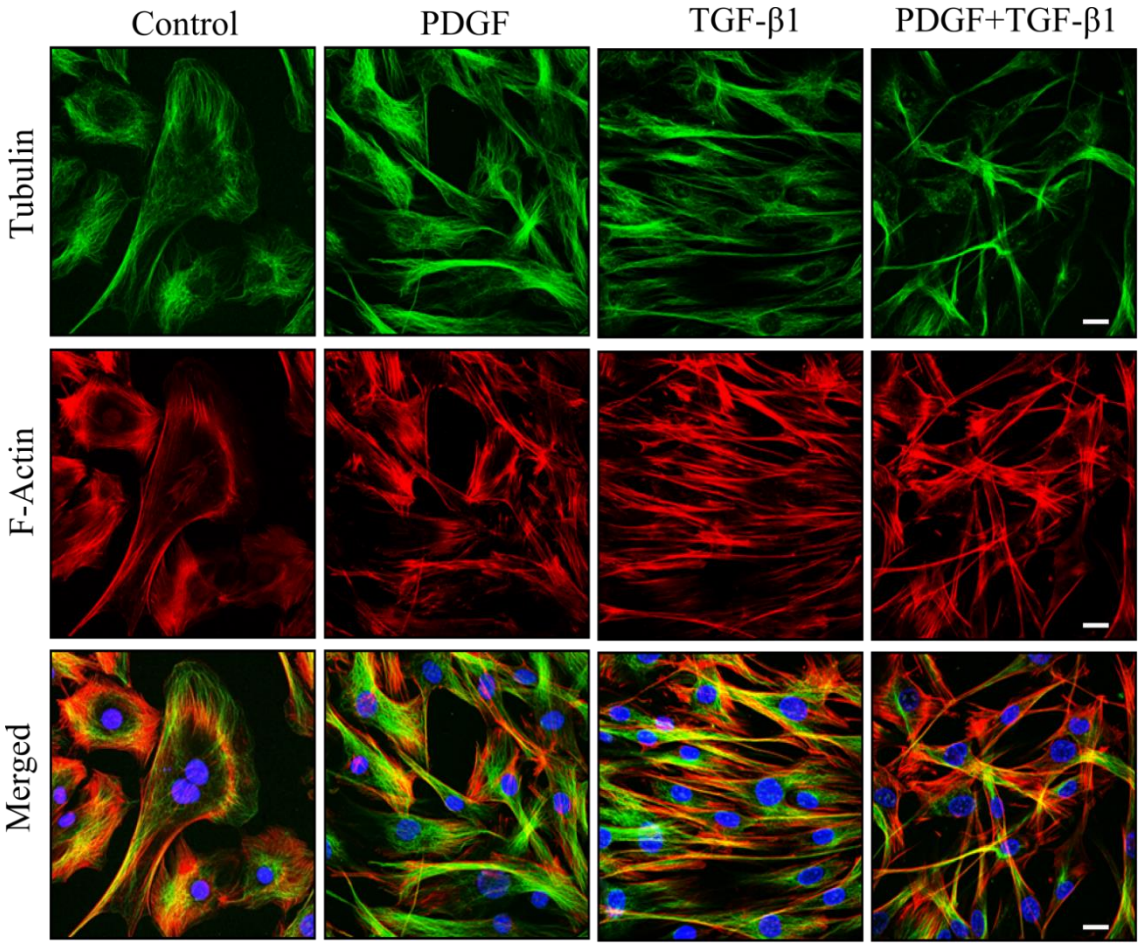

Figure 4-4. *MSCs reorganize their cytoskeleton in response to TGF-β1 after 24 hours.* (A) Confocal images of soluble factor-treated MSCs stained with Phalloidin (F-actin, red), anti-α-tubulin (microtubules, green), and DAPI (nucleus, blue). The shape and cytoskeletal organization of CM and PDGF-treated MSCs were similar; whereas, TGF-β1 with or without PDGF treated MSCs were elongated with condensed cytoskeletal filaments (scale bar: 20μm).

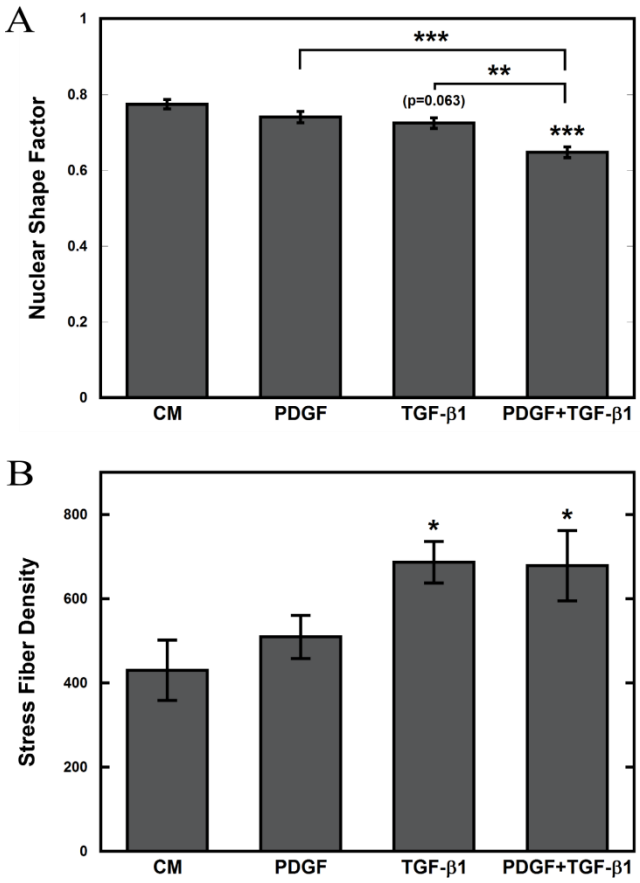

Figure 4-5. *Cytoskeletal parameters (A) nuclear shape factors and (B) stress fiber density were determined by analysis of confocal images with custom MATLAB routine.* (A) The nuclear shape factors were used to characterize the elongation of the nucleus, with a shape factor of 1 indicating a perfect circle and 0 indicating a straight line respectively. (B) The stress fiber density was used to characterize the density of actin stress fibers per cell area. Cytoskeletal changes observed in TGF-β1-treated (with or without PDGF) MSCs were confirmed using the cytoskeletal parameters, which indicated reductions in cell and nuclear shape factors and increase in stress fiber densities. Results are reported as average ± s.e.m. (n=3).

Both PDGF and TGF-β1 signaling are essential for cellular stiffening: TGF-β1 profoundly influenced the morphology, cytoskeletal structure, mechanical stiffness of MSCs. Although the individual effects of PDGF on these aspects were not always identifiable, the addition of PDGF to TGF-β1 treatment amplified these cellular responses, indicating possible interaction between these two signaling pathways. To begin to understand this interaction, flow cytometry analysis was performed to analyze the surface expression of PDGFR-β in all four conditions (Figure 4-6A-C). Though the percentage of positive cells (PPC) was only decreased for conditions containing PDGF (Figure 4-6B), mean fluorescence intensity (MFI) was significantly ($p<0.005$) decreased for all three treatments indicating that TGF-β1 treatment also results in reduced binding sites for PDGF ligand (Figure 4-6C). Additional studies suggest that this decrease in MFI was not due to a decrease in PDGFR-β surface expression, but increased binding of PDGF to its receptor blocking the antibody binding. Incubation with PDGF at short time scales (~1hour) revealed a rapid decrease in PDGFR MFI before changes in receptor levels from altered gene expression would be able to occur, suggesting the decrease is due to increased levels of bound PDGF (Figure 4.7A-C). This result inferred that the cells treated with TGF-β1 alone were also experiencing increased levels of PDGF signaling through the activation of autocrine PDGF signaling loop.

To better elucidate the roles of PDGF and TGF-β1 signaling on mechanical stiffening, we decoupled these interactions with small molecule inhibitors JNJ-10198409 and SB-505124 in tandem with soluble factor treatment. SB-505124 binds to intracellular domain of TGF-βR type I (ALK4, ALK5 and ALK7) and stops phosphorylation of SMADs to inhibit downstream TGF-β1 signaling [22]. JNJ-10198409 is a selective

PDGFR-β kinase inhibitor, which blocks downstream PDGF signaling [23]. We chose the concentration of each inhibitor (JNJ-10198409-50nM; SB-505124-1μM) based on 24 hour viability given a range of inhibitor concentrations. MSCs incubated for one hour with SB-505124 prior to treatment with TGF-β1 alone or in combination with PDGF maintained their viscous cytosolic property similar to that of control MSCs (Fig 4-8). More interestingly, JNJ-10198409 incubation completely prevented both TGF-β1 and combination of PDGF and TGF-β1 induced stiffening (Figure 4-8). These results suggest an integral role of the PDGFR-β signaling pathway in regulating TGF-β1 induced cell stiffening.

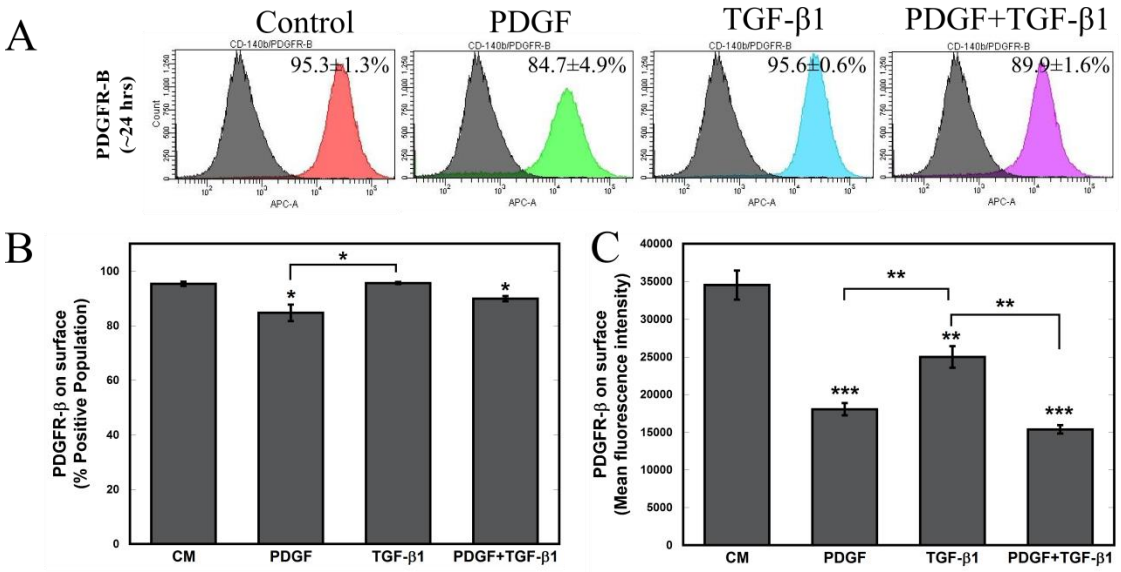

Figure 4-6. *Role of PDGFR-β in TGF-β1 signaling.* (A) Flow cytometric analysis of surface PDGFR-β expression on MSCs in response to soluble factor treatment at 24 hours. (B-C) Percent positive population and mean fluorescence intensity of treated cells were calculated from FACS-DIVA. PDGF and combination of PDGF and TGF-β1 resulted in reduced available surface receptors after 24 hours; TGF-β1 treatment also reduced available PDGFR-β. Results are reported as average ± s.e.m. (n=3).

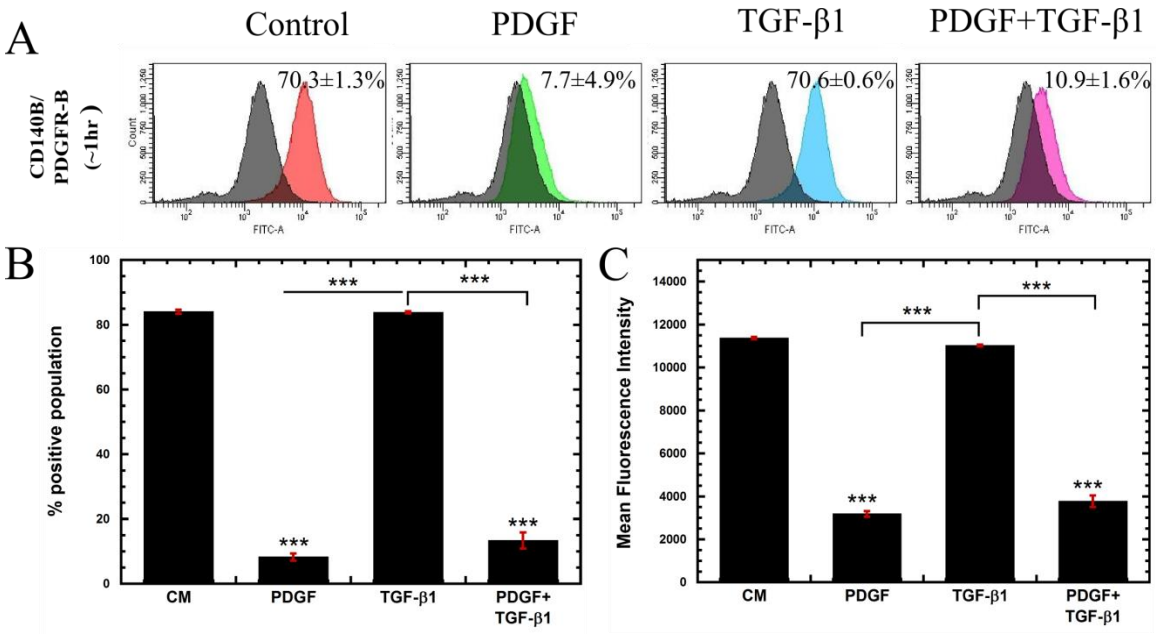

Figure 4-7. *TGF-β1 does not interact with PDGFR-β at short time scales* (A) Histograms of soluble factor MSCs from flow cytometry for PDGFR-β (after 1 hour). Gated percent positive population of MSCs compared to the negative population (black histogram) is indicated as mean±s.e.m. (B) PPC and (C) MFI calculated for CD140b/PDGFR-β after 1hour. Results are reported as average ± s.e.m. (n=3).

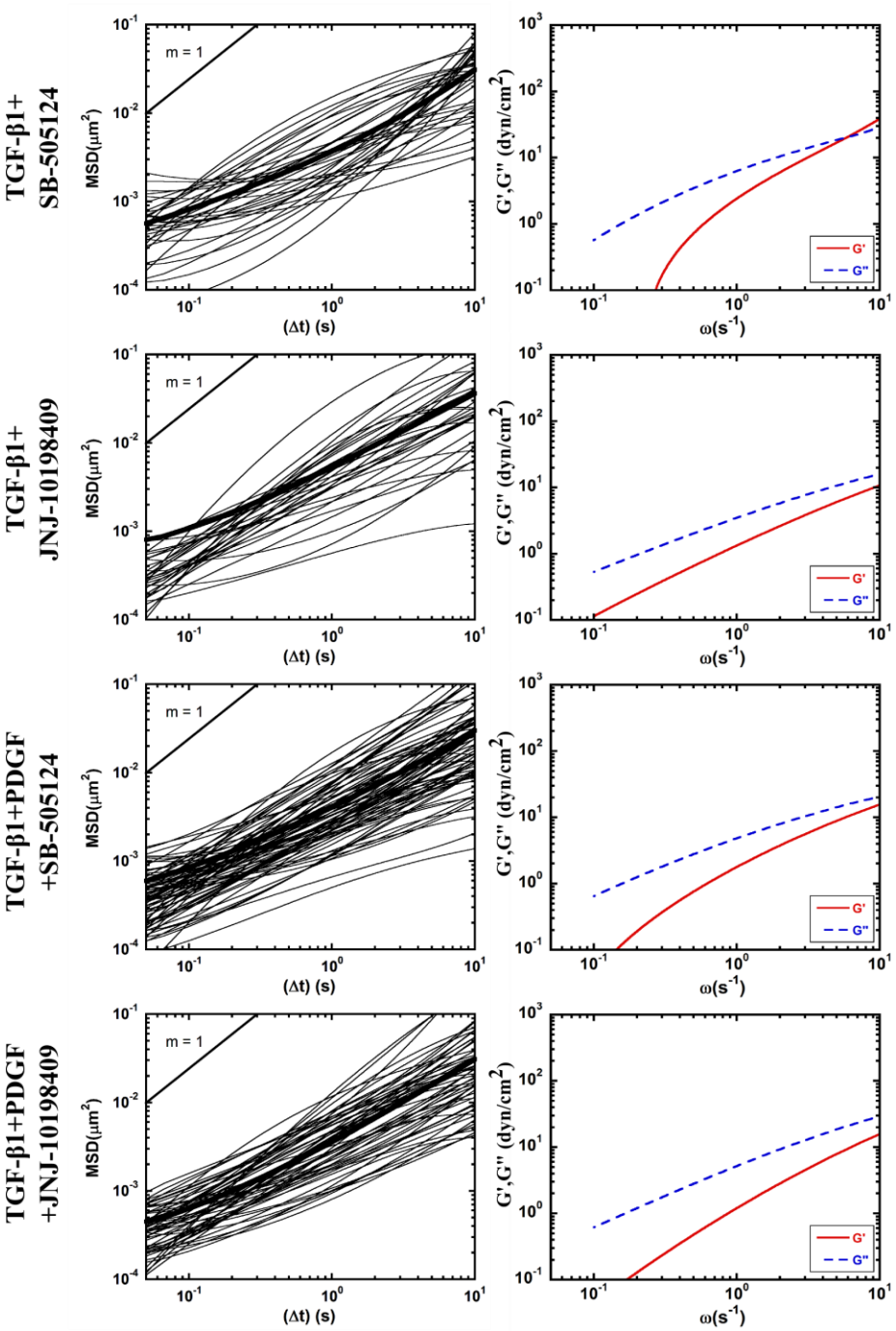

Figure 4-8. *PDGFR-β inhibitor reverses TGF-β1 mediated mechanical response.* Effect of small molecule chemical inhibitors SB-505124 (blocks TGF-βRI mediated signaling) and JNJ-10198409 (inhibits PDGFR-β mediated signaling) on the viscoelastic properties of soluble factor-treated MSCs were evaluated after 24 hours. The average mean squared displacements of 100 nm particles embedded in the cytoplasm of cells and frequency-dependent elastic (G') and viscous (G") moduli of inhibitor treated MSCs were similar to the control cells.

TGF-β1 regulates cellular stiffness and morphology via close control of actin-binding proteins: The structure and function of cytoskeletal actin is controlled by actin-binding proteins (ABPs) [24,25], which bind to actin filaments and modulate their length, stability, and cytoskeletal attachments. With the high impact of TGF-β1 on cytoskeletal structure, its effects on subset of ABPs were assessed using RT-PCR analysis. We investigated the effects of soluble factor treatment on 5 different genes belonging to the ABP family. Tensin, a scaffolding protein that connects the actin cytoskeleton to the membrane via focal adhesion complexes has shown actin-bundling activity. *Tensin-1* (*Tns1*) was upregulated in a TGF-β1 dependent manner in MSCs (Figure 4-9, 4-10) and treatment with SB-505124 (TGF-βRI inhibitor) but not JNJ10198409 (PDGFR-β inhibitor) abrogated the positive response. We also found very similar response for troponin-t2 (*Tnnt2*) which interacts with stabilizing protein tropomyosin (stabilizes actin bundles by protecting them from ADF/cofilin) to regulate the interaction of actin and myosin. Bundling and crosslinking proteins regulate cell tension through close association with actin stress fibers and the gene for bundling protein α-actinin-1 (*Actn1*) was upregulated in TGF-β1 treated cells. Interestingly, the positive regulation of this actin crosslinking gene was dependent on both PDGF and TGF-β1 signaling pathway because both SB-505124 and JNJ-1019409 inhibited the gene upregulation. Finally, we examined the effect of soluble factor treatments on the expression of *ezrin (Ezr) and moesin* (*Msn*) that belongs to ERM family of membrane anchoring proteins which tether intracellular actin domains to cell membrane. *Msn*, which directly regulates cortical rigidity in dividing cells, was up-regulated in TGF-β1 treated cells; however, *Ezr*

expression was downregulated. These regulation patterns of ERM proteins are in agreement with previous studies with TGF-β1 treated epithelial cells [26].

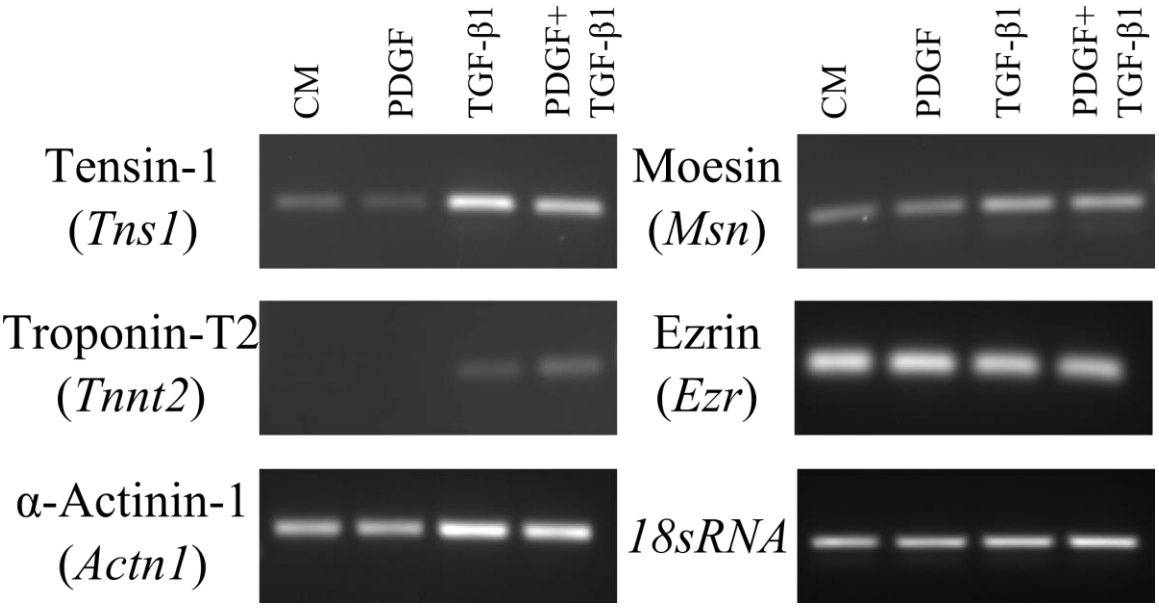

Figure 4-9. *TGF-β1 closely regulates ABPs.* (A) PCR amplified gene expression of actin-binding proteins were confirmed using 2% (w/v) agarose gel. Four lanes are corresponding to CM, PDGF, TGF-β1 and the combination of PDGF and TGF-β1 (from left to right). *Tensin-1 (Tns-1), troponin t2 (Tnnt2), moesin (Msn), and α-actinin-1 (Actn1)* were all upregulated; whereas, *ezrin* (*Ezr)* was downregulated. 18s RNA was used as control.

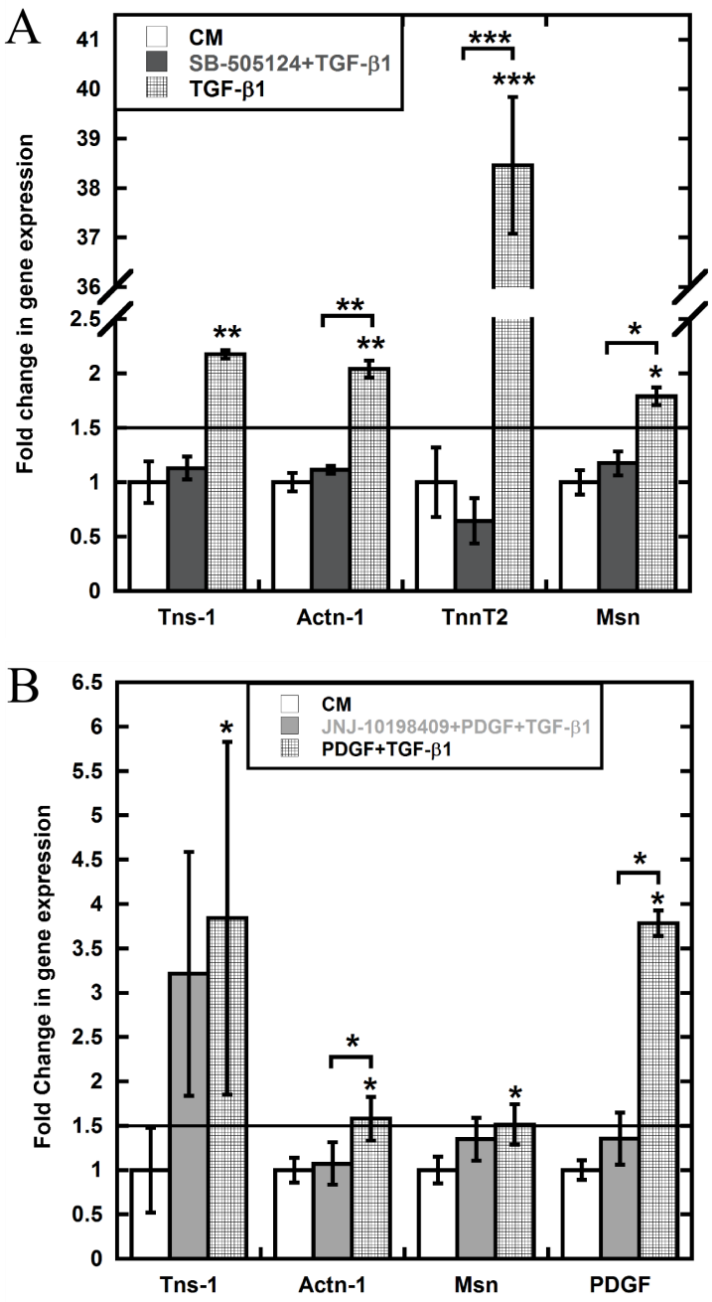

Figure 4-10. *PDGF signaling influences TGF-β1 mediated mechanical stiffening.* (A) SB-505124 blocked the upregulation of TGF-β1 mediated expression of actin-binding proteins *tensin-1 (Tns-1), α-actinin-1 (Actn1), troponin T2 (Tnnt2) and moesin (Msn)* compared to control after 24 hours. (B) JNJ-10198409 selectively blocked *Actn1* and p*dgfb* gene activation in PDGF and TGF-β1 treated cells compared to control. Gene expression was normalized using 18sRNA as internal control. Results are reported as average ± s.e.m. (n=3).

4.4. DISCUSSIONS

MSCs are highly proliferative adult stem cells that are involved in wound healing and tissue regeneration [27]. They have been shown to change their mechanical properties both during differentiation [9] as well as recruitment to sites of inflammation such as wound sites and tumor tissue [27]. Though soluble factors are critical for both of these processes [28,29], little is known about the effects of individual growth factors on the intracellular mechanical properties of MSCs. In this study, we investigated changes in mechanical properties, including intracellular rheology, cytoskeletal organization, as well as molecular pathways differentially regulated by 24-hour treatment with PDGF and/or TGF-β1.

The cytoskeleton that underlies cell rheological properties is a network of highly heterogeneous and dynamic filamentous proteins that not only provide the cell with structural support but also actively rearrange to permit motility. Alterations in morphology and cytoskeletal have been correlated with changes in the intracellular mechanical properties [1]. Particle-tracking methods probe the local viscoelastic nature of the cell, which is determined from the transport rates of particles embedded in cytoplasm. Particle tracking has been used *in vitro* to characterize the mechanical properties of networks of reconstituted cytoskeletal proteins [30,31] and *in vivo* to probe the dynamic mechanical properties of filamentous proteins in the cell cytoskeleton [32]. Kole *et al.* previously found that Swiss 3T3 fibroblasts migrating at the edge of a scratch wound assay undergo heterogeneous stiffening response, characterized by increased rigidity of cortical actin, to PDGF treatment [3].

Multiple particle tracking microrheology was used in this study to determine the effects of TGF-β1 and PDGF on the microscopic mechanical properties of MSCs (Figure 4-1). MSCs underwent a homogenous stiffening response to TGF-β1 treatment with the cytoplasm transforming into an elastic solid. The average MSD was used to determine the elastic moduli at $\omega=1\ s^{-1}$and treatment with TGF-β1 resulted in 9-fold increased rigidity (Figure 4-1, Table 4-1). This homogeneous stiffening response was also seen in PDGF and TGF-β1 treated cells; however, the elasticity of the cytoplasm was increased further 10-fold ($p<0.05$) with the addition of PDGF. These marked shifts in viscoelastic properties of cells may be due to enhanced crosslinking among actin filaments, as similar mechanical strengthening of *in vitro* actin solutions is demonstrated from the formation of both orthogonal networks and ordered bundles, mediated by F-actin cross-linking/bundling proteins. *In vitro,* α-actinin increased actin solution elasticity by 15-fold, at a molar ratio of 1:50 (0.03 μM α-actinin in 15μM actin) [33]. Further studies with other cross-linking (Filamin) and bundling proteins (Fascin) individually or in combination with α-actinin increased the formation of entangled and crosslinked structures of bundled fibers, resulting in stiffer actin gel mechanics [31,34]. The difference in elasticity of combination of PDGF and TGF-β1 treated cells compared to TGF-β1 alone may be due to a more balanced role between cross-linkers and bundlers which gives rise to superior ordered architecture with higher stiffness. This surprising result highlights the importance of studying the effects of soluble factors on the mechanical properties of MSCs. Differences in the viscoelastic behavior of cells have been associated with differentiation potential [35], malignant transformation, and disease [36]. For instance, activation of latent TGF-β1 in soft tissues such as the kidney has been

deemed critical for tissue fibrosis [37] which may be due to stiffening of both cells and their remodeled environments.

We further investigated more macroscopic cytoskeletal changes in response to TGF-β1 and PDGF by evaluating the cell shape factor and actin stress fiber density. Treatment with TGF-β1, but not PDGF, resulted in increased stress fiber density and cell elongation. Surprisingly, the effect of TGF-β1 was enhanced by the addition of PDGF, indicating that crosstalk in signaling pathways, is important in mediating this response (Figure 4-4, 4-5). Interestingly, TGF-β1 treated cells were aligned in parallel but introduction of PDGF with TGF-β1 increased the randomness in their orientation. The parallel alignment of TGF-β1 treated cells may be associated with increased production of fibrillar collagen [38,39]. Mannose-6-phosphate [40] and other TGF-β inhibitors [41,42] are used to prevent hypertrophic scars, which are often associated with increased collage I expression and parallel alignment of ECM proteins.

TGF-β1 is also known for its role in directing MSC differentiation into bone, cartilage, and muscle [43] and for regulating the expression of other growth factors, including PDGF [44], important in stem cell growth, maintenance, and differentiation [45]. Although PDGF and TGF-β1 affect many cellular processes over longer time periods, the molecular and mechanical response to these factors was measured after a 24-hour exposure, which minimized the effects of these processes on cellular mechanics. Over the 24-hour time period used in our studies, PDGF and TGF-β1 did not affect MSC differentiation, as determined by histological screening.

Previous studies have explored molecular mechanism behind TGF-β1 dependent cytoskeletal remodeling and found important roles of small Rho-GTPases (RhoA,

CDC42, and Rac1) [46-48]. To correlate with cytoskeletal re-organization and mechanical stiffening response to TGF-β1 treatment, we examined the role of multiple genes belonging to the family of actin-binding proteins that directly control actin remodeling [24,25]. The actin-binding protein α-actinin acts as a crosslinker and bundler in reconstituted actin solutions [49] and organizes F-actin filaments in orthogonal or parallel structures in cells, contributing to both stress fiber formation and cellular stiffness [34]. Other proteins like fascin and transgelin interact more selectively with F-actin, which is important for generating more structured actin networks like parallel bundles found in filopodia and stress fiber formation [50-52]. Increasing the thickness of these parallel bundles or reducing the degrees of freedom for polymeric actin movement through orthogonal crosslinking may contribute to high cell stiffness.

Due to the complexities of intracellular control of actin mechanics originating from protein interactions and post-translation modifications, it is difficult to isolate the mechanical response to a particular protein or protein complex. Instead we focused on the roles of the principal signaling pathways affected by TGF-β1 and PDGF. The initial studies suggested PDGF can augment the effects of TGF-β1. Multiple studies have provided evidence of cross-talk between these two pathways [53,54]. We used small molecule receptor inhibitors to explore the role of PDGF and TGF- β1 signaling in the mechanical response (Figure 4-8). SB-505124 binds to TGF-βRI and inhibits phosphorylation of Smad2/3 to block TGF-β signaling. It has been shown to successfully block recruitment of MSCs to arteries [55] and block ALK5 mediated chondrogenesis of MSCs [18]. JNJ-10198409 is PDGFR-β tyrosine kinase inhibitor and it has been primarily examined to inhibit proliferation of different cell types [20,56]. Both inhibitors

have been tested independently to curb tumor growth, albeit through different mechanisms [20,57]. SB-505124 expectedly inhibited elongation and stiffening response; however, more interestingly, PDGFR-β inhibitor–JNJ-10198409 blocked these responses as well for both TGF-β1 alone and in combination with PDGF. We further investigated role of these inhibitors on relevant gene activation of ABPs such as *tensin-1 (Tns1), α-actinin-1(Actn1), troponin t2 (Tnnt2), moesin (Msn),* using PCR and gel electrophoresis. After initial screening, we focused on 4 genes for each inhibitor based on differential response. SB-505124 completely blocked the TGF-β1 mediated upregulation of all four genes (Figure 4-9A). Since PDGF individually does not regulate ABPs, we used JNJ-10198409 to examine the role of PDGF signaling in combined soluble factor treated cells. Expectedly, JNJ-10198409 abrogated *Pdgfb* gene activation (Figure 4-9B). More interestingly, it selectively only blocked *Actn1* activation. Combined with the previous results of complete inhibition of TGF-β1 mediated cell stiffening with JNJ-10198409, this data suggests that *Actn1* is one of the key regulators of cell stiffening. However, a more detailed screening of ABPs with JNJ-10198409 is required to explore all the key elements of stiffening response. These studies provided evidence of integral role of PDGFR-β mediated signaling for individual TGF-β1 treatment. Furthermore, two different time scales, including short (~1 hour) (Figure 4-7) and long (~24 hours) (Figure 4-6), were used to determine possible interaction between TGF-β1 treatment and PDGFR-β expression. At short time scale, available surface PDGFR-β expression was down-regulated for PDGF treated cells individually and in combination with TGF-β1 compared to control (both by PPC and MFI, (Figure 4-7)). Similar trends were found to be true at longer time scale for PDGF and combination of PDGF and TGF-β1 (Figure 4-

6A-C). For TGF-β1 treated cells, surface expression of PDGFR-β was comparable to that of control cells at shorter time scale. However, surface expression of PDGFR-β on TGF-β1 treated cells were significantly ($p<0.005$) lower compared to control cells after 24 hours (Figure 4-6B). Analysis of microarray data exhibit 0.5-fold ($p<0.05$) increase in *PDGFB* expression for TGF-β1 treated cells compared to control. This result was also confirmed using PCR.

Data presented here strongly indicate cross-talk between PDGF and TGF-β1 signaling pathways in regulating certain aspects of the mechanical and chemical response of MSCs. Up-regulation of *Pdgfb* and *Pdgfrb* in TGF-β1 treated cells might be due to the autocrine induction of PDGF signaling (Figure 4-11). Other studies have suggested establishment of the autocrine PDGF-loop in TGF-β1 treated cells albeit in different cell types [58,59]. This study suggests that this PDGF loop may be integral for TGF-β1 mediated mechanical response. And for combination treatment, addition of recombinant PDGF protein amplifies the response from PDGF loop which later interacts with intracellular TGF-β1 signaling to modulate the rheological and cytoskeletal response.

4.5. CONCLUSIONS

Soluble factors like PDGF and TGF-β1 are essential for normal tissue remodeling and wound healing and play an important role in the development of malignant diseases. The mechanical response of cells to these soluble factors in the niches remains poorly understood. This study indicates at the cellular level, TGF-β1 can induce cytoskeletal remodeling to change cell rheology and shape to modify cell behavior. Additionally, we found that PDGF signaling is integral for TGF-β1 mediated mechanical response of cells. The TGF-β1 signaling pathway is manipulated in numerous therapeutic applications from

regenerative medicine to cancer. This study shows that PDGF may be a viable target in manipulating certain aspects of this signaling pathway.

Previous studies have correlated PDGF and TGF-β1 induced cytoskeletal remodeling and mechanical response of cells to small Rho GTPases [46-48] that control actin organization via intermediate actin binding proteins. However, the genetic manipulation of Rho GTPases to specifically control cell shape and mechanics can be complicated since they directly participate in multiple signaling pathways. Here we demonstrated that PDGF and TGF-β1 signaling uniquely regulate key ABPs to induce mechanical changes. Such a finding can lead to more specific control of mechanical properties of MSCs that can be tailored to meet tissue specific applications.

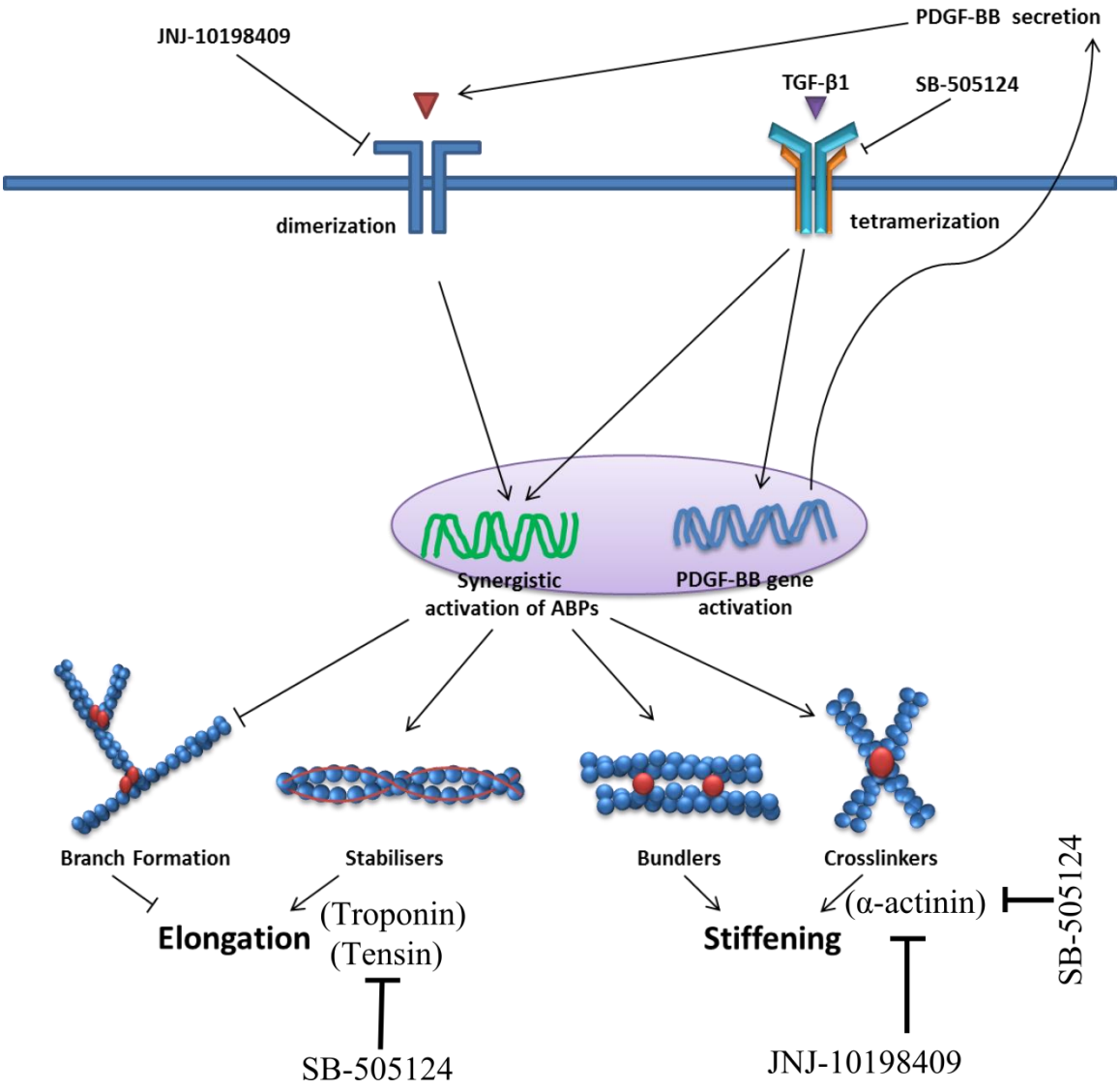

Figure 4-11. *Schematic presentation of TGF-β1 mediated stiffening response.* A simplified diagram correlating mechanical response of MSCs to the treatment with TGF-β1 by molecular regulation of actin-binding proteins such as stabilization and crosslinking factors. After 24 hour exposure to TGF-β1, alterations in morphology and stiffness can be explained by differential gene expression in actin binding proteins (ABPs).

4.6. REFERENCE

1. McGrail DJ, D Ghosh, ND Quach and MR Dawson. (2012). Differential mechanical response of mesenchymal stem cells and fibroblasts to tumor-secreted soluble factors. PloS one 7:e33248.

2. Ji JF, BP He, ST Dheen and SSW Tay. (2004). Interactions of chemokines and chemokine receptors mediate the migration of mesenchymal stem cells to the impaired site in the brain after hypoglossal nerve injury. Stem cells 22:415-427.

3. Kole TP, Y Tseng, I Jiang, JL Katz and D Wirtz. (2005). Intracellular Mechanics of Migrating Fibroblasts. Molecular Biology of the Cell 16:328-338.

4. McGrail DJ, KM McAndrews and MR Dawson. (2012). Biomechanical analysis predicts decreased human mesenchymal stem cell function before molecular differences. Exp Cell Res.

5. Klopp AH, EL Spaeth, JL Dembinski, WA Woodward, A Munshi, RE Meyn, JD Cox, M Andreeff and FC Marini. (2007). Tumor Irradiation Increases the Recruitment of Circulating Mesenchymal Stem Cells into the Tumor Microenvironment. Cancer Research 67:11687-11695.

6. Birnbaum T, J Roider, C Schankin, C Padovan, C Schichor, R Goldbrunner and A Straube. (2007). Malignant gliomas actively recruit bone marrow stromal cells by secreting angiogenic cytokines. Journal of Neuro-Oncology 83:241-247.

7. Dittmar T and F Entschladen. (2013). Migratory Properties of Mesenchymal Stem Cells. In: *Mesenchymal Stem Cells - Basics and Clinical Application I*. Weyand B, M Dominici, R Hass, R Jacobs and C Kasper eds. Springer Berlin Heidelberg. pp 117-136.

8. Byfield FJ, RK Reen, T-P Shentu, I Levitan and KJ Gooch. (2009). Endothelial actin and cell stiffness is modulated by substrate stiffness in 2D and 3D. Journal of biomechanics 42:1114-1119.

9. Darling EM, M Topel, S Zauscher, TP Vail and F Guilak. (2008). Viscoelastic properties of human mesenchymally-derived stem cells and primary osteoblasts, chondrocytes, and adipocytes. Journal of biomechanics 41:454-464.

10. Pang C, Z Gao, J Yin, J Zhang, W Jia and J Ye. (2008). Macrophage infiltration into adipose tissue may promote angiogenesis for adipose tissue remodeling in obesity. American Journal of Physiology-Endocrinology And Metabolism 295:E313-E322.

11. Leitzel K, W Bryce, J Tomita, G Manderino, I Tribby, A Thomason, M Billingsley, E Podczaski, H Harvey and M Bartholomew. (1991). Elevated plasma platelet-derived growth factor B-chain levels in cancer patients. Cancer research 51:4149-4154.

12. Hudkins KL, DG Gilbertson, M Carling, S Taneda, SD Hughes, MS Holdren, TE Palmer, S Topouzis, AC Haran and AL Feldhaus. (2004). Exogenous PDGF-D is a potent mesangial cell mitogen and causes a severe mesangial proliferative glomerulopathy. Journal of the American Society of Nephrology 15:286-298.

13. Meyer A, W Wang, J Qu, L Croft, JL Degen, BS Coller and J Ahamed. (2012). Platelet TGF-β1 contributions to plasma TGF-β1, cardiac fibrosis, and systolic dysfunction in a mouse model of pressure overload. Blood 119:1064-1074.

14. Wakefield LM, JJ Letterio, T Chen, D Danielpour, RS Allison, LH Pai, AM Denicoff, MH Noone, KH Cowan and JA O'Shaughnessy. (1995). Transforming growth factor-beta1 circulates in normal human plasma and is unchanged in advanced metastatic breast cancer. Clinical Cancer Research 1:129-136.

15. Kortesidis A, A Zannettino, S Isenmann, S Shi, T Lapidot and S Gronthos. (2005). Stromal-derived factor-1 promotes the growth, survival, and development of human bone marrow stromal stem cells. Blood 105:3793-3801.

16. Cassiede P, JE Dennis, F Ma and AI Caplan. (1996). Osteochondrogenic potential of marrow mesenchymal progenitor cells exposed to TGF-β1 or PDGF-BB as assayed *in vivo* and *in vitro*. Journal of Bone and Mineral Research 11:1264-1273.

17. Tang Y, X Wu, W Lei, L Pang, C Wan, Z Shi, L Zhao, TR Nagy, X Peng and J Hu. (2009). TGF-β1–induced migration of bone mesenchymal stem cells couples bone resorption with formation. Nature medicine 15:757-765.

18. Hellingman CA, ENB Davidson, W Koevoet, EL Vitters, WB van den Berg, GJ van Osch and PM van der Kraan. (2011). Smad signaling determines chondrogenic differentiation of bone-marrow-derived mesenchymal stem cells: inhibition of Smad1/5/8P prevents terminal differentiation and calcification. Tissue Engineering Part A 17:1157-1167.

19. Fujitani, M., Grinshtein, N., Smith, K. M., & Kaplan, D. R. (2012). Potent and selective cytotoxic and cytostatic activity of JNJ-10198409 against neuroblastoma cells. *Chiba Med J*, *88*, 27-34.

20. D'Andrea MR, JM Mei, RW Tuman, RA Galemmo and DL Johnson. (2005). Validation of *in vivo* pharmacodynamic activity of a novel PDGF receptor tyrosine kinase inhibitor using immunohistochemistry and quantitative image analysis. Molecular Cancer Therapeutics 4:1198-1204.

21. Tee S-Y, J Fu, CS Chen and PA Janmey. (2011). Cell shape and substrate rigidity both regulate cell stiffness. Biophysical journal 100:L25-L27.

22. DaCosta Byfield S, C Major, NJ Laping and AB Roberts. (2004). SB-505124 Is a Selective Inhibitor of Transforming Growth Factor-β Type I Receptors ALK4, ALK5, and ALK7. Molecular Pharmacology 65:744-752.

23. Ho CY, DW Ludovici, US Maharoof, J Mei, JL Sechler, RW Tuman, ED Strobel, L Andraka, H-K Yen and G Leo. (2005). (6, 7-Dimethoxy-2, 4-dihydroindeno [1, 2-c] pyrazol-3-yl) phenylamines: Platelet-Derived Growth Factor Receptor Tyrosine Kinase Inhibitors with Broad Antiproliferative Activity against Tumor Cells. Journal of medicinal chemistry 48:8163-8173.

24. Uribe R and D Jay. (2009). A review of actin binding proteins: new perspectives. Molecular biology reports 36:121-125.

25. Winder SJ and KR Ayscough. (2005). Actin-binding proteins. Journal of cell science 118:651-654.

26. Haynes J, J Srivastava, N Madson, T Wittmann and DL Barber. (2011). Dynamic actin remodeling during epithelial–mesenchymal transition depends on increased moesin expression. Molecular biology of the cell 22:4750-4764.

27. Djouad F, P Plence, C Bony, P Tropel, F Apparailly, J Sany, D Noel and C Jorgensen. (2003). Immunosuppressive effect of mesenchymal stem cells favors tumor growth in allogeneic animals. Blood 102:3837-44.

28. Barrientos S, O Stojadinovic, MS Golinko, H Brem and M Tomic-Canic. (2008). Growth factors and cytokines in wound healing. Wound Repair and Regeneration 16:585-601.

29. Hanahan D and RA Weinberg. (2011). Hallmarks of cancer: the next generation. Cell 144:646-674.

30. Tseng Y, E Fedorov, JM McCaffery, SC Almo and D Wirtz. (2001). Micromechanics and ultrastructure of actin filament networks crosslinked by human fascin: a comparison with alpha-actinin. J Mol Biol 310:351-66.

31. Esue O, Y Tseng and D Wirtz. (2009). α-Actinin and filamin cooperatively enhance the stiffness of actin filament networks. PLoS One 4:e4411.

32. Kole TP, Y Tseng and D Wirtz. (2004). Intracellular microrheology as a tool for the measurement of the local mechanical properties of live cells. Methods Cell Biol 78:45-64.

33. Xu J, D Wirtz and TD Pollard. (1998). Dynamic Cross-linking by α-Actinin Determines the Mechanical Properties of Actin Filament Networks. Journal of Biological Chemistry 273:9570-9576.

34. Tseng Y, TP Kole, JS Lee, E Fedorov, SC Almo, BW Schafer and D Wirtz. (2005). How actin crosslinking and bundling proteins cooperate to generate an

enhanced cell mechanical response. Biochemical and biophysical research communications 334:183-192.

35. González-Cruz RD, VC Fonseca and EM Darling. (2012). Cellular mechanical properties reflect the differentiation potential of adipose-derived mesenchymal stem cells. Proceedings of the National Academy of Sciences 109:E1523-E1529.

36. Guck J, S Schinkinger, B Lincoln, F Wottawah, S Ebert, M Romeyke, D Lenz, HM Erickson, R Ananthakrishnan and D Mitchell. (2005). Optical deformability as an inherent cell marker for testing malignant transformation and metastatic competence. Biophysical journal 88:3689-3698.

37. Pohlers D, J Brenmoehl, I Löffler, CK Müller, C Leipner, S Schultze-Mosgau, A Stallmach, RW Kinne and G Wolf. (2009). TGF-β and fibrosis in different organs—molecular pathway imprints. Biochimica et Biophysica Acta (BBA)-Molecular Basis of Disease 1792:746-756.

38. Warstat K, D Meckbach, M Weis-Klemm, A Hack, G Klein, P de Zwart and WK Aicher. (2010). TGF-beta enhances the integrin alpha2beta1-mediated attachment of mesenchymal stem cells to type I collagen. Stem Cells Dev 19:645-56.

39. D'Angelo M, JM Chen, K Ugen and RM Greene. (1994). TGF beta 1 regulation of collagen metabolism by embryonic palate mesenchymal cells. J Exp Zool 270:189-201.

40. Xia C, XY Yang, Y Wang and S Tian. (2011). Inhibition effect of mannose-6-phosphate on expression of transforming growth factor Beta receptor in flexor tendon cells. Orthopedics 34:21.

41. Zhang Z, TM Garron, XJ Li, Y Liu, X Zhang, YY Li and WS Xu. (2009). Recombinant human decorin inhibits TGF-beta1-induced contraction of collagen lattice by hypertrophic scar fibroblasts. Burns 35:527-37.

42. Lu L, AS Saulis, WR Liu, NK Roy, JD Chao, S Ledbetter and TA Mustoe. (2005). The temporal effects of anti-TGF-beta1, 2, and 3 monoclonal antibody on wound healing and hypertrophic scar formation. J Am Coll Surg 201:391-7.

43. Park JS, JS Chu, AD Tsou, R Diop, Z Tang, A Wang and S Li. (2011). The effect of matrix stiffness on the differentiation of mesenchymal stem cells in response to TGF-beta. Biomaterials 32:3921-30.

44. Zhao F, YF Zhang, YG Liu, JJ Zhou, ZK Li, CG Wu and HW Qi. (2008). Therapeutic effects of bone marrow-derived mesenchymal stem cells engraftment on bleomycin-induced lung injury in rats. Transplant Proc 40:1700-5.

45. Ng F, S Boucher, S Koh, KS Sastry, L Chase, U Lakshmipathy, C Choong, Z Yang, MC Vemuri, MS Rao and V Tanavde. (2008). PDGF, TGF-beta, and FGF signaling is important for differentiation and growth of mesenchymal stem cells

(MSCs): transcriptional profiling can identify markers and signaling pathways important in differentiation of MSCs into adipogenic, chondrogenic, and osteogenic lineages. Blood 112:295-307.

46. Edlund S, M Landstrom, C-H Heldin and P Aspenstrom. (2002). Transforming Growth Factor-beta -induced Mobilization of Actin Cytoskeleton Requires Signaling by Small GTPases Cdc42 and RhoA. Mol. Biol. Cell 13:902-914.

47. Vardouli L, E Vasilaki, E Papadimitriou, D Kardassis and C Stournaras. (2008). A novel mechanism of TGFβ-induced actin reorganization mediated by Smad proteins and Rho GTPases. FEBS Journal 275:4074-4087.

48. Arber S, FA Barbayannis, H Hanser, C Schneider, CA Stanyon, O Bernard and P Caroni. (1998). Regulation of actin dynamics through phosphorylation of cofilin by LIM-kinase. Nature 393:805-809.

49. Wachsstock DH, W Schwartz and TD Pollard. (1993). Affinity of alpha-actinin for actin determines the structure and mechanical properties of actin filament gels. Biophysical journal 65:205-214.

50. Tojkander S, G Gateva and P Lappalainen. (2012). Actin stress fibers–assembly, dynamics and biological roles. Journal of Cell Science 125:1855-1864.

51. Goodman A, BL Goode, P Matsudaira and GR Fink. (2003). The Saccharomyces cerevisiae calponin/transgelin homolog Scp1 functions with fimbrin to regulate stability and organization of the actin cytoskeleton. Molecular biology of the cell 14:2617-2629.

52. Vignjevic D, S-i Kojima, Y Aratyn, O Danciu, T Svitkina and GG Borisy. (2006). Role of fascin in filopodial protrusion. The Journal of cell biology 174:863-875.

53. Qi Y-X, J Jiang, X-H Jiang, X-D Wang, S-Y Ji, Y Han, D-K Long, B-R Shen, Z-Q Yan and S Chien. (2011). PDGF-BB and TGF-β1 on cross-talk between endothelial and smooth muscle cells in vascular remodeling induced by low shear stress. Proceedings of the National Academy of Sciences 108:1908-1913.

54. Leof EB, JA Proper, AS Goustin, GD Shipley, PE DiCorleto and HL Moses. (1986). Induction of c-sis mRNA and activity similar to platelet-derived growth factor by transforming growth factor beta: a proposed model for indirect mitogenesis involving autocrine activity. Proceedings of the National Academy of Sciences 83:2453-2457.

55. Wan M, C Li, G Zhen, K Jiao, W He, X Jia, W Wang, C Shi, Q Xing and YF Chen. (2012). Injury-Activated Transforming Growth Factor β Controls Mobilization of Mesenchymal Stem Cells for Tissue Remodeling. Stem Cells 30:2498-2511.

56. Kim Y, MI Fiel, E Albanis, HI Chou, W Zhang, G Khitrov and SL Friedman. (2012). Anti-fibrotic activity and enhanced interleukin-6 production by hepatic stellate cells in response to imatinib mesylate. Liver International 32:1008-1017.

57. Biswas S, TL Criswell, SE Wang and CL Arteaga. (2006). Inhibition of Transforming Growth Factor-β Signaling in Human Cancer: Targeting a Tumor Suppressor Network as a Therapeutic Strategy. Clinical Cancer Research 12:4142-4146.

58. Gotzmann J, A Fischer, M Zojer, M Mikula, V Proell, H Huber, M Jechlinger, T Waerner, A Weith and H Beug. (2006). A crucial function of PDGF in TGF-β-mediated cancer progression of hepatocytes. Oncogene 25:3170-3185.

59. Battegay EJ, EW Raines, RA Seifert, DF Bowen-Pope and R Ross. (1990). TGF-β induces bimodal proliferation of connective tissue cells via complex control of an autocrine PDGF loop. Cell 63:515-524.

CHAPTER 5: EFFECT OF TGF-β1 AND PDGF-BB ON ADHESION AND MOTILITY OF MESENCHYMAL STEM CELLS

Cell adhesion and migration are critical processes that play key roles in normal and pathological tissue development. Several studies have investigated the role of specific *in vivo* factors in regulating adhesion and migration of multiple cell types including mesenchymal stem cells (MSCs). The primary objective of this study is to develop MSCs that can adhere and migrate in the wound bed. Therefore, we examined the effect of two wound healing site specific factors, TGF-β1 and PDGF, on MSC migration and adhesion. Combining these results with the mechanical characterization from previous studies (chapter 4) can provide new insights into MSC behavior *in vivo.*

5.1. INTRODUCTION

The adhesion of cells to the extracellular matrix (ECM) or cell surface receptors (like VCAM-1) is essential for cell survival and viability [1]. Anchorage dependent cells bind to the ECM via surface adhesion molecules such as integrins, cadherins, and selectins to avoid programmed cell death by anoikis [2,3]. Integrins initiates the adhesion process and essentially perform as both linkers and sensors for cells by bridging the bond between the cell cytoskeleton and the ECM [2]. Activated integrins are heterodimeric transmembrane glycoprotein receptors that consist of α and β subunits [4]. There are 24 non-covalent dimers that have been identified to form from the family of 18 ‘α’ and 8 ‘β’ subunits (total 26) in mammalian cells. Among these combined 26 individual subunits,

αv (CD51) and β1 (CD29) participate in forming the majority of the heterodimeric clusters in MSCs [4]. The cytoplasmic domain of the bound and activated integrins recruits a host of intracellular cytoplasmic molecules to form focal adhesion complexes [2], which contain mechanical (talin, vinculin, filamin, α-actinin) and chemical signal transducers (FAK, paxilin, src family kinases) [5-7]. After cells are anchored to surfaces, bound integrins provide bidirectional relay of both biophysical and biochemical signals for cells carry out a plethora of activity in the tissue regeneration site including migration [6,8].

Cell migration is important for both normal tissue regeneration and growth of pathological processes like cancer. During growth and regeneration, migration process allows cells to distribute and replace damaged cells, actively participate in tissue remodeling and angiogenesis [9-11]. Adhesive strength does not directly correlate with cell migration; however, it is critical and controls certain aspects of cell motility [12,13]. The migration process begins with the protrusion of lamellipodia and the formation of new focal adhesions at the leading edge of the cell [12,14]. The cytoskeleton undergoes rapid reorganization during this event. Polymerized actin binds to the focal adhesion complex and the contractile force created by myosin motors acts via polymerized actin to pull up the trailing edge of the cell and push it in the forward direction [12,13]. During migration, cells dynamically establish and break bonds on the migrating surface [15]. Migrating cells require an intermediate level of adhesive forces, since highly adhesive cells would have difficulty breaking these bonds during migration and non-adhesive cells could not generate the traction forces required for engaging the ECM [16,17].

Chemical and physical stimuli have been shown to alter cell shape and cytoskeletal organization and influence cell migration by activating cytoskeletal mediators [18-22]. PDGF has been universally reported to be a very potent chemoattractant [23] and plays key role to recruit smooth muscle cells and MSC-like pericytes for angiogenesis *in vivo* [24,25]. In case of TGF-β1, migration results remain intriguingly cell specific. For example, TGF-β1 can induce epithelial to mesenchymal transition (EMT) of epithelial cells that contributes to invasiveness of cells with increased motility both *in vitro* and *in vivo* [26-28]. In contradiction, TGF-β1 has been shown to inhibit migration of endothelial cells [29,30]. In fact, independent studies have reported contradictory effects of TGF-β1 on MSCs, underlining the importance of more thorough characterization of such interaction. Here, we found that TGF-β1 treatment resulted in increased expression of integrins and enhanced adhesion of MSCs with different ECM proteins. We also examined the effects of the soluble factors on regulating cell motility to close an artificially created scratch. Although, PDGF controlled motility of MSCs predominantly, TGF-β1 enhanced the PDGF-mediated migration effect in a directional motility assay mimicking a scratch wound. Since the effects of the soluble factors on these functions can vary from cell type to cell type significantly, it is necessary to investigate the functional outcome of MSCs under the influence of the soluble factors both individually and in combination.

5.2. MATERIALS AND METHODS

Materials: IMDM, DMEM, L-glutamine, penicillin-streptomycin and trypsin were purchased from Mediatech and fetal bovine serum (FBS) was purchased from Atlanta Biologicals. Recombinant human proteins TGF-β1 and PDGF-BB (referred to as PDGF)

and antibodies for flow Cytometry were purchased from Biolegend. Rhodamine-Phalloidin, were purchased from Invitrogen. All other reagents were purchased from VWR unless otherwise specified.

MSC isolation and culture: Murine MSCs were isolated from the bone marrow of 6-10 weeks old adult male Balb/C mice (Charles River Laboratories, Wilmington, MA) and cultured in normal growth media (IMDM media supplemented with 20% FBS, 2 mM L-glutamine, 100U/ml penicillin, and 100U/ml streptomycin). Purified MSCs between passages 2-6 were used for all studies.

Centrifugal force based adhesion assay: This fluorometric assay was used to evaluate the effect of soluble factor treatment on MSC adhesion to native ECM, collagen (COL), or fibronectin (FBN). Briefly, MSCs were trypsinized and seeded in a 96 well plate that was coated with 10 µg/ml desired ECM molecule or left uncoated for native ECM control (n = 8 wells per condition). After 24 hours treatment with soluble factors, cells were labeled with a transmembrane fluorescent viability marker, Calcein AM (Anaspec), and an initial fluorescence reading was recorded. Cells were detached by centrifuging inverted plates at 500 x g for 5 minutes before recording a final fluorescence reading. The adherent fraction was determined by normalizing the final florescence values with the initial pre-spin values.

Flow cytometry: MSCs were analyzed with a BD LSR-II flow cytometer to capture the effects of soluble factor treatment on the cell surface adhesion markers. Briefly, both treated and untreated cells were detached from 10 cm dishes, centrifuged, and suspended in 100 µl cold FACS buffer (2% FBS, 1mM EDTA in PBS). Cells were then incubated with one of the following anti-mouse antibodies (dilutions in parentheses): PE-CD51

(1:20), FITC-CD29 (1:100), AF-647-MVCAM1/CD106 (1:200); APC- MVCAM1/ CD106 (1:200). All studies were performed in triplicate with at least n = 50,000 events per sample.

Immunofluorescence staining: To visualize focal adhesion protein vinculin, MSCs were cultured and treated on glass cover-slips in 24-well plates. Cells were then fixed with 4% formaldehyde before permeabilization with Triton X-100 and blocking with horse serum. Cells were stained for one hour at room temperature with 1 µg/mL rabbit anti-vinculin, followed by combination of 1:1000 goat anti-rabbit Alexa Flour 488 (secondary for vinculin Ab) and 1:200 Rhodamine Phalloidin. Coverslips were then washed three times before sealing with Vectashield (Vector Labs) containing DAPI. All cells were visualized using Zeiss LSM 510 UV/NLO confocal microscope. All image analysis was performed in custom-written MATLAB algorithms.

Motility and scratch assay: MSCs were cultured at a sub-confluent density for motility assay. For the scratch assay, cells were cultured as a confluent monolayer on uncoated 24-well plate and a gap was created by removing cells with a pipette tip. Wells were then washed to remove detached cells before staining with NucBlue Live Cell dye (Invitrogen, Carlsbad, CA) or Hoechst for 30 minutes. Cells were then treated with soluble factors before placing them on Nikon Eclipse Ti inverted epifluorescent microscope, which was maintained at 37°C and 5% carbon dioxide throughout the experiment using an *In vivo* Scientific environmental cell chamber. Both brightfield (BF) and DAPI images were taken at multiple points at 10 minutes interval for 6-8 hours at 10x magnification. The locations of cell nuclei, segmented from fluorescent images, were tracked in MATLAB to define cell traces. The cell migration coefficients and directional velocities were

determined by fitting the traces to the persistent random walk model [31]. Briefly, mean square displacements were calculated ($MSD = d^2(\tau)$) from the two dimensional tracking data and was used for fitting the following equation:

$$\langle d^2(\tau)\rangle = 4\mu\{t - P[1 - e^{-t/P}]\}$$

P= persistence time and μ=migration coefficient.

Statistics: Each experiment was performed with 3 or more replicates, and all values expressed as the mean ± s.e.m. One way Anova test with repeated measures was used to determine statistical significance of experiments involving four groups. For comparison between groups, Tukey's HSD post-test was used. Significance was reported as * (for $p<0.05$), ** (for $p<0.005$) and *** (for $p<0.0005$).

5.3. RESULTS

TGF-β1 and PDGF alter adhesive strength of MSCs: A functional adhesion analysis with a centrifugation force based adhesion assay (Figure 5-1) revealed MSCs treated with PDGF were significantly ($p<0.05$) less adhesive than control cells on tissue culture plastic (32.9%); whereas, TGF-β1 treated cells were up to 54% more adhesive than control ($p<0.0005$). Combination treatment with PDGF and TGF-β1 also resulted in increased MSC adhesion ($p<0.0005$) relative to control (75%), indicating that cell adhesion is largely regulated by TGF-β1. After 24 hours, the adhesion of MSCs with COL and FBN was similar to tissue culture plastic (TCP), since MSCs likely had sufficient time to secrete their own ECM proteins.

TGF-β1 and PDGF alter expression and distribution of cell adhesion molecules: We next sought to analyze the changes in the expression of the focal adhesion complexes that

link the actin cytoskeleton to the extracellular environment and adjacent cells by staining for the focal adhesion marker vinculin (Figure 5-2A). Though the overall vinculin

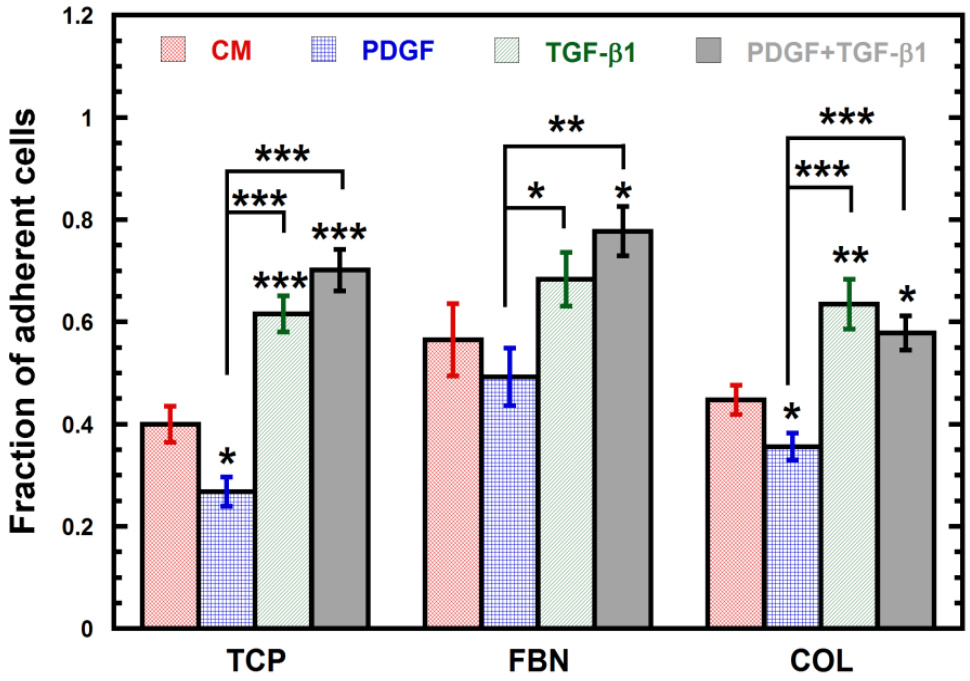

Figure 5-1. *TGF-β1 enhanced adhesive strength of MSC on substrate.* Centrifuge-based adhesion assay was used to determine the effects of soluble factor treatment on the adhesion of MSCs on tissue culture plastic (TCP) coated with collagen -10ug/ml (COL) or fibronectin-10ug/ml (FBN). TGF-β1 treatment resulted in an increased fraction of adherent cells.

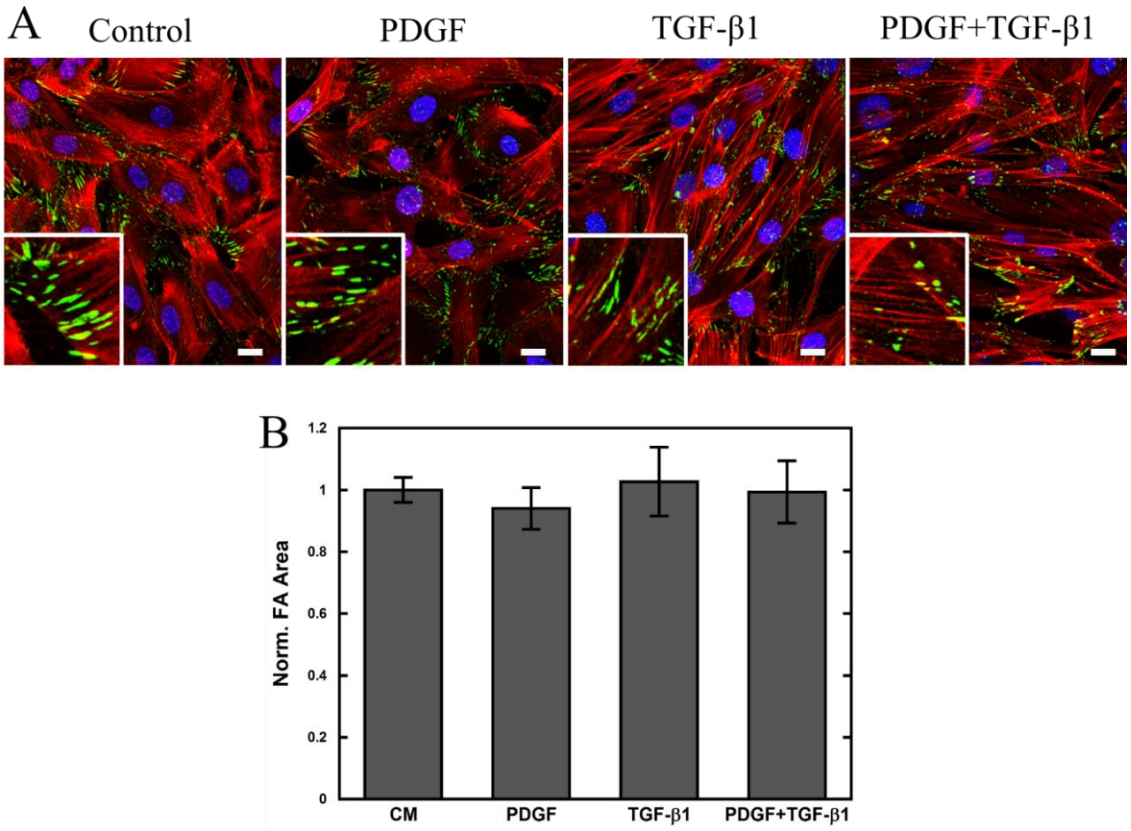

Figure 5-2. *Vinculin expression remain unchanged after soluble factor treatment.* (A) Confocal images of soluble factor-treated MSCs stained with Phalloidin (F-actin, red), anti-vinculin (green), and DAPI (nucleus, blue) (scale bar: 20μm). (B) Normalized focal adhesion areas were calculated by analysis of confocal images with custom MATLAB routine.

expression (quantified using confocal micrographs in MATLAB) did not change significantly (Figure 5-2B), the pattern of expression was more distributed throughout the population of cells and localized to tips on an individual cell level when exposed to TGF-β1.

To reconcile these differences, flow cytometry was used to analyze differences in expression of integrin subunits β_1 (CD29, Figure 5-3A) and α_v (CD51, Figure 5-3A), which bind directly to the extracellular matrix, and cell adhesion molecules vascular cell adhesion molecule-1 (VCAM-1) (Figure 5-4A), which mediate cell-cell adhesion (also ICAM-1 Figure 5-4A) with endothelial cells and leukocytes. PDGF treatment had very little effect on the expression of these integrin molecules, with only significant differences in mean fluorescence intensity (MFI, Figure 5-3B) for α_v (reduced expression) but not β1 integrin. In contrast, treatment with TGF-β1 significantly altered both integrin expressions as demonstrated by increased MFI for CD29 ($p<0.005$) and CD51 ($p<0.0005$). However, both TGF-β1 and PDGF treated cells demonstrated similar trend for the examined cell-cell adhesion molecules and significantly reduced percentage of positive cells (PPC) for VCAM-1 and ICAM-1 (Figure 5-4B). The altered integrin expression for TGF-β1 treated cells may explain the observed differences in adhesion and further demonstrates the important role of TGF-β1 in cell adhesion.

PDGF controls cell motility *in vitro*: A random motility assay was used to evaluate the effect of soluble factors on cell motility. For these studies, MSCs were seeded on uncoated 24 wells plate and grown to subconfluency prior to treatment. In presence of

soluble factors, the directed motility and migration coefficients were determined by tracking the cell nuclei with NucBlue live cell dye. PDGF enhanced random migration speed of MSCs

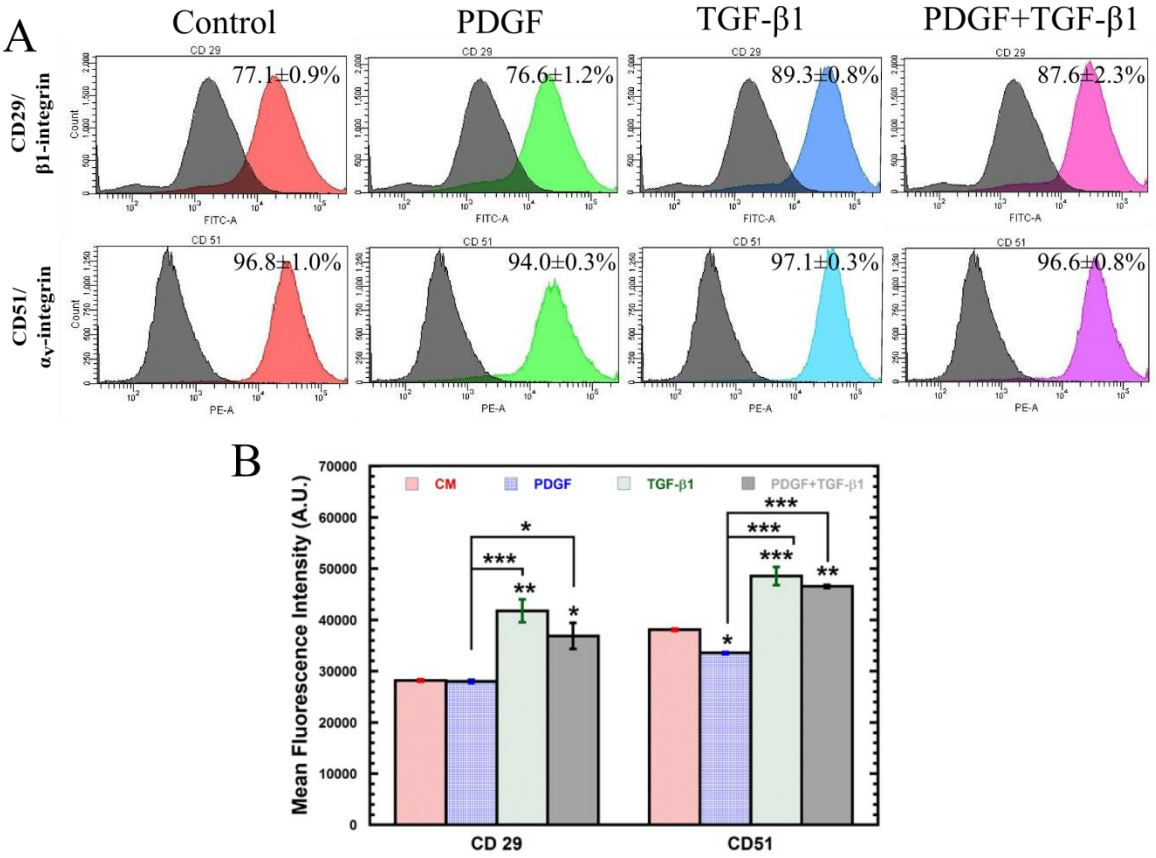

Figure 5-3. *TGF-β1 increased cell surface integrin expression.* (A) Histograms from flow cytometric analysis of surface cell adhesion molecules using fluorescent labeled antibodies for α_v (PE) and β_1 (FITC) integrins on MSCs after 24 hours treatment with soluble factors. Gated percent positive population of MSCs compared to the negative population (black histogram) are indicated as mean±s.e.m. on top right of overlayed histograms (red for CM, green for PDGF, blue for TGF-β1 and violet for PDGF+TGF-β1). Histograms from flow cytometry were analyzed using FACS-DIVA for mean fluorescence intensity (MFI). Surface integrin expressions of PDGF-treated cells were unaffected; whereas TGF-β1 individually and in combination increased both integrin expression significantly compared to the control. Results are reported as average ± s.e.m. (n=3).

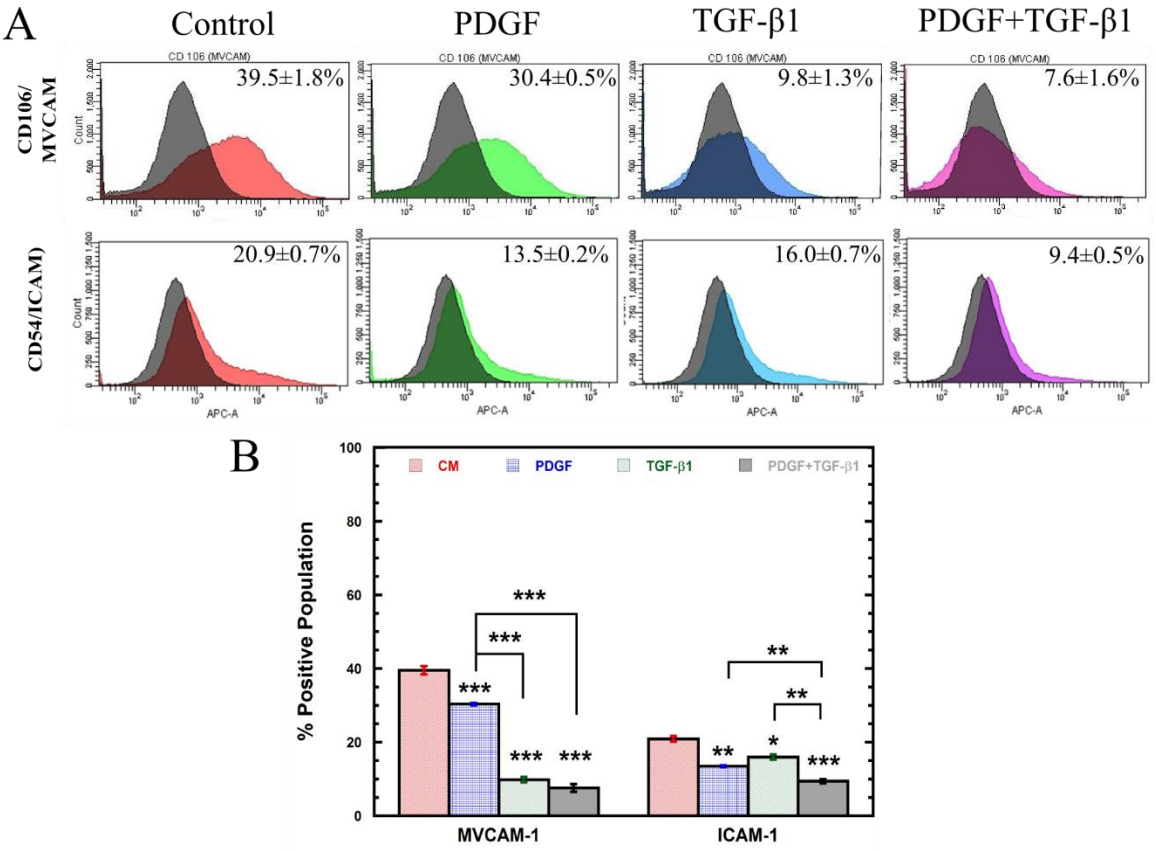

Figure 5-4. *PDGF and TGF-β1 downregulated surface cell-cell interaction* (A) Histograms from flow cytometric analysis of surface cell-cell adhesion molecules using fluorescent labeled antibodies for VCAM-1 (APC) and ICAM-1 (APC) on MSCs after 24 hours treatment with soluble factors. Gated percent positive population of MSCs compared to the negative population (black histogram) are indicated as mean±s.e.m. on top right of overlayed histograms (red for CM, green for PDGF, blue for TGF-β1 and violet for PDGF+TGF-β1). (B) Histograms from flow cytometry were analyzed using FACS-DIVA for percent positive population (PPC). Surface VCAM-1 and ICAM-1 expressions of PDGF-treated cells were decreased; whereas TGF-β1 individually and in combination reduced both CAM expression significantly compared to the control. Results are reported as average ± s.e.m. (n=3).

both individually and in combination with TGF-β1, however; no significant difference was observed between individual PDGF treatment and combination. Both migration coefficient and mean directional velocity were increased significantly for PDGF treated cells compared to control (Figure 5-5). TGF-β1 failed to generate any motility response from the cells both individually and in combination. Similar PDGF dominant migration activities were observed for an *in vitro* scratch assay (that mimics the wound site) as cells migrated toward an artificially created gap to establish new cell-cell contact. PDGF alone and in combination drove MSCs towards the scratch bed to close the gap more efficiently. Though TGF-β1 alone did not induce a directional motility response, the effects of PDGF were enhanced when TGF-β1 was added (Figure 5.6.).

5.4. DISCUSSION

MSC adhesion to ECM can modulate cell spreading, mechanotransduction and migration [32]. Tissue specific soluble factors interact with MSCs to mediate their engraftment and migration [33]. Here we investigated effect of two such soluble factors PDGF and TGF-β1 on MSC adhesion and migration *in vitro*.

TGF-β1 treatment induced significant increase in cell adhesion ($p<0.0005$ for plastic), whereas, addition of PDGF did not enhance the effects of TGF-β1, indicating that crosstalk between these signaling pathways (Figure 4-11) is likely not important in regulating adhesion to ECM. Previous studies have suggested that increase in integrin binding to ECM and clustering can lead to adhesion strengthening. Since α_v (CD51) and β_1 (CD29) participate in forming most integrin heterodimers, we examined effect of the

soluble factor treatments on their surface expression. Both integrin expressions were enhanced in a TGF-β1 dependent manner ($p<0.0005$). Moreover, reduced VCAM-1

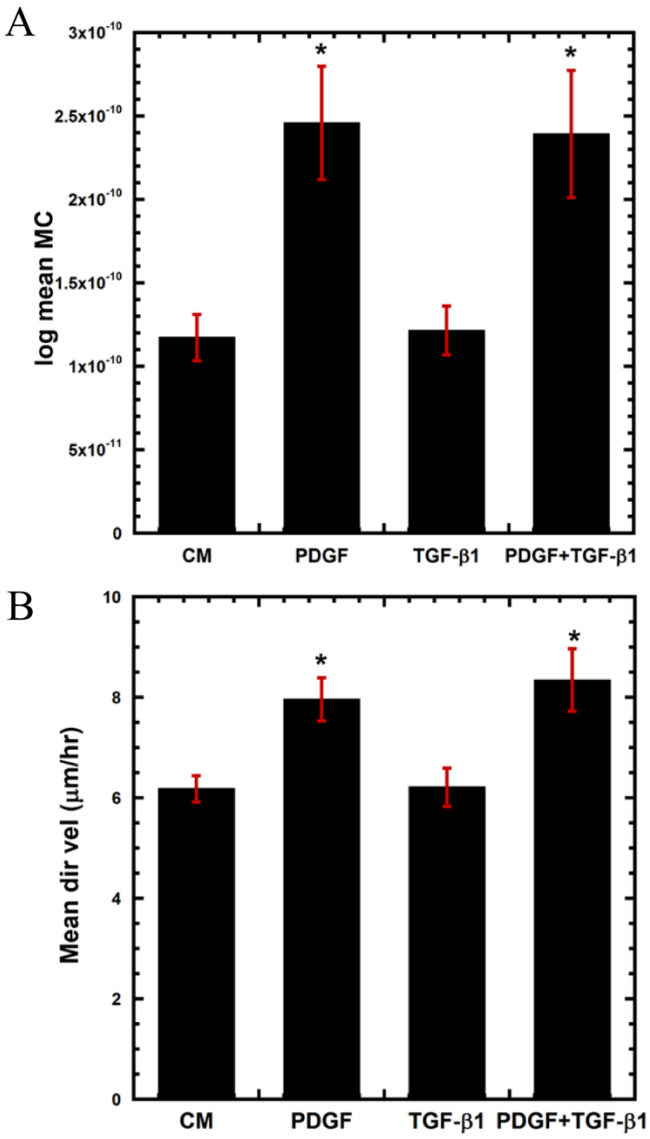

Figure 5-5. *PDGF control random cell motility (chemokinesis) on 2D plastic surface***.** (A, B) Cell motility was evaluated in soluble factor treated MSCs by (A) random cell migration coefficient and (B) directional velocity. (6-8 hours)

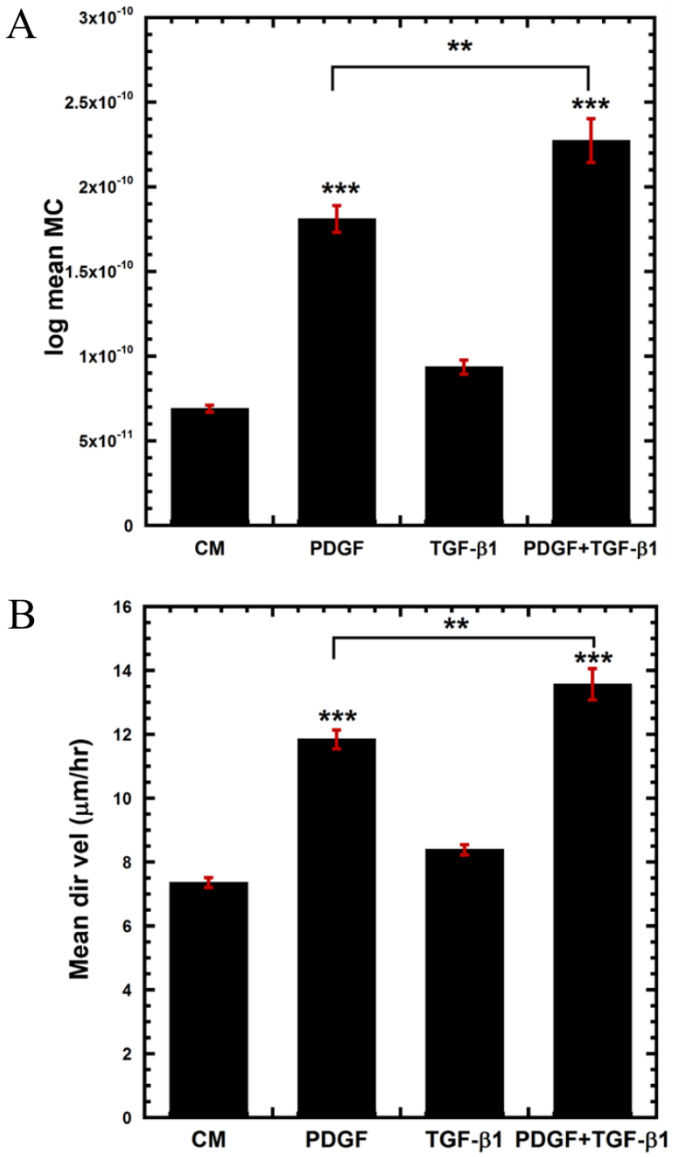

Figure 5-6. *TGF-β1 enhanced PDGF mediated cell migration towards "wound" gap on 2D plastic surface.* (A, B) Cell motility was evaluated in presence of soluble factors after creating scratch on a confluent monolayer of MSCs by (A) cell migration coefficient and (B) directional velocity. (6-8 hours)

expressions for the same TGF-β1 dependent conditions suggest that increased integrin expression does not lead to integrin-CAM mediated cell-cell adhesion. We also investigated the effect of soluble factors on focal adhesion (FA) complex protein vinculin. Adhesion and migration processes are shown to be dependent on FA-related parameters including, spatio-temporal distribution and size of FAs [7,15,20]. Interestingly, overall expression of vinculin (the load bearing member of FA complex) did not change; however, vinculin was more distributed. A possible explanation can be that with the enhanced number of stress fibers and increased intracellular stiffness, the force distribution can be optimized by distributing sites of interaction between FA and actin-fibers. Additionally, more surface integrins can form clusters at these new sites of interactions leading to adhesive strengthening with enhanced number of cell-ECM bonds.

MSC migration is critical for *in vivo* events such as cancer growth and wound healing [34,35]. We investigated role of PDGF and TGF-β1 in regulating MSC migration in both random (motility assay) and directed manner (scratch assay). and PDGF was found to enhance the MSC motility in both assays in agreement with literature [23]. PDGF receptor mediated activation of PI3-K (Phosphoinositide-3-kinase)-AKT pathway is central for cell migration [36,37] and it is possibly contributing to the enhanced migration observed in our studies. However, the role of TGF-β1 is not as straightforward as PDGF and we found both in literature and our studies that it can be much more complex. TGF-β1 individually did not have any effect on migration of MSCs. Interestingly, TGF-β1 enhanced PDGF dependent MSC migration in a scratch assay. For

individual TGF-β1 treatment, adhesive strengthening can be detrimental to migration albeit generating higher intracellular contractile forces. And it is only in presence of PDGF; TGF-β1 treated cells can generate enough contractility elongation to overcome the adhesive force barrier to induce migration. However, due to formation of high density of actin stress fibers in this case, cells prefer more persistent migration in one direction leading to enhanced motility in scratch assay. Taken together, these results suggest that TGF-β1 plays a profound role in controlling the individual cell and overall tissue mechanical behavior in tumors and wound sites.

5.5. CONCLUSIONS

Both PDGF and TGF-β1 have been shown interact with MSCs *in vivo* regenerative niches and their influence on MSC function can be complementary. TGF-β1 has been shown to induce differentiation of MSCs into contractile smooth muscle cells (SMCs); whereas, endothelial cell-secreted PDGF is important in recruitment SMCs and stabilization of the newly formed blood vessels. We found that TGF-β1 increased integrin-dependent adhesion strength and enhanced directional migration of cells in the presence of other chemotactic factors such as PDGF. The enhanced integrin based adhesion can increase engraftment efficiency and the increased directional migration can be beneficial for homing towards inflamed tissues. Combined with the previously observed morphological elongation and mechanical stiffening of MSCs (chapter 4) after TGF-β1 treatment, these results provide new insights into MSC function in presence of these soluble factors at regeneration sites. More importantly, this study can be used to design preconditioning of MSCs prior to transplantation (both locally and systemically) to increase efficacy of cell based therapeutics.

5.6. REFERENCES

1. Discher DE, DJ Mooney and PW Zandstra. (2009). Growth factors, matrices, and forces combine and control stem cells. Science 324:1673-1677.

2. Parsons JT, AR Horwitz and MA Schwartz. (2010). Cell adhesion: integrating cytoskeletal dynamics and cellular tension. Nature reviews Molecular cell biology 11:633-643.

3. Chiarugi P and E Giannoni. (2008). < i> Anoikis</i>: A necessary death program for anchorage-dependent cells. Biochemical pharmacology 76:1352-1364.

4. Barczyk M, S Carracedo and D Gullberg. (2010). Integrins. Cell and tissue research 339:269-280.

5. Bershadsky AD, NQ Balaban and B Geiger. (2003). Adhesion-dependent cell mechanosensitivity. Annual review of cell and developmental biology 19:677-695.

6. Vogel V and MP Sheetz. (2009). Cell fate regulation by coupling mechanical cycles to biochemical signaling pathways. Current opinion in cell biology 21:38-46.

7. Wozniak MA, K Modzelewska, L Kwong and PJ Keely. (2004). Focal adhesion regulation of cell behavior. Biochimica et Biophysica Acta (BBA)-Molecular Cell Research 1692:103-119.

8. Evans EA and DA Calderwood. (2007). Forces and bond dynamics in cell adhesion. Science 316:1148-1153.

9. Bendeck MP, N Zempo, AW Clowes, RE Galardy and MA Reidy. (1994). Smooth muscle cell migration and matrix metalloproteinase expression after arterial injury in the rat. Circulation Research 75:539-45.

10. Mason DP, RD Kenagy, D Hasenstab, DF Bowen-Pope, RA Seifert, S Coats, SM Hawkins and AW Clowes. (1999). Matrix Metalloproteinase-9 Overexpression Enhances Vascular Smooth Muscle Cell Migration and Alters Remodeling in the Injured Rat Carotid Artery. Circulation Research 85:1179-1185.

11. Friedl P and D Gilmour. (2009). Collective cell migration in morphogenesis, regeneration and cancer. Nature reviews Molecular cell biology 10:445-457.

12. Ridley AJ, MA Schwartz, K Burridge, RA Firtel, MH Ginsberg, G Borisy, JT Parsons and AR Horwitz. (2003). Cell Migration: Integrating Signals from Front to Back. Science 302:1704-1709.

13. Gardel ML, IC Schneider, Y Aratyn-Schaus and CM Waterman. (2010). Mechanical integration of actin and adhesion dynamics in cell migration. Annual review of cell and developmental biology 26:315-333.

14. Vicente-Manzanares M, DJ Webb and AR Horwitz. (2005). Cell migration at a glance. Journal of Cell Science 118:4917-4919.

15. Gupton SL and CM Waterman-Storer. (2006). Spatiotemporal feedback between actomyosin and focal-adhesion systems optimizes rapid cell migration. Cell 125:1361-1374.

16. DiMilla PA, JA Stone, JA Quinn, SM Albelda and DA Lauffenburger. (1993). Maximal migration of human smooth muscle cells on fibronectin and type IV collagen occurs at an intermediate attachment strength. The Journal of Cell Biology 122:729-737.

17. Palecek SP, JC Loftus, MH Ginsberg, DA Lauffenburger and AF Horwitz. (1997). Integrin-ligand binding properties govern cell migration speed through cell-substratum adhesiveness. Nature 385:537-540.

18. Lo C-M, H-B Wang, M Dembo and Y-l Wang. (2000). Cell movement is guided by the rigidity of the substrate. Biophysical journal 79:144-152.

19. Isenberg BC, PA DiMilla, M Walker, S Kim and JY Wong. (2009). Vascular smooth muscle cell durotaxis depends on substrate stiffness gradient strength. Biophysical journal 97:1313-1322.

20. Plotnikov SV, AM Pasapera, B Sabass and CM Waterman. (2012). Force fluctuations within focal adhesions mediate ECM-rigidity sensing to guide directed cell migration. Cell 151:1513-1527.

21. Petrie RJ, AD Doyle and KM Yamada. (2009). Random versus directionally persistent cell migration. Nature Reviews Molecular Cell Biology 10:538-549.

22. Raftopoulou M and A Hall. (2004). Cell migration: Rho GTPases lead the way. Developmental biology 265:23-32.

23. Ponte AL, E Marais, N Gallay, A Langonne, B Delorme, O Herault, P Charbord and J Domenech. (2007). The *in vitro* migration capacity of human bone marrow mesenchymal stem cells: comparison of chemokine and growth factor chemotactic activities. Stem cells 25:1737-1745.

24. Andrae J, R Gallini and C Betsholtz. (2008). Role of platelet-derived growth factors in physiology and medicine. Genes & development 22:1276-1312.

25. Hellstrom M, P Lindahl, A Abramsson and C Betsholtz. (1999). Role of PDGF-B and PDGFR-beta in recruitment of vascular smooth muscle cells and pericytes

during embryonic blood vessel formation in the mouse. Development 126:3047-3055.

26. Zhen X, MX SHEN, D Zhu, LY WANG and XL ZHA. (2003). TGF-β1-promoted epithelial-to-mesenchymal transformation and cell adhesion contribute to TGF-β1-enhanced cell migration in SMMC-7721 cells. Cell research 13:343-350.

27. Giehl K and A Menke. (2006). Moving on: Molecular mechanisms in TGFβ-induced epithelial cell migration. Signal Transduction 6:355-364.

28. Deng B, X Yang, J Liu, F He, Z Zhu and C Zhang. (2010). Focal adhesion kinase mediates TGF-β1-induced renal tubular epithelial-to-mesenchymal transition *in vitro*. Molecular and cellular biochemistry 340:21-29.

29. Schabort EJ, M Van der Merwe and CU Niesler. (2011). TGF-β isoforms inhibit IGF-1-induced migration and regulate terminal differentiation in a cell-specific manner. Journal of muscle research and cell motility 31:359-367.

30. Castañares C, M Redondo-Horcajo, N Magán-Marchal, P ten Dijke, S Lamas and F Rodríguez-Pascual. (2007). Signaling by ALK5 mediates TGF-β-induced ET-1 expression in endothelial cells: a role for migration and proliferation. Journal of Cell Science 120:1256-1266.

31. Dickinson RB and RT Tranquillo. (1993). Optimal estimation of cell movement indices from the statistical analysis of cell tracking data. AIChE journal 39:1995-2010.

32. Cavalcanti-Adam EA, T Volberg, A Micoulet, H Kessler, B Geiger and JP Spatz. (2007). Cell spreading and focal adhesion dynamics are regulated by spacing of integrin ligands. Biophysical journal 92:2964-2974.

33. Kean TJ, P Lin, AI Caplan and JE Dennis. (2013). MSCs: Delivery Routes and Engraftment, Cell-Targeting Strategies, and Immune Modulation. Stem Cells International 2013:13.

34. Sasaki M, R Abe, Y Fujita, S Ando, D Inokuma and H Shimizu. (2008). Mesenchymal stem cells are recruited into wounded skin and contribute to wound repair by transdifferentiation into multiple skin cell type. the Journal of immunology 180:2581-2587.

35. Li L and J Jiang. (2011). Regulatory factors of mesenchymal stem cell migration into injured tissues and their signal transduction mechanisms. Frontiers of medicine 5:33-39.

36. Goncharova EA, AJ Ammit, C Irani, RG Carroll, AJ Eszterhas, RA Panettieri and VP Krymskaya. (2002). PI3K is required for proliferation and migration of human pulmonary vascular smooth muscle cells. American Journal of Physiology-Lung Cellular and Molecular Physiology 283:L354-L363.

37. Jiménez C, RA Portela, M Mellado, JM Rodríguez-Frade, J Collard, A Serrano, C Martínez-A, J Avila and AC Carrera. (2000). Role of the PI3K regulatory subunit in the control of actin organization and cell migration. The Journal of cell biology 151:249-262.

CHAPTER 6: MOLECULAR PROFILING OF MESENCHYMAL STEM CELLS AFTER TREATMENT WITH TGF-β1 AND PDGF

Though a variety of soluble factors have been shown to increase MSC migration and engraftment [1,2], the complex signaling cascades controlling this response remain poorly understood. Our earlier work showed that both murine [3] and human [4] MSCs undergo dramatic cytoskeletal stiffening in response to the cocktail of pro-migratory molecules released by tumor cells. These soluble factors include PDGF and TGF-β1, which play important roles in recruiting MSCs to target sites and influencing their growth and regenerative capacity [5]. To gain molecular insight into the role of these two factors in regulating MSC behavior, we characterized their effects individually and in combination on the transcriptional profile of MSCs using high-throughput genome wide microarray analysis.

6.1. INTRODUCTION

Mesenchymal stem cells (MSCs) migrate from their *in vivo* niche and engraft in the damaged tissues and tumors where they aid in tissue regeneration and growth by secreting soluble growth factors, interacting with immune cells, and differentiating into tissue-specific cell types [6-9]. Soluble growth factors secreted by inflamed tissues and tumors interact with MSCs in their *in vivo* niche and control their mobilization and recruitment to the target sites [7]. When the cells are infused systemically or directly transplanted locally for therapeutic applications, the initial interaction with these niche specific factors (especially after reaching the target site) can largely determine the fate of

incorporated MSCs and is not completely understood. Here we have investigated the role of two representative factors present in inflammatory niches, including PDGF-BB (referred as PDGF) and TGF-β1, on MSC gene expression.

Platelets at the site of inflammation release PDGF and TGF-β1 to orchestrate recruited cell functions that benefit regeneration process [9,10]. In chronic illness, the rapid degradation of these growth factors has been associated with impaired cellular function in wound bed [11,12]. In previous chapters, treatment of MSCs with TGF-β1 resulted in pronounced elongation, cytoskeletal reorganization, increased stress fiber density, enhanced adhesion and increased stiffness; whereas, PDGF profoundly increased cell motility but did not modify other physical aspects of the cells. To explore the broader molecular impact of these growth factors on MSCs, we conducted a detailed gene expression analysis (Affymetrix) of MSCs grown in media supplemented with PDGF and TGF-β1 alone and in combination. Molecularly high-throughput gene expression analysis (Affymetrix MG430 2.0) demonstrated significant gene expression changes when MSCs were treated either with TGF-β1 alone or in combination with PDGF; however, PDGF alone resulted in relatively few changes in comparison to TGF-β1. Pair-wise comparisons of the genome-wide expression profiles of treated and control cells revealed TGF-β1 regulated genes involved in cytoskeletal organization, cell adhesion and extracellular matrix (ECM) remodeling, production of actin-binding proteins, and epithelial-to-mesenchymal transition (EMT).

6.2. MATERIALS AND METHODS

Materials: IMDM, DMEM, L-glutamine, penicillin-streptomycin and trypsin were purchased from Mediatech and fetal bovine serum (FBS) was purchased from Atlanta

Biologicals. Recombinant human proteins TGF-β1 and PDGF-BB (referred to as PDGF) were purchased from Biolegend. All other reagents were purchased from VWR unless otherwise specified.

MSC isolation and culture: Murine MSCs were isolated from the bone marrow of 6-10 weeks old adult male Balb/C mice (Charles River Laboratories, Wilmington, MA) and cultured in normal growth media (IMDM media supplemented with 20% FBS, 2 mM L-glutamine, 100U/ml penicillin, and 100U/ml streptomycin). Briefly, tibiae and femurs of the mice were extracted and crushed in FBS. Cold PBS and collagenase I (2mg/ml) solutions were added subsequently to facilitate cell extraction from bone with minimal cell damage. Finally, the solution mixture was filtered (70 μm cell strainer) and centrifuged (1000xg for 10 minutes) to recover the bone marrow cell population in pellet form. Media was supplanted regularly to remove non-adherent BM cell populations. Once the adherent cells reached 80-90% confluency, the cell culture was expanded and subsequently purified using EasySep™ Mouse SCA1 Positive Selection Kit (StemCell Technologies). Purified MSCs between passages 2-6 were used for all studies.

Soluble factor treatment: Soluble factor dilutions were created in serum-free DMEM immediately before use. All experiments were carried out with four conditions: serum-free control media, 5ng/ml PDGF, 5ng/ml TGF-β1 and combination of PDGF and TGF-β1- each 5ng/ml. MSCs were treated for 24 hours unless otherwise specified.

Microarray data analysis: Gene expression analysis of treated and untreated MSCs was performed in triplicate using three independent replicates per condition. The Affymetrix GeneChip Mouse Genome 430 2.0 microarray chips were used for these studies. Affymetrix .CEL files were processed using Expression Console Software Version 1.1

with the RMA algorithm (Robust Microarray Analysis). The normalized expression values of each gene were $\log_2$ transformed and used for further analysis.

Unsupervised analysis: From the initial 45,101 probe sets (genes) on the Affymetrix Mouse Genome 430 2.0 chip, 42,129 displayed marginal differences in expression across all samples (standard deviation ≤ 0.5 from the mean of all samples) and were filtered out. The remaining 2,972 probe sets were employed in the unsupervised clustering analysis using the Spotfire Decision Site 9.1.2 (TIBCO Software: http://spotfire.tibco.com/) with the UPGMA (unweighted average) method and the Euclidean distance as the similarity measure.

Supervised analysis: From the initial 45,101 probe sets (genes) on the Affymetrix Mouse Genome 430 2.0 chip, 13,777, 19,672 and 19,618 genes displayed expression values ≥ 0.2 SD from the mean across the control and the cell treatments of PDGF, TGF- β1 and PDGF-TGF-β1 respectively. From these, the differentially expressed genes between each cell treatment (PDGF, TGF-β1 and PDGF-TGF-β1) and the control samples were computed using stringent false discovery rate (FDR) criteria. The significant probe sets were 842 (FDR of 1.5%), 10,617 (FDR of 2.4%) and 8,117 (FDR of 2.13%) for the PDGF, TGF-β1 and PDGF-TGF-β1 respectively. These genes were employed in pathway enrichment analyses using the GeneGO software.

6.3. RESULTS

Expression profiling reveals distinct genes and pathways in MSC treated with the TGF-β1, PDGF and the combined PDGF and TGF-β1: From the initial 45,101 probe sets of the Affymetrix Mouse Genome 430 2.0 chip, any housekeeping genes and

potential experimental noise was excluded by discarding all probe sets with expression variation of standard deviation ≤ 0.5 among the 12 samples of cell treatments and controls. The remaining 2,972 probe sets were used for the unsupervised hierarchical clustering and initial expression pattern discovery (Figure 6-1). Unsupervised analysis showed expression profiles of TGF-β1 grouped with the combined PDGF and TGF-β1 cell treatment and did not group with the PDGF and control treatments.

In order to investigate further the differences between each cell treatment and control, and between treatments, we estimated the number of significantly differentially expressed probe sets. The Significance Analysis of Microarrays (SAM) revealed greater number of differentially expressed probe sets for TGF-β1 (10,617 probe sets of FDR 2.4% or 23.5% of the initial 45,101 probe sets of the Affymetrix Mouse Genome 430 2.0 chip) but fewer probe sets for the combined TGF-β1 and PDGF (8,117 differentially expressed probe sets of FDR 2.13% or 18.0% of the initial 45,101 genes of Affymetrix Mouse Genome 430 2.0 chip). Even fewer probe sets were estimated for PDGF (only 842 differentially expressed probe sets of FDR 1.5% or 1.87% of the initial 45,101 genes of Affymetrix Mouse Genome 430 2.0 chip).

The number of significantly differentially expressed genes between treatments and controls were 589, 6,751, and 5,292 for the PDGF, TGF-β1 and the combined PDGF and TGF-β1 treatments respectively (Figure 6-2). We identified the most highly regulated (both up and down) genes for each treatment condition sorting by the $\log_2$ratio value. The top 15 upregulated genes and downregulated genes for each treatment conditions compared to control are listed in Appendix C (Table C-2 and Table C-4).

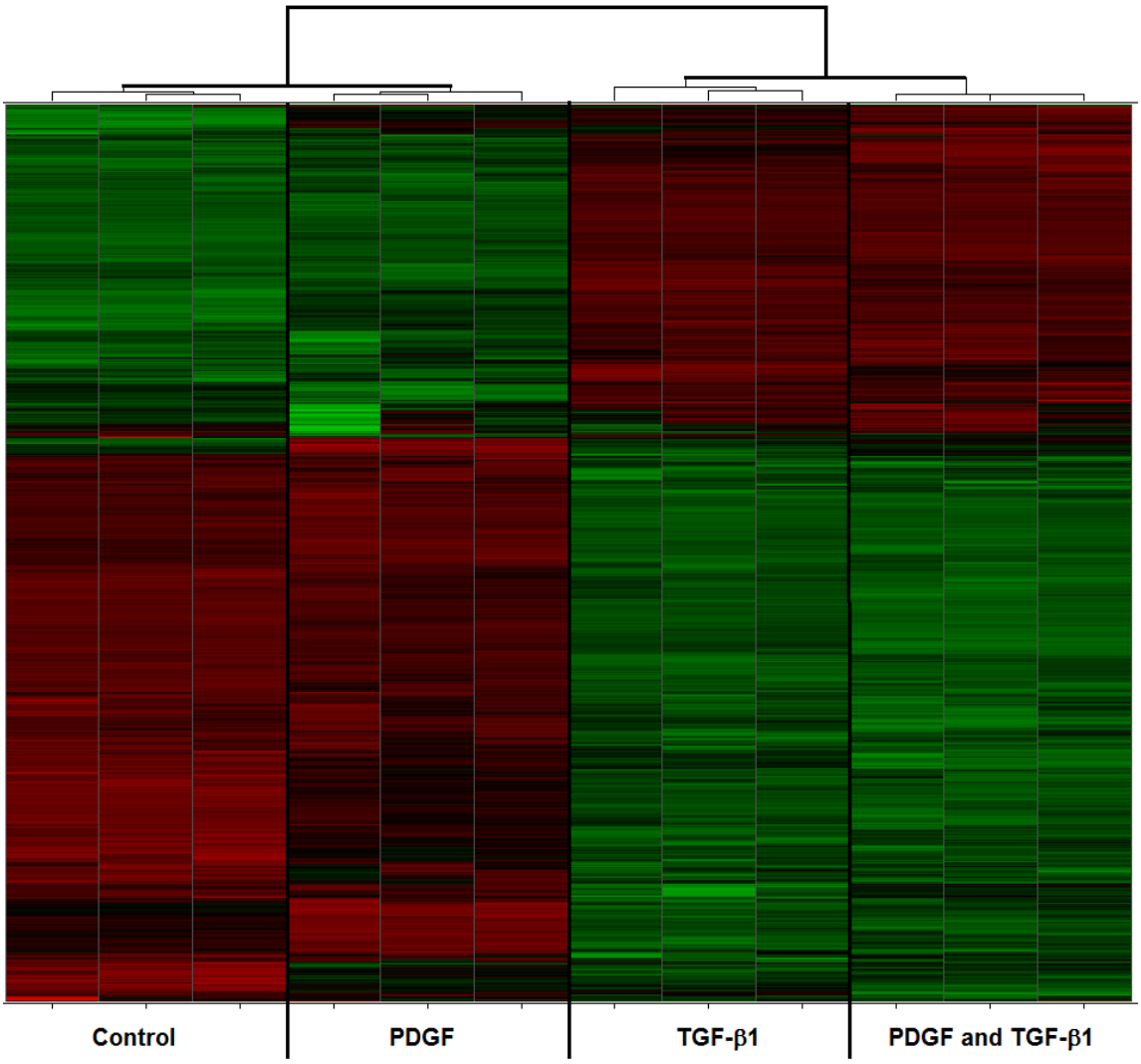

Figure 6-1. *Heatmap of Unsupervised clustering of all microarray probes***.** Heatmap indicating significant changes (FDR p value ≤ 0.05) in gene expression (black, no change; red, increase; green, decrease) due to serum-free, PDGF, TGF-β1 and combination of PDGF and TGF-β1 (n=3).

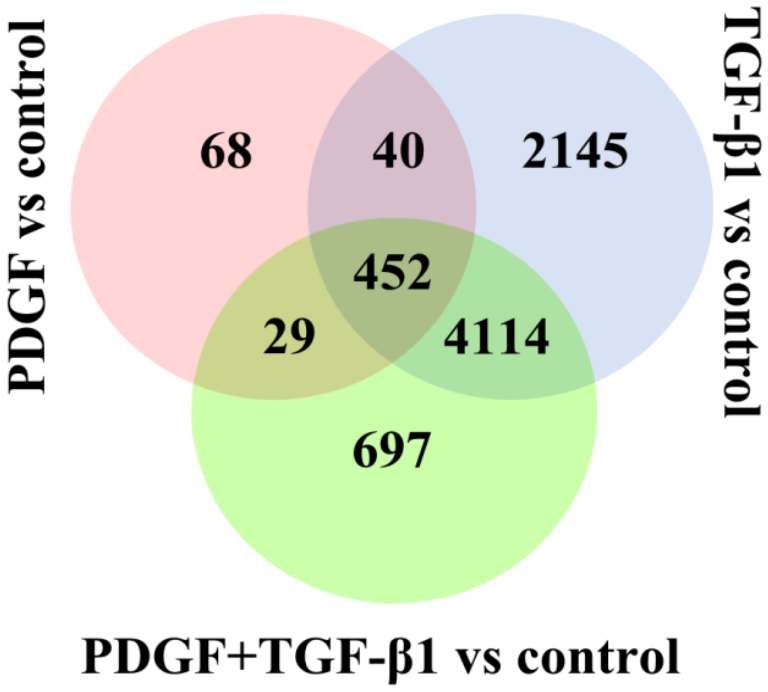

Figure 6-2. *Venn diagram depicts the number of genes regulated in a soluble factor treatment-specific and non-specific manner within each segment (n=3).*

Adiponectin (Adipoq), endothelial cell-specific molecule 1 (Esm1), insulin-like growth factor 2 (Igf2) and vascular cell adhesion molecule 1 (Vcam1) genes were all downregulated for all three conditions; however, no such commonality was observed for upregulated genes. Additionally the genes regulated for the combination treatment were heavily populated by the genes controlled by TGF-β1 treatment, suggesting that TGF-β1 plays the dominant role in the combination treatment. It is also noteworthy that for both TGF-β1 and combination treatment, the most upregulated genes were associated with adhesion and extracellular matrix (ECM) remodeling (example: *Periostin (Postn), tenascin C (Tnc), hyaluronan synthase 2 (Has2)*).

Differentially expressed genes display distinct pathway enrichment in TGF-β1 and PDGF: The most significantly enriched pathways for each treatment regime are listed in Table 6-1. Consistent with the highly upregulated gene list, the most significantly enriched pathway across all treatments was the Cell Adhesion and ECM remodeling pathway. Other significantly enriched pathways among TGF-β1 treated cells were cytoskeletal remodeling and developmental processes related to epithelial-to-mesenchymal transition (EMT). The pathways significantly enriched after the combined PDGF and TGF-β1 treatments were a mixture of pathways significantly enriched in one or other of the individual treatments. The role of TGF-β1 became more prominent when we clustered the total number of regulated genes for a particular pathway (Figure 6-3). TGF-β1 alone and in combination regulated most genes for motility, adhesion, EMT, cytokines, chemokines, and chemokine receptors. Since TGF-β1 has most profoundly influenced the transcriptional profile of MSCs, we analyzed the three significantly regulated networks to provide further insight (Figure 6-4, Figure 6-5 and Figure 6-6). Networks depicting cytoskeletal remodeling and adhesion pathways share a number of molecules due to the interconnectivity between the processes. Genes encoding actin binding proteins (α-actinin, arp2/3), focal adhesion proteins (talin, vinculin) and wnt signaling pathway molecules that actively participate in actin reorganization were all upregulated. Similar constitutive upregulation was also noticeable for the cell surface integrins that connect the cytoskeletal network to ECM. Although the small RhoGTPases were not differentially regulated at the mRNA level, other elements of the actin-myosin contractility pathway were differentially regulated in

Table 6-1. Treatment specific 10 most significant enriched pathways.

PDGF vs Control	pValue	TGF-β1 vs Control	pValue	PDGF+TGF-β1 vs Control	pValue
Cell Adhesion and ECM remodeling	3.52e-6	Cell Adhesion and ECM remodeling	8.90e-10	Cell Adhesion and ECM remodeling	2.60e-10
Immune response: IL17 signaling pathways	1.20e-5	Cytoskeleton remodeling	2.08e-9	Development: regulation of EMT	6.11e-9
Immune response: IL16 signaling pathway	8.22e-5	Chemokines and cell adhesion	3.40e-9	Development: TGF-beta-dependent induction of EMT via SMADs	1.00e-8
Protein folding and Bradykinin/Kallidin maturation	9.92e-5	Development: regulation of EMT	6.39e-9	Immune response: Oncostatin M signaling via JAK-Stat in human cells	8.72e-7
Immune response: Lectin induced complement pathway	1.58e-4	TGF,WNT dependent cytoskeletal remodeling	1.68e-8	Signal transduction: cAMP signaling	2.07e-6
Immune response: Oncostatin M signaling via MAPK	1.67e-4	Development: TGF-beta-dependent induction of EMT during via SMADs	1.79e-8	TGF,WNT dependent cytoskeletal remodeling	4.61e-6
Immune response: Oncostatin M signaling via MAPK in human cells	2.30e-4	Some pathways of EMT in cancer cells	7.46e-8	PGE2 pathways in cancer	4.82e-6
Immune response: Classical complement pathway	2.31e-4	PGE2 pathways in cancer	1.28e-7	Development: Transcription regulation of granulocyte development	6.87e-6
Mechanism of Pioglitazone/Metformin and Rosiglitazone /Metformin cooperative action in Diabetes mellitus, Type 2	4.80e-4	Development: Flt3 signaling	9.34e-7	Development: WNT signaling pathway, Part 2	1.20e-5
		Development: TGF-beta-dependent induction of EMT via MAPK	9.46e-7	Role of Diethylhexyl Phthalate and Tributyltin in fat cell differentiation	1.25e-5

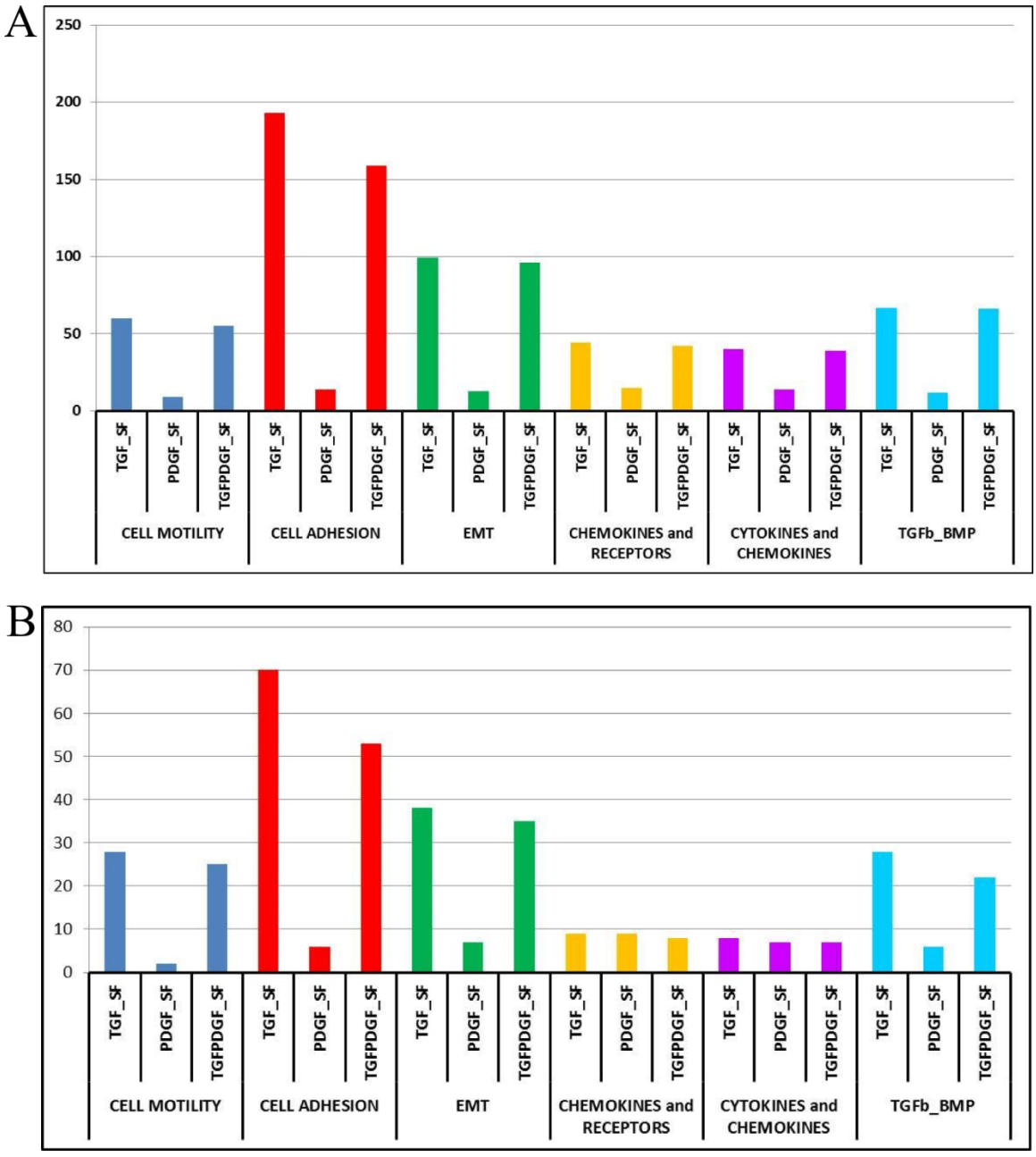

Figure 6-3. *(A) Total number of differentially expressed genes of specific pathways (B) Total number of upregulated genes of specific pathways (without duplicate probes)*

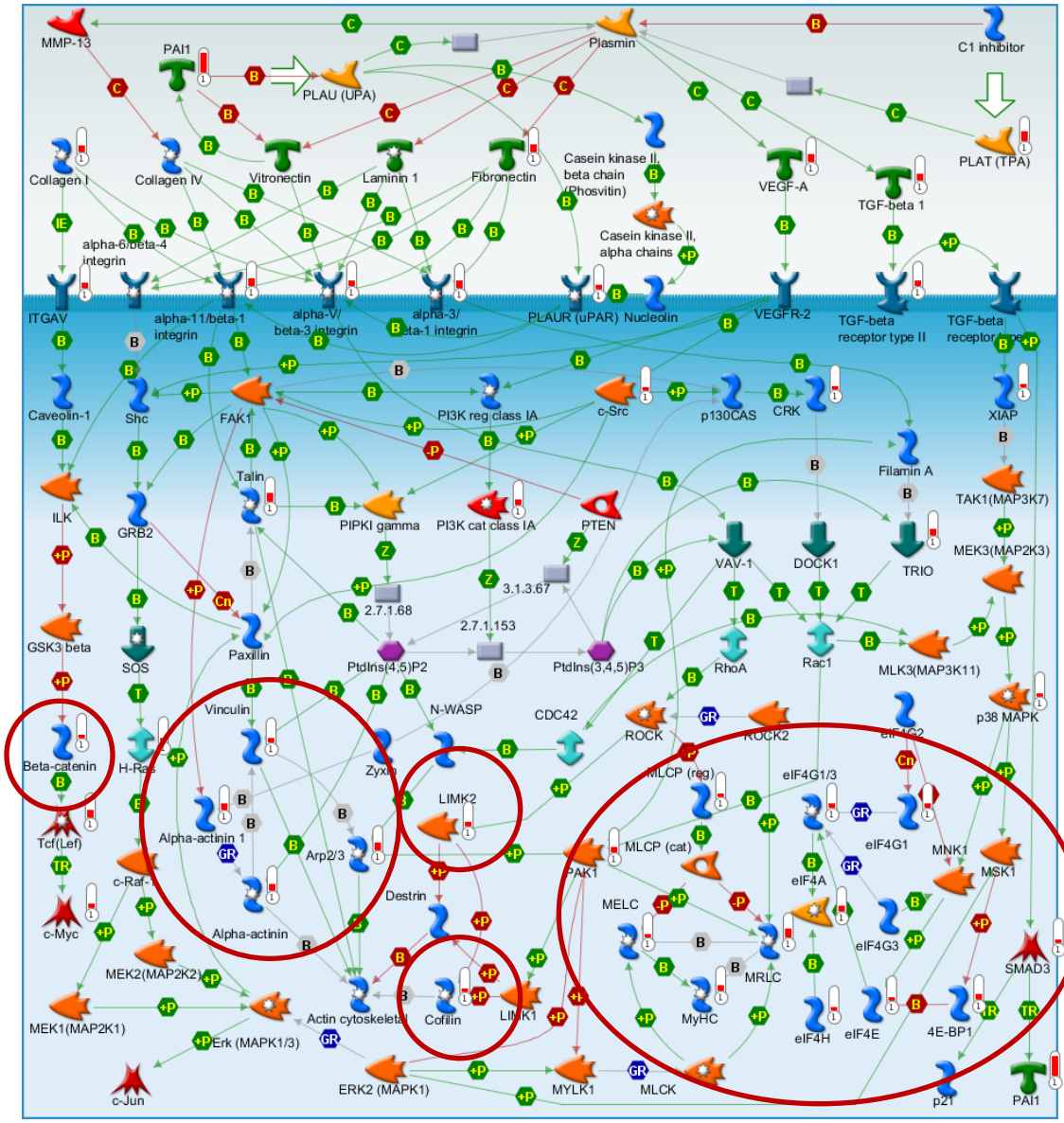

Figure 6-4. *Regulated genes related to cytoskeletal remodeling in TGF-β1 treated cells compared to control.* Red thermometer: genes transcriptionally up-regulated in MSCs; blue thermometer: genes transcriptionally down-regulated in MScs.

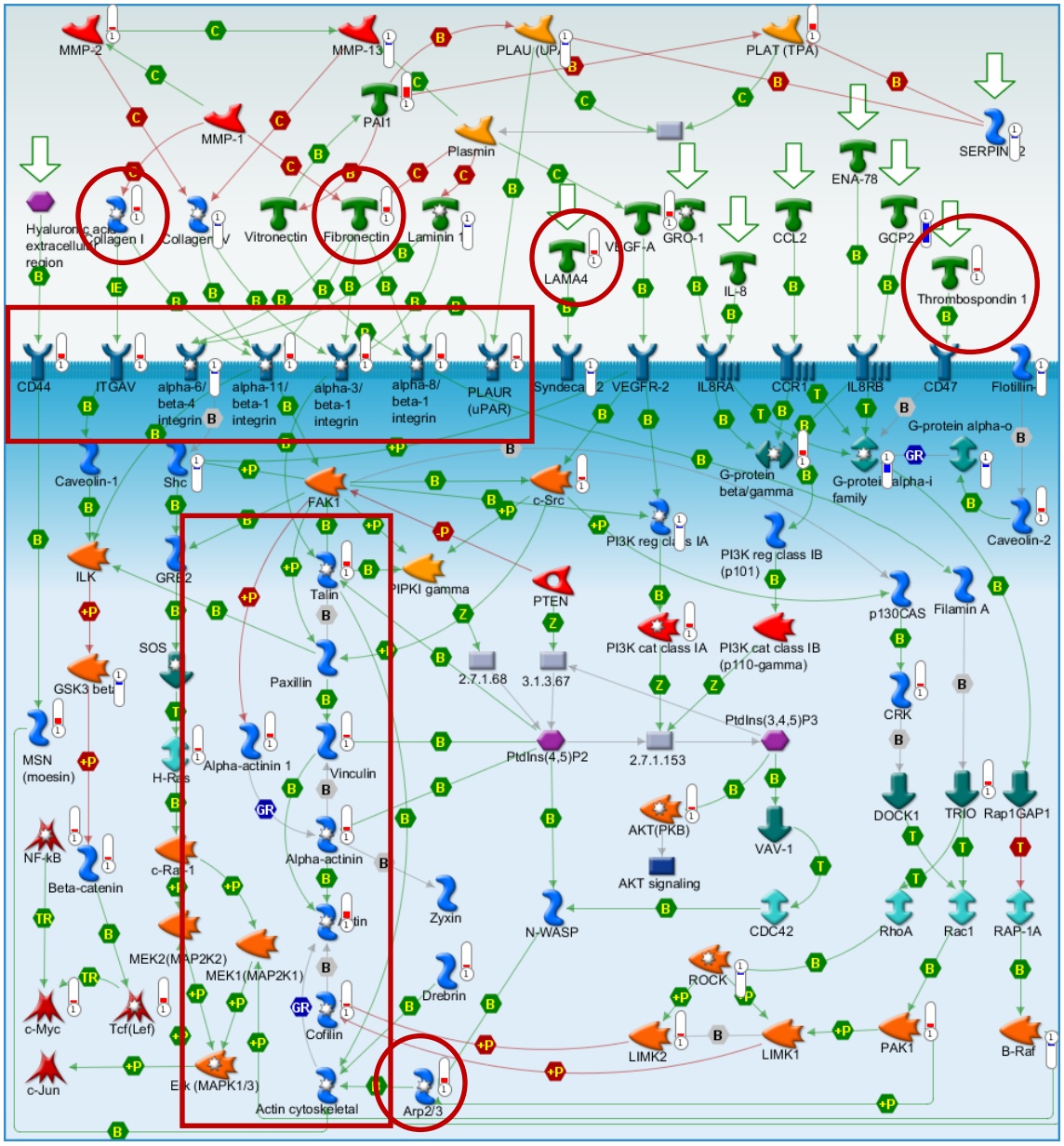

Figure 6-5. *Regulated genes related to Chemokines and Adhesion in TGF-β1 treated cells compared to control.* Red thermometer: genes transcriptionally up-regulated in MSCs; blue thermometer: genes transcriptionally down-regulated in MScs.

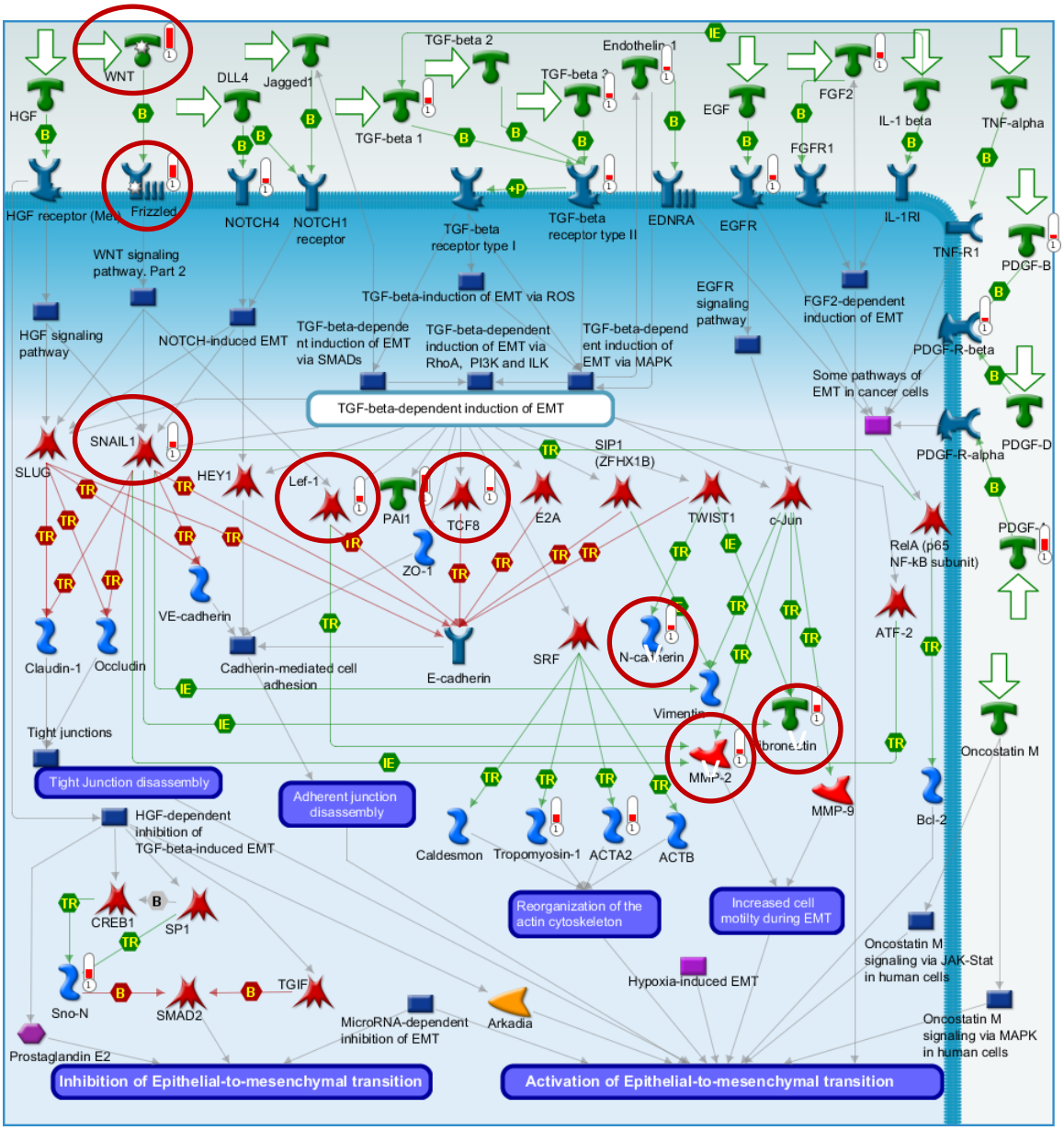

Figure 6-6. *Regulated genes related to Epithelial to mesenchymal transition (EMT) in TGF- β1 treated cells compared to control*. Red thermometer: genes transcriptionally up-regulated in MSCs; blue thermometer: genes transcriptionally down-regulated in MSCs

TGF-β1 treated cells, including nucleotide exchange factors that regulate RhoGTPases like *EIF, myosin light chain phosphatase (MLCP) and LIM kinase-2 (LIMK2)*. During EMT, transcription factors like TCF, LEF (associates with β catenin in Wnt signaling pathway), snail mediate cytoskeletal remodeling that contribute to invasive phenotype of the cells. These transcription factors along with expression of N-cadherin (mesenchymal marker) are used a biomarker for EMT process. All these factors were found to be upregulated in TGF-β1 treated MSCs.

TGF-β1 closely control of actin-binding proteins: The structure and function of cytoskeletal actin is controlled by actin-binding proteins (ABPs), which bind to actin filaments and modulate their length, stability, and cytoskeletal attachments [13,14], . With the high impact of TGF-β1 on cytoskeletal structure, its effects on ABPs were assessed using microarray analysis from curated GO gene sets available from Broad Institute's Molecular Signature Database (MSigDB) (Table 6-2). Stabilizing proteins were constitutively up-regulated in TGF-β1 treated MSCs; whereas, capping and severing proteins were constitutively down-regulated (Table 6-2). Tropomyosin stabilizes actin bundles by protecting them from ADF/cofilin and interacts with troponin to regulate the interaction of actin and myosin. *Tropomyosin-1* (*Tpm1*) along with *troponin* (*Tnnt2*) was up-regulated; whereas, its inhibitor *tropomodulin* (*Tmod3*) was down-regulated in TGF-β1 treated cells. Bundling and crosslinking proteins regulate cell tension through close association with actin stress fibers. Bundling proteins *α-actinin-1* (*Actn1*) and *transgelin* (*Tagln*) were up-regulated and other cross-linkers such as *α2 and β2 spectrins* (*Spna2, Spnb2*) which play a key role in membrane anchoring of actin, were down-regulated. Membrane anchoring proteins, which tether intracellular domains of actin to membrane

proteins, were mostly up-regulated with the exception of *ezrin* (*Ezr*) and aforementioned *spectrins*. *Ezr* belongs to ERM family of anchoring proteins with other members being *moesin* (*Msn*) and *radixin* (*Rdx*). *Msn*, which directly regulates cortical rigidity in dividing cells, was up-regulated in TGF-β1 treated cells; however, change in *Rdx* expression was not significant. These regulation patterns of ERM proteins are in agreement with previous studies with TGF-β1 treated epithelial cells.

6.4. DISCUSSION

We have previously characterized the effects of soluble growth factors PDGF and TGF-β1 both alone and in combination on the physical and functional properties of MSCs. While PDGF did not significantly influence the physical properties of MSCs, cells exhibited enhanced motility in its presence. On the other hand TGF-β1 enormously affected both physical and functional behavior of the cells as suggested by dramatic elongation, cytoskeletal reorganization, intracellular stiffening and adhesion strengthening on matrix. For the combined treatment, cellular properties were dictated predominantly by TGF-β1, however, synergistic effects were identified for certain aspects such as intracellular stiffening, elongation and directed migration towards scratch.

To understand cytoskeletal re-organization and mechanical stiffening response, we focused on genes that encode for actin-binding proteins (ABPs) that directly control actin remodeling. The filamentous actin cytoskeletal network is dynamically regulated by several classes of ABPs: cross-linkers and bundlers, which construct higher order network structure; stabilizers that sustain unidirectional growth and protection from

Table 6-2. Regulation of actin-binding proteins (ABPs) in response to soluble factor treatment.

	Probe Set ID	Gene Symbol	Gene Title	PDGF vs Control	TGF-β1 vs Control	(PDGF+TGF-β1) vs Control	TGF-β1 vs PDGF	(PDGF+TGF-β1) vs TGF-β1
	1434013_at	*Ablim3*	actin binding LIM protein family, member 3	NS	0.86	1.39	NS	0.85
Bundling and crosslinking	1427735_a_at	*Acta1*	actin, alpha 1, skeletal muscle	NS	1.80	1.03	1.87	1.02
	1422340_a_at	*Actg2*	actin, gamma 2, smooth muscle, enteric	NS	2.12	1.08	2.56	1.53
	1452415_at	*Actn1*	actinin, alpha 1	NS	1.08	1.07	0.83	0.78
	1423505_at	*Tagln*	transgelin	NS	2.46	1.13	2.91	1.60
Membrane anchoring	1450850_at	*Ezr*	ezrin	NS	-1.33	-1.97	-0.99	-1.66
	1450379_at	*Msn*	moesin	NS	1.96	2.13	1.61	1.76
	1427889_at	*Spna2*	spectrin alpha 2	NS	-0.94	-1.18	NS	-0.71
	1419256_at	*Spnb2*	spectrin beta 2	NS	-0.92	-1.06	NS	-0.66
Stabilising	1435287_at	*Add2*	adducin 2 (beta)	NS	0.99	1.54	1.02	1.30
	1417917_at	*Cnn1*	calponin 1	NS	2.40	1.84	2.58	1.98
	1418726_a_at	*Tnnt2*	troponin T2, cardiac	NS	2.85	3.57	3.35	3.89
	1428650_at	*Tns1*	tensin 1	NS	2.28	2.10	2.50	2.28
	1456623_at	*Tpm1*	tropomyosin 1, alpha	NS	1.07	1.00	NS	NS
Capping and severing	1435557_at	*Fhod1*	formin homology 2 domain containing 1	NS	-0.56	-0.48	NS	NS
	1423088_at	*Tmod3*	tropomodulin 3	NS	-0.40	-0.63	NS	NS
	1449969_at	*Tmod4*	tropomodulin 4	NS	-0.89	-1.22	-0.76	-0.95

severing; nucleation and branch forming proteins, which initiate filament formation; monomer binders, capping and severing proteins controls the polymerization and depolymerization of actin filaments. Cells treated with TGF-β1 and combination of PDGF and TGF-β1 up-regulated gene expression of bundling, crosslinking and stabilizing proteins. Other groups of proteins associated with branch formation, capping and severing were generally down-regulated, facilitating unidirectional growth of actin filaments and stress fibers. Crosslinking and bundling proteins can affect both the overall network architecture and the ability to dynamically re-organize these networks.

MSC treatment with TGF-β1 also resulted in enhanced expression of matrix proteins, like *collagen (Col), fibronectin (Fbn), and tenascin C (Tnc),* and *matrix metalloproteinases (Mmp)* (Table C-2) important in remodeling the ECM of the wound bed and tumor microenvironment. Intracellular mechanical forces on the local environment may induce further remodeling of the extracellular matrix through physical interactions. Taken together, these results suggest that TGF-β1 has a profound role in controlling the individual cell and overall tissue mechanical behavior in tumors and wound sites.

6.5. CONCLUSIONS

In summary, genome wide microarray analysis demonstrated the effect of TGF-β1 on the transcriptional profile of MSCs, which was much more profound than PDGF; however, cross talk between the two signaling pathways can synergistically enrich and influence certain MSC behavior. Genes essential for cytoskeletal reorganization, adhesion and matrix remodeling were constitutively upregulated in a TGF-β1-dependent manner. Changes in gene expression after treatment with TGF-β1 were corroborated with the

functional differences observed in chapter 4-5, including (1) actin-binding protein mediated elongation and stiffening and (2) integrin mediated adhesive strengthening. Interestingly, genes related to multiple differentiation pathways were also regulated by TGF-β1, suggesting that short-term treatment with TGF-β1 simultaneously influences multiple lineage-specific differentiation pathways. Combined with high number of upregulated soluble factors, and ECM related genes, these results suggest that TGF-β1 plays a very critical role in inflammatory niches to regulate MSC function and fate at both short and longer time scales.

6.6. REFERENCES

1. Wang L, Y Li, X Chen, J Chen, S Gautam, Y Xu and M Chopp. (2002). MCP-1, MIP-1, IL-8 and ischemic cerebral tissue enhance human bone marrow stromal cell migration in interface culture. Hematology 7:113-117.

2. An P, H Lei, J Zhang, S Song, L He, G Jin, X Liu, J Wu, L Meng, M Liu and C Shou. (2004). Suppression of tumor growth and metastasis by a VEGFR-1 antagonizing peptide identified from a phage display library. Int J Cancer 111:165-73.

3. McGrail DJ, D Ghosh, ND Quach and MR Dawson. (2012). Differential mechanical response of mesenchymal stem cells and fibroblasts to tumor-secreted soluble factors. PloS one 7:e33248.

4. McGrail DJ, KM McAndrews and MR Dawson. (2012). Biomechanical analysis predicts decreased human mesenchymal stem cell function before molecular differences. Exp Cell Res.

5. Zhang Z, TM Garron, XJ Li, Y Liu, X Zhang, YY Li and WS Xu. (2009). Recombinant human decorin inhibits TGF-beta1-induced contraction of collagen lattice by hypertrophic scar fibroblasts. Burns 35:527-37.

6. Uccelli A, L Moretta and V Pistoia. (2008). Mesenchymal stem cells in health and disease. Nature Reviews Immunology 8:726-736.

7. Chamberlain G, J Fox, B Ashton and J Middleton. (2007). Concise review: mesenchymal stem cells: their phenotype, differentiation capacity, immunological features, and potential for homing. Stem cells 25:2739-2749.

8. da Silva Meirelles L, AM Fontes, DT Covas and AI Caplan. (2009). Mechanisms involved in the therapeutic properties of mesenchymal stem cells. Cytokine & growth factor reviews 20:419-427.

9. Spaeth E, A Klopp, J Dembinski, M Andreeff and F Marini. (2008). Inflammation and tumor microenvironments: defining the migratory itinerary of mesenchymal stem cells. Gene therapy 15:730-738.

10. Coussens LM and Z Werb. (2002). Inflammation and cancer. Nature 420:860-867.

11. Barrientos S, O Stojadinovic, MS Golinko, H Brem and M Tomic-Canic. (2008). PERSPECTIVE ARTICLE: Growth factors and cytokines in wound healing. Wound Repair and Regeneration 16:585-601.

12. Schultz GS, G Ladwig and A Wysocki. (2005). Extracellular matrix: review of its roles in acute and chronic wounds. World Wide Wounds 2005.

13. Uribe R and D Jay. (2009). A review of actin binding proteins: new perspectives. Molecular biology reports 36:121-125.

14. Winder SJ and KR Ayscough. (2005). Actin-binding proteins. Journal of cell science 118:651-654.

CHAPTER 7: TGF-β1 PRETREATMENT OF MESENCHYMAL STEM CELLS SUSTAINED IMPROVED FUNCTION BOTH *IN VITRO* AND *IN VIVO*

Wound healing is a complex biological process where recruited cells play a central role in regeneration. In cases of both acute and chronic wounds, this cellular response is arrested, contributing to non-healing wounds. The ability of mesenchymal stem cells (MSCs) to self-renew and differentiate into multiple connective cell lineages has distinguished them as ideal candidates for wound healing. Previous studies have demonstrated that transplanted MSCs can revive the wound healing process with improved wound closure rate and neovascularization in diabetic mice. However, the interaction of MSCs with soluble factors already present in these regenerative niches is not well characterized. Increased understanding of these interactions can lead to avenues for more efficient design of MSC-based therapeutics. We have previously demonstrated that transforming growth factor (TGF-β1), highly expressed in inflammatory sites, can stimulate MSCs to dramatically alter their physical and mechanical properties. More importantly, genome wide microarray results suggest that treated cells exhibit upregulated genes for adhesion, migration, and differentiation. In this study, we show MSCs pre-treated with TGF-β1 for 24 hours, show improved adhesion, and differentiation even after removal of stimulus leading to improved wound healing in mice.

7.1. INTRODUCTION

Injury to the skin results in the activation of the wound healing process, which is a complex series of events that includes inflammation, formation of granulation tissue, remodeling of an extracellular matrix (ECM), re-epithelialization, and scar tissue formation [1,2]. Growth factors are essential in mediating these wound healing stages, which proceed continuously from the time the skin is damaged until a scar is formed [3,4]. Elderly patients and patients suffering from chronic illness, including diabetes, ischemia, or hypertension, develop chronic wounds when the wound healing process is arrested in a state of chronic inflammation [1,5-8]. Two of the factors that have been associated with the formation of chronic wounds are: (1) impaired production of cytokines and growth factors and (2) reduced angiogensis (blood vessel formation) [9]. Mesenchymal stem cells (MSCs) (adult stem cells derived from bone marrow) have previously been shown to promote more rapid wound healing in diabetic mice, which was attributed to increased cytokine production [5]. Our study focused on the optimization of MSC migration in the wound bed. We hypothesized that migrating MSCs that disseminated throughout the wound bed would contribute to the formation of granulation tissue, which would constrict the wound for more rapid wound closure. Improved MSC migration could also improve the spatial and temporal activity of growth factors and cytokines since they were secreted from MSCs that disseminated throughout the wound tissue. More effective treatments for chronic wounds are urgently needed. Current therapies, which include wound debridement, negative-pressure therapy, growth factor replacement, biological dressing, skin grafts and cell-based therapies, have only increased the healing rate by up to 50%, and often times, this result was only temporary.

This study sought to understand if TGF-β1 pretreatment induced a sustained modification in MSC phenotype and behavior. TGF-β1 treatment resulted in dramatically elongated morphology and this phenotype was maintained even after 24 hours of removal of the stimulus. Similarly, TGF-β1 pretreated cells sustained the enhanced surface expression of α_v, β_1 and β_3 integrins as determined by flow cytometry and subsequent higher adhesion to both glass and substrate compared to control cells. Pretreated MSCs demonstrated enhanced differentiation potential along multiple lineages including, osteogenic, adipogenic and myogenic phenotypes. Injection of TGF-β1 pretreated MSCs at the periphery of skin wounds resulted in increased wound closure rates compared to control MSCs. TGF-β1 pretreated MSCs also demonstrated greater distribution and migration towards the center of the wound compared to control cells. The persistent characteristics of TGF-β1 pretreated cells can be beneficial for treatment of chronic wounds, where cell functions are arrested due to rapid degradation of soluble factors.

7.2. MATERIALS AND METHODS

Materials: IMDM, DMEM, L-glutamine, penicillin-streptomycin and trypsin were purchased from Mediatech and fetal bovine serum (FBS) was purchased from Atlanta Biologicals. Recombinant human TGF-β1 protein and flow cytometry antibodies were purchased from Biolegend. All other reagents were purchased from VWR unless otherwise specified.

MSC isolation and culture: Murine MSCs were isolated from the bone marrow of 6-10 weeks old adult male Balb/C mice (Charles River Laboratories, Wilmington, MA) and cultured in normal growth media (IMDM media supplemented with 20% FBS, 2 mM L-

glutamine, 100U/ml penicillin, and 100U/ml streptomycin). Purified MSCs between passages 2-6 were used for all studies.

Soluble factor pretreatment: Soluble factor dilutions were created in serum-free DMEM or IMDM immediately before use. Initially, MSCs were pretreated with serum-free control media (CM), and 5 ng/ml TGF-β1 (diluted in serum free media) for 24 hours. Afterwards, the stimulations were removed and both control and pretreated cells were moved to serum free or specific differentiation induction media to determine the effects of pretreatment on MSC functions. To avoid confusion with the previous results, the removal of growth factor stimulus was assigned as t_0; whereas the time points for each experiment was indicated as t_0+t hours. For example centrifugation based adhesion assays described in this section were carried out at t_0+24 hours.

Fabrication of Polyacrylamide Substrates: Substrates were synthesized based on the protocol described before [10]. Briefly, glass coverslips were activated using 3-aminopropyltrimethoxysilane and a mixture of the acrylamide and bis-acrylamide solution (10% acrylamide to 0.3% bis) was polymerized on the activated glass coverslips (Young' modulus (E) ~ 34kPa). Substrates were coated with type I collagen solution (0.2 mg/ml) before cell culture.

Adhesion Assay: Control and pretreated MSCs were trypsinized and labeled with a transmembrane fluorescent viability marker, Calcein AM (Anaspec), in HBSS with divalents. Then the cells were allowed to adhere for three hours after stimulus was removed (t_0+3h) in HBSS before taking an initial florescence reading. A final reading was taken after removing non-adherent cells by washing with HBSS to determine the adherent fraction.

Centrifugal force based adhesion assay: This fluorometric assay was used to evaluate the effect of soluble factor pretreatment on MSC adhesion to native ECM. Briefly, control and pretreated MSCs were trypsinized and labeled with Calcein AM. Then the cells were seeded in an uncoated 96 well plate in serum-free media. At 24 hours after stimulus was removed (t_0+24h), an initial fluorescence reading was recorded. Cells were detached by centrifuging inverted plates at 500 x g for 3 minutes before recording a final fluorescence reading. The adherent fraction was determined by normalizing the final florescence values with the initial pre-spin values.

Morphological analysis: Control and pretreated MSCs were cultured for 24 hours after the removal of stimulus (t_0+24h) and were stained with crystal violet. Cells were then imaged with stereoscope microscope and Motic camera. Cell borders were traced manually and cell shape factors, defined as $4*\pi*\text{Area}/ (\text{Perimeter})^2$, were determined using Image J.

Microarray data analysis for differentiation related genes: Gene expression results from previously reported microarray analysis (chapter 6) was used for differentiation related gene analysis (CM vs TGF-β1)(t_0). Lists of genes related to specific differentiation pathways were obtained from NCBI Biosystems and KEGG pathway databases.

Differentiation studies: The effects of pretreatment on MSC differentiation were investigated for the following cell lineages: smooth muscle cells, adipocytes, and osteoblasts. Briefly, cells were cultured and pretreated on 24-well plates (CM vs TGF-β1) before switching to differentiation induction media. The induction media formulation and the staining method for each differentiation studies are described below.

Smooth muscle cell differentiation: For myogenic induction, IMDM was supplemented with 10% (v/v) FBS and 50 µM trans-retinoic acid for culturing the cells for 7 days (t_0+7d). The medium was changed every day. Cells were stained with Cy3 conjugated alpha-smooth muscle actin antibody (dilution 1:200). All cells were visualized using either an inverted Nikon Eclipse Ti or Zeiss LSM 510 UV confocal microscope.

Adipogenesis: Adipogenic induction media was formulated using IMDM media supplemented with 10% FBS, 10% HS, 1% L-glutamine, 1% Pen-Strep, 5µg/ml Insulin, 1.0 µM Dexamethasone, 0.5 µM Isobutylmethylxanthine, and 50 µM Indomethacin. Cells were cultured for 3 weeks after stimulus was removed (t_0+21d) with induction media and negative control media before they were stained with Oil-Red O to visualize lipid rich vacuoles inside the cells. Cells were fixed in 4% formaldehyde for an hour before being stained with freshly made Oil-Red O solution (3 parts of 0.5% (w/v) Oil-Red O stock solution in isopropyl alcohol mixed with 2 parts of PBSD (PBS with 1% dextrin)).

Osteogenesis: Cells were cultured in IMDM media with 20% FBS, 1% L-glutamine, 1% Pen-Strep, 1 nM Dexamethasone, 20 mM B-glycerophosphate, 50 µM Ascorbate-2-phosphate, and 50 ng/ml L-thyroxine sodium pentahydrate. Osteogenic differentiation was analyzed after 3 weeks (t_0+21d) using von-Kossa staining. Cells were fixed with neutral buffered 10% formalin solution for an hour and were subsequently exposed to 5% (w/v) silver nitrate solution in water under UV light. Osteogenic differentiation was evaluated by visualizing the silver deposition which replaced the calcium.

Wound preparation and Mesenchymal stem cell transplantation: An *in vivo* punch biopsy wound healing model was used to determine the effects of MSC pretreatment on

wound healing. Briefly, hair was removed from the dorsal surface of anesthetized (100 mg/kg ketamine and 10 mg/kg xylazine or isofluorane gas) 12-week old male Balb/C mice by shaving and Nair hair removal reagent. One 5 mm full-thickness skin wound was made on each side of the dorsal midline using a punch biopsy tool (to trace the wound perimeter) and iris scissors (to remove the tissue). Concurrently, pretreated MSCs were detached and labeled with the lipophilic tracer dye DiD (Invitrogen). Mouse mesenchymal stem cells ($5.0x10^5$) suspended in a small volume of PBS solution (~100 µl) were injected (30 gauge needle) intradermally at the periphery of wound tissue of anesthetized mice.

Wound healing analysis*:* After seven days, animals were sacrificed and wound tissues were collected to image the fluorescently labeled MSCs. Wound tissues were stained with DAPI to highlight the nuclei and were then mounted on slide for imaging. The wound bed was imaged using Nikon Eclipse Ti inverted fluorescence microscope and an image of the entire wound area was created by stitching together all the individual images in Nikon Elements.

Statistics: Each experiment was performed with 3 or more replicates, and all values expressed as the mean ± s.e.m. For comparison between two groups student t-test was used. One way Anova test with repeated measures was used to determine statistical significance of experiments involving more than two groups. For comparison between groups, Tukey's HSD post-test was used. Significance was reported as * (for $p<0.05$), ** (for $p<0.005$) and *** (for $p<0.0005$).

7.3. RESULTS

TGF-β1 pretreatment enhances adhesive strength of MSCs: MSCs pretreated with TGF-β1 displayed higher adhesivity on both glass and polyacrylamide gel substrates (E~34kPa) after 3 hours (t_0+3h) of removal of stimulus (Figure 7-1). In both cases, the adherent fraction of pretreated cells was normalized to the control cells. TGF-β1 pretreated cells exhibited greater than 1.7 fold increase in adhesivity in both cases ($p<0.05$). A centrifugation force based adhesion assay was used to investigate the adhesive properties at longer time scales (~24 hours) (Figure 7-2). For this purpose, pretreated cells were seeded on uncoated tissue culture plastic (TCP) and were then subjected to centrifugation (500xg) at t_0+24h. TGF-β1 pretreated cells maintained their higher adhesivity to ECM and exhibited a 4.2 fold increase in the adherent fraction compared to control.

Effect of soluble factor pretreatment on distribution of cell adhesion molecules: We next sought to analyze the changes in the expression of cell surface adhesion molecules that control cell adhesivity to the extracellular environment and adjacent cells (Figure 7-3). Integrin subunits α_v (CD51), β_1 (CD29), β_3 (CD61), and vascular cell adhesion molecule-1 (VCAM-1) were analyzed using flow cytometry at 24 hours (t_0+24h) after removal of stimulus. TGF-β1 pretreated cells significantly upregulated the expressions of the integrins while reducing VCAM-1 expression (Figure 7-3). Mean fluorescence intensity (MFI) of histograms further confirmed the trends of integrin upregulation and VCAM-1 downregulation due to TGF-β1 pretreatment (Figure 7-4). This result correlated with the observed adhesive strengthening response.

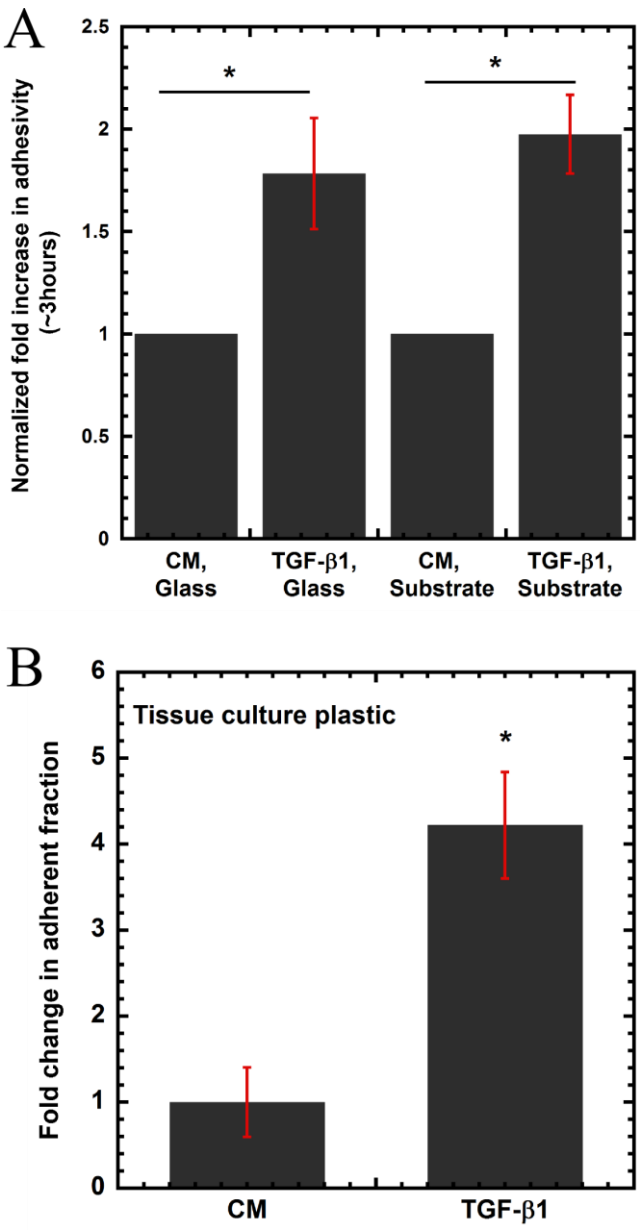

Figure 7-1. *Pretreated MSCs exhibit higher adhesive strength at both short (~3 hours) and longer time scales (~24 hours).* (A) Pretreated MSCs (CM vs TGF-β1) plated on glass and polyacrylamide gels were washed after 3 hours to remove detached cells. (B) Centrifuge-based adhesion assay was used to determine the effect of soluble factor pretreatment on the adhesion of MSCs on tissue culture plastic (TCP).

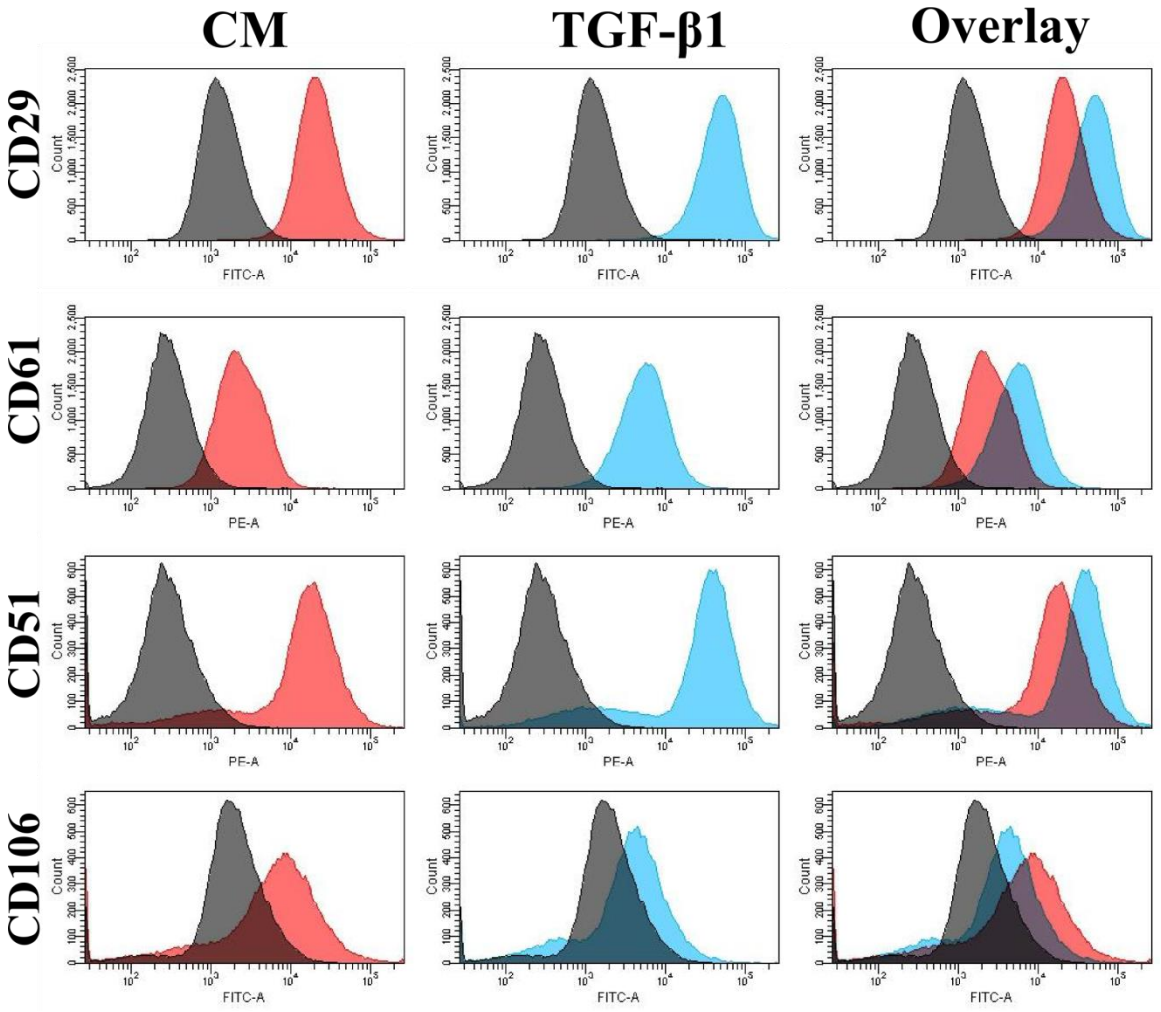

Figure 7-2. *Analysis of cell surface adhesion molecules α_v (CD51-PE), β_1 (CD29-FITC) and β_3 (CD61-PE), integrins and VCAM-1 (CD106 - FITC) using flow cytometry after 24 hours of removal of stimulus.* Black indicates negative cell population; whereas red and blue represent control and TGF-β1 pretreated cells respectively. TGF-β1 pretreated cells exhibit higher integrin expression and lower VCAM-1 expression at 24 hours after removal of the stimulus compared to control cells.

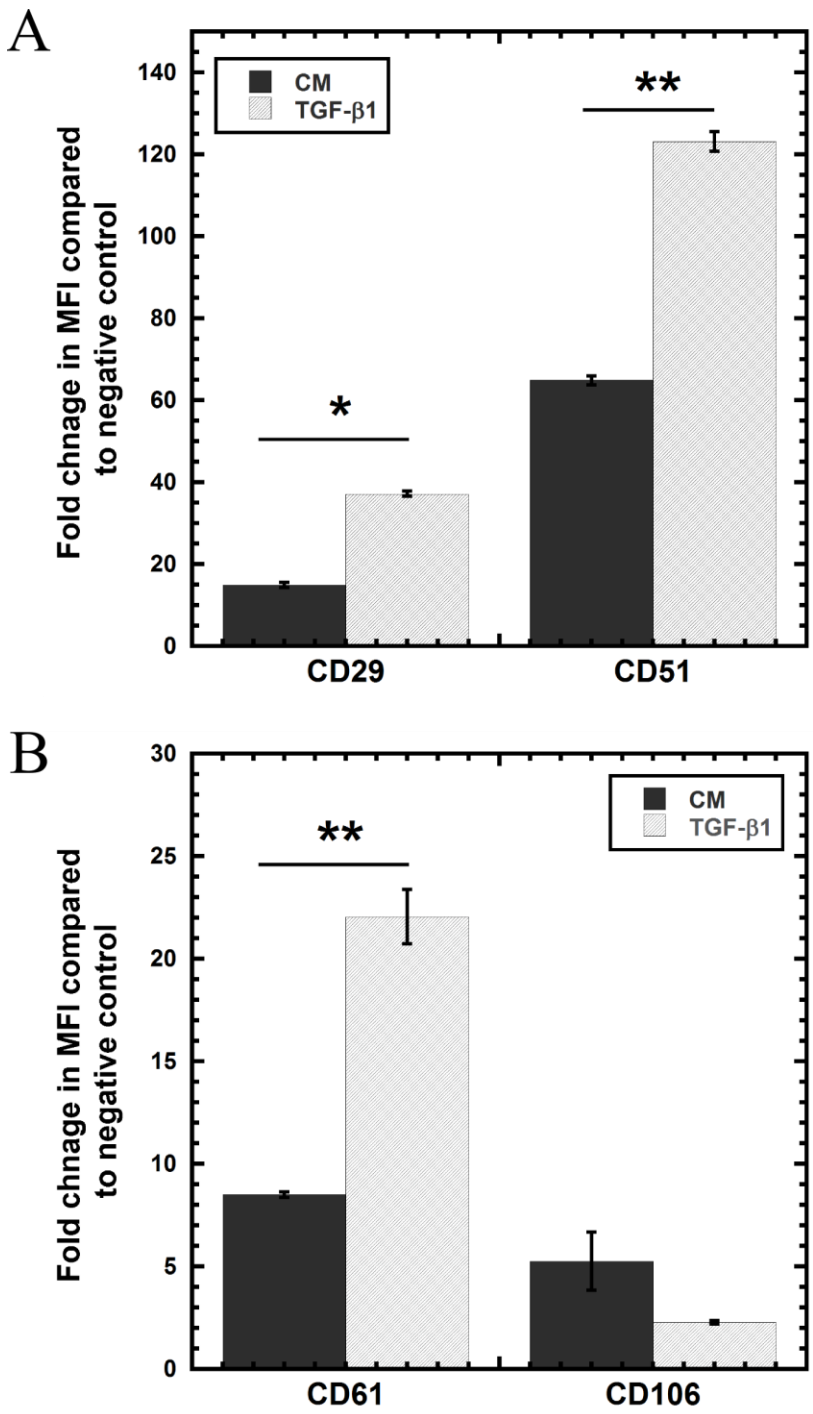

Figure 7-3. *TGF-β1 pretreated MSCs maintain surface adhesion.characteristics.* Histograms from flow cytometry were analyzed using FACS-DIVA for mean fluorescence intensity (MFI). Expressions of surface integrins αv (CD51), β1 (CD 29) and β3 (CD61) were increased significantly in TGF-β1 pretreated cells compared to the control; whereas TGF-β1 pretreatment reduced VCAM1 (CD106) expression significantly compared to the control. Results are reported as average. (n=2).

Sustained morphological changes at 24 hours after TGF-β1 pre-treatment: MSCs undergo dramatic elongation in response to TGF-β1 treatment. To examine the persistent effect of TGF-β1 on cell shape, pretreated MSCs were detached and reseeded on a new surface (TCP) with serum free media in the absence of stimulus for 24 hours (t_0+24h). Cells were fixed and stained with crystal violet to analyze cell morphology using a cell shape factor (CSF) which varies from 0 for a line to 1 for a perfect circle. TGF-β1 pretreated cells retained the elongation effect even after 24 hours (t_0+24h) (Figure 7-5). The cell shape factor of TGF-β1 pretreated cells was significantly lower than its control counterpart indicating dramatic elongation ($p<0.05$).

TGF-β1 pretreatment enhances the differentiation potential of MSCs: MSCs can differentiate into both mesodermal and non-mesodermal lineages and TGF-β1 is reported to have profound effects on MSC differentiation and cell fate. Here, the effects of short-term exposure to soluble factors on the long-term differentiation potential of MSCs were characterized for multiple lineages. TGF-β1 pretreated MSCs along with the control cells were exposed to myogenic, adipogenic, and osteogenic differentiation media and were stained after 1 week (t_0+7d) for myogenesis [11] and 3 weeks (t_0+21d) for adipogenesis and osteogenesis [12] (Figure 7-5). To determine smooth muscle cell differentiation, cells were immunostained with Cy3 conjugated alpha-smooth muscle actin (α-SMA). Pretreated MSCs exhibited higher expression of α-SMA compared to control indicating more mature smooth muscle cell (SMC) phenotype. For adipogenesis, oil red o staining was used to visualize lipid vacuoles; whereas, von Kossa stained calcium nodules for osteogenesis. The percent of the total area that stained positive was quantified in all three cases to determine the degree of differentiation.

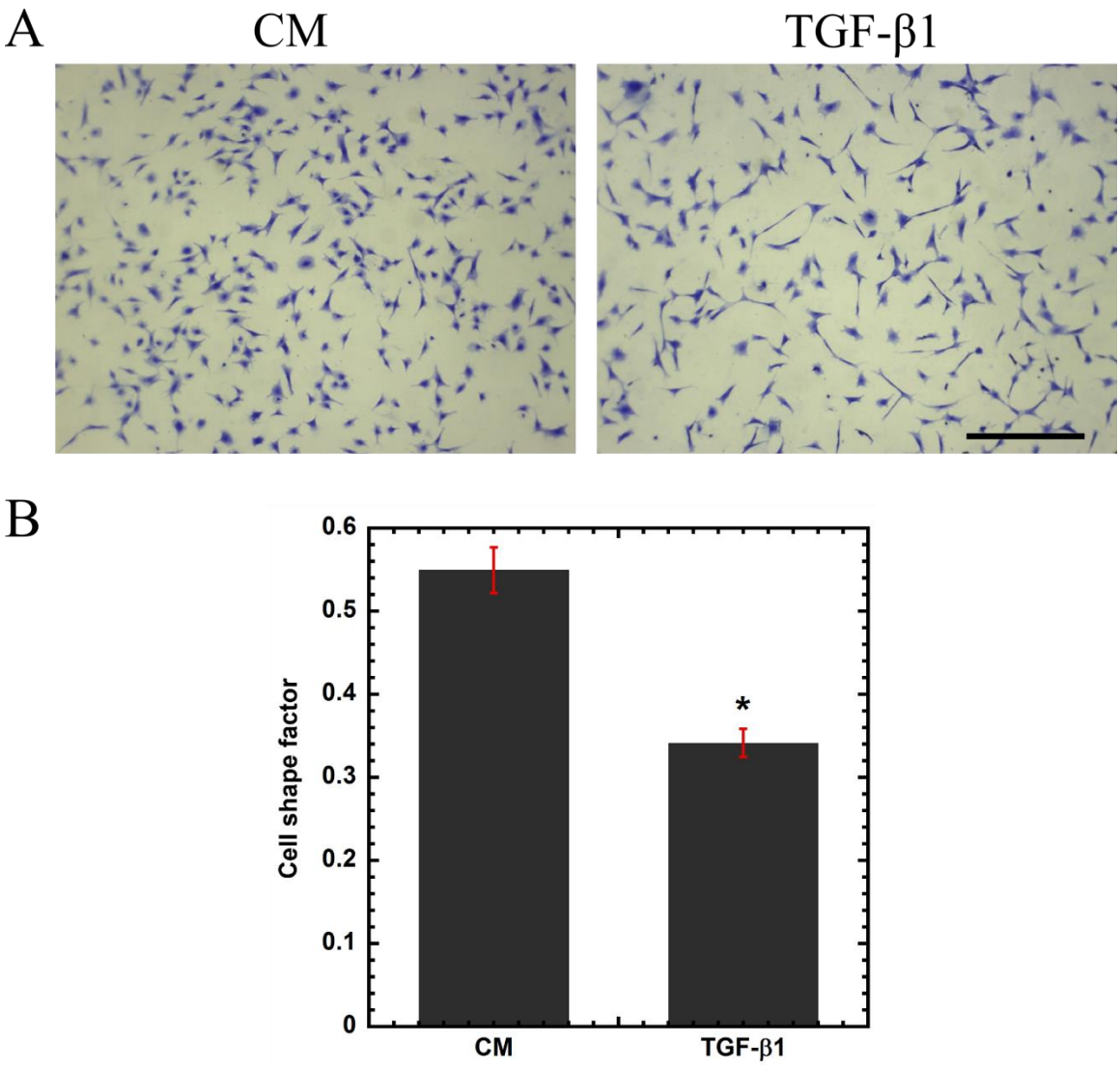

Figure 7-4. *Pretreated MSC maintain elongated phenotype* (A) Brightfield images pretreated MSCs after 24 hours stained with crystal violet. TGF-β1 pretreated MSCs sustained elongated morphology in serum free media for 24 hours. (scale bar: μm). (B) Cell shape factor (CSF) was determined by analysis of bright field images with image J. CSF was used to characterize the elongation of the cell, with a shape factor of 1 indicating a perfect circle and 0 indicating a straight line. Results are reported as average ± s.e.m. (n=2).

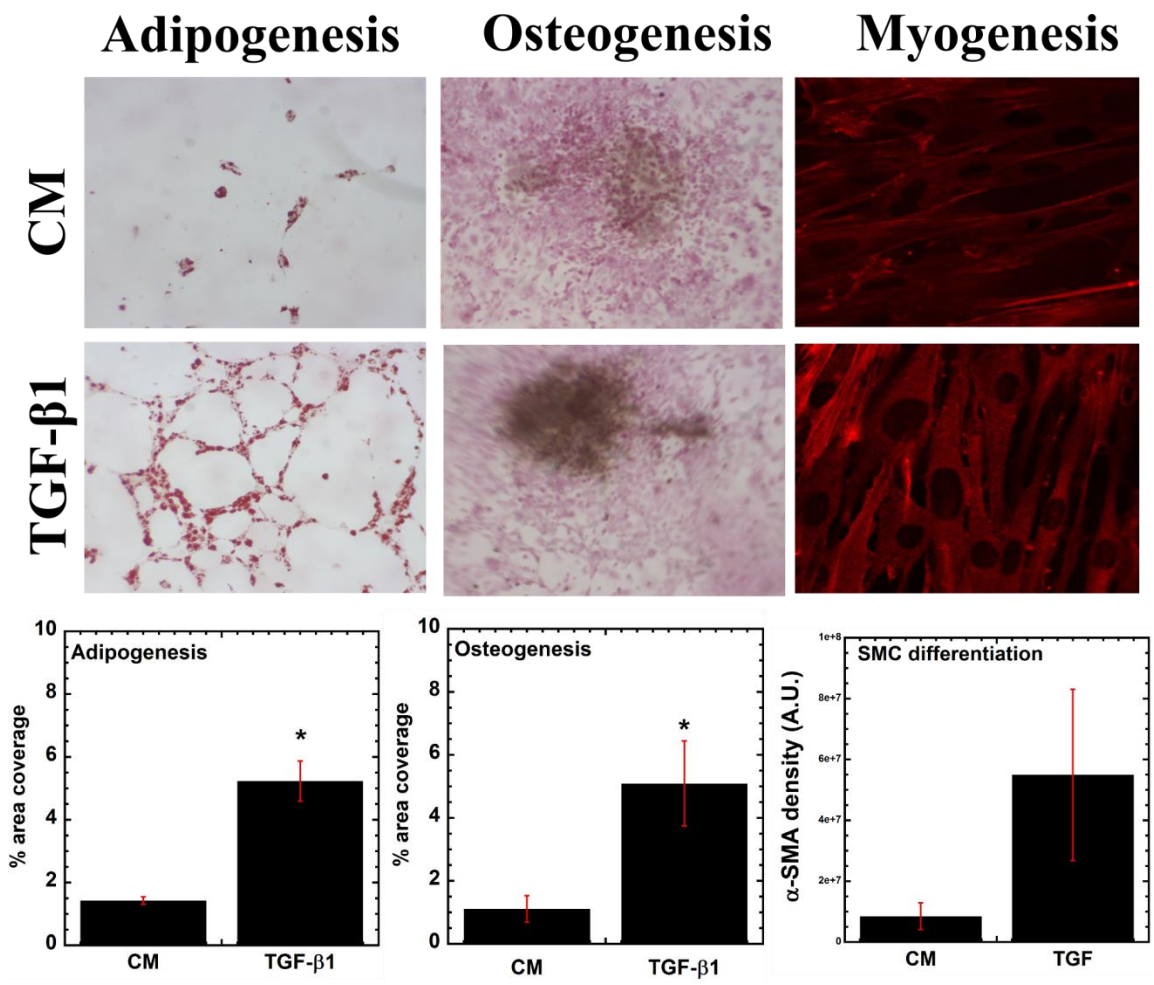

Figure 7-5. *Enhanced differentiation potential of TGF-β1 pretreated MSCs along multiple lineages.* MSCs differentiated into adipocytes (column 1), osteoblasts (column 2) and smooth muscle cells (column 3) in lineage-specific differentiation media as shown by staining. Adipocytes and osteoblasts were stained with oil red o and von Kossa respectively; whereas smooth muscle cells were stained with immunofluorescent dye Cy3 conjugated α-Smooth Muscle Actin (shown in red).

TGF-β1 pretreated cells demonstrated significantly higher coverage area for both osteogenesis and adipogenesis compared to control cells. For myogenic differentiation, normalized α-SMA expression was increased compared to control suggesting enhanced differentiation.

TGF-β1 pretreatment enhances wound healing: Previous studies demonstrated that MSCs could be used to increase the rate of wound closure in full thickness skin wounds; however, untreated MSCs used in these studies resulted in a modest change in the rate of wound healing and long-term engraftment of MSCs was not clearly established [13]. We hypothesized that the sustained changes observed in TGF-β1pretreated MSCs would lead to more rapid wound closure and longterm engraftment in the tissue for improved healing of chronic wounds. A syngeneic mouse wound healing model was used to test this hypothesis with murine MSCs injected in immunocompetent mice. Each adult Balb/C mouse (n=3) used in this study was given two full thickness skin wounds, and fluorescently labeled MSCs (control and TGF-β1 pretreated) were injected at the periphery of each wound. After 5 days, the area of the open wound was significantly lower for TGF-β1 preconditioned cells. After 7 days, skins were isolated from the sacrificed mice to image the entire wound area and to identify the distribution of fluorescently labeled MSCs in the wound bed (Figure 7-6A). TGF-β1 pretreated cells migrated more towards the center of the wound as image analysis in MATLAB revealed a 2.5 fold increase in directed migration for pretreated cells compared to control (Figure 7-6B).

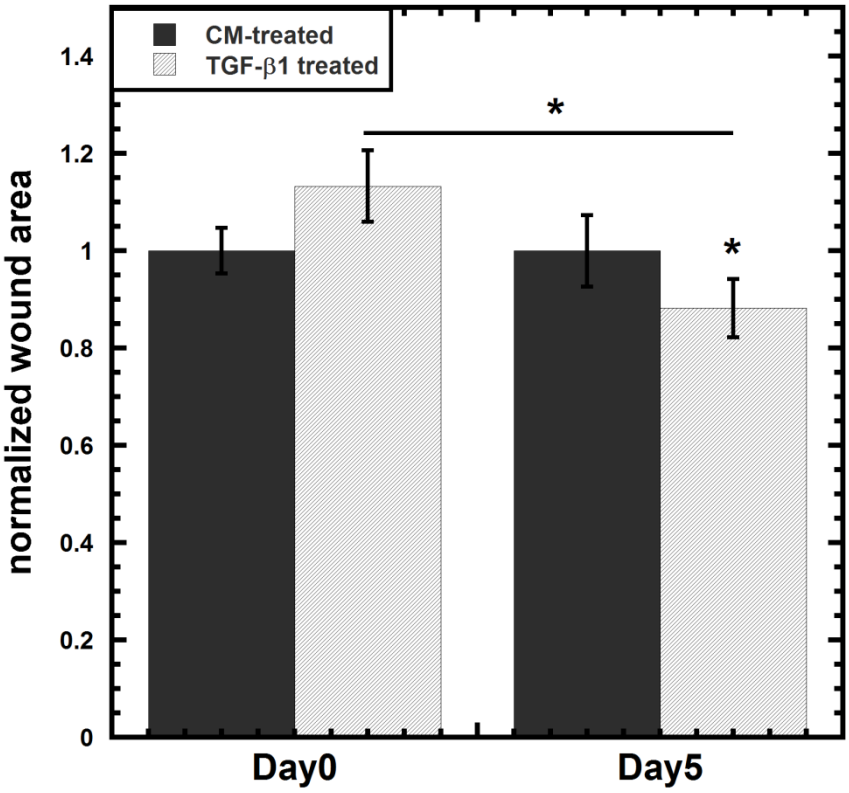

Figure 7-6. *TGF-β1 pretreated MSCs close wound gap more rapidly*. Open area of TGF-β1 pretreated MSC injected wound was normalized to its respective control.

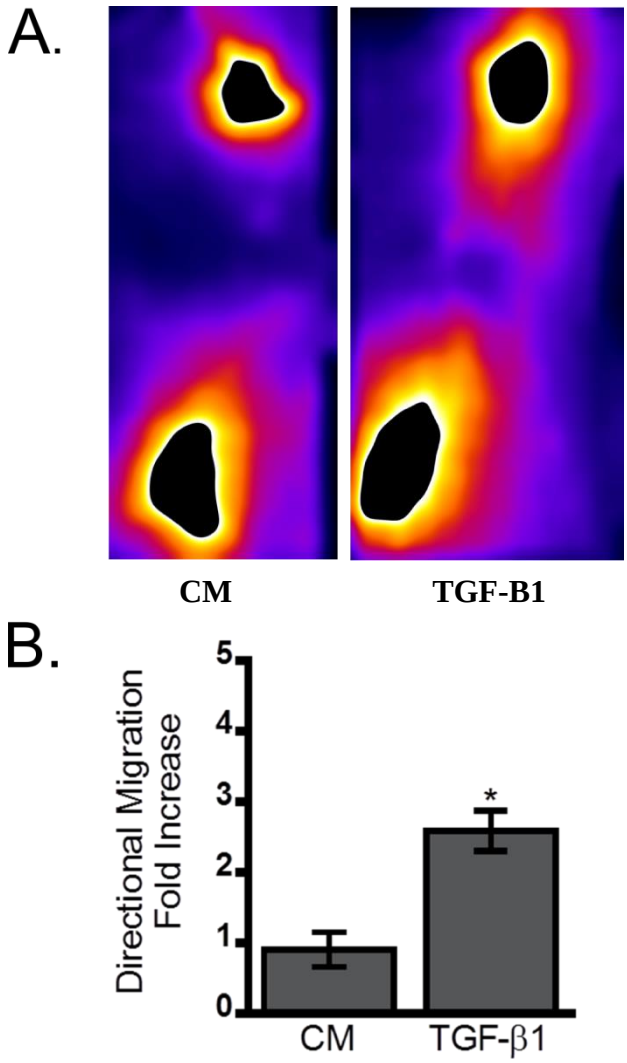

Figure 7-7. *Pretreated MSCs exhibit enhanced migration in vivo.* (A) Thresholded fluorescence images of skin tissue showed enhanced distribution of MScs towards center of the wound. (B) Quantification of directed migration towards the center of the wound.

7.4. DISCUSSION

Chronic wounds, which predominantly affect elderly and chronically ill patients, are a major health care burden. Although a plethora of wound healing treatments are clinically available, these are often unsuccessful in treating chronic wounds. Wound healing is a very complex process and understanding the coordinated action of the different types of cells and niche specific soluble and insoluble factors is of utmost importance for the development of modern wound care. Growth factors and bioactive materials have been used increasingly in recent times; however, on their own, there efficacy remains limited [14]. Recent studies have highlighted the benefits of using mesenchymal stem cells for wound healing that holds high hope for the future of the wound care [15,16]. However, characterization of MSCs with niche specific factors is still in its early stages. In this study, we have investigated interaction between mesenchymal stem cells and TGF-β1 a growth factor that plays an important role both in normal wound healing and in fibrosis. The current study was designed to determine if TGF-β1 induces a persistent alteration in MSC phenotype, leading to more efficient wound healing *in vivo*.

Adhesion to substrates is essential for the survival of anchorage dependent cells like MSCs. We have initially characterized the adhesion profile of TGF-β1 pretreated cells at both short (~3 hours (t_0+3h)) and longer time scales (~24 hour (t_0+24h)). To determine the initial adhesion response at 3 hours, both glass and more compliable polyacrylamide (PA) gel substrates (E ~ 34kPa) were used. The stiffness of the substrate was chosen within the range of reported values for skin tissue [17]. A similar number of control and TGF-β1 pretreated MSCs were adherent to glass and PA gels before washing; however, fewer TGF-β1 pretreated cells were detached upon washing, indicating that

TGF-β1 pretreatment increased the adhesivity. This behavior of the pretreated cells can be traced back to the fact that surface integrin expression was increased in the presence of TGF-β1 and MSCs retained the surface phenotype even after removal of stimulus for 24 hours (Figure 7-2, Figure B-1). Subsequently, we were interested in probing the effects of TGF-β1 pretreatment on the adhesivity of MSCs at longer time scales when the cells are no longer exposed to TGF-β1. A centrifuge-based adhesion assay was used to measure the adherent fraction on uncoated tissue culture plastic. These results would account for the adhesive strengthening due to changes in integrin expression and the secretion of native ECM proteins by MSCs. Previous studies have demonstrated enhanced ECM and other growth factor secretion from cells in response to TGF-β1 and transcriptional activation of the ECM genes were found to be upregulated previously (Figure 6-4, Appendix C). At 24 hours (t_0+24h) after removal of stimulus, pretreated MSCs displayed more than 4 fold increase in the adherent cell fraction compared to the 2 fold increase measured in our washing study after 3 hours (t_0+3h) (Figure 7-1). Also, the surface expression of β1, β3 and αv integrins remained upregulated after 24 hours (t_0+24h) with similar magnitudes in the mean fluorescence intensity as measured in Appendix B (Figure B-1). Additionally, pretreated cells maintained their elongated shape even after detachment and replating compared to the control cells.

Due to their multilineage differentiation potential and capacity for *in vitro* expansion, MSC based therapeutics for wound healing hold distinct advantages over the currently used cell types such as fibroblasts and keratinocytes [15,18]. In addition, TGF-β1 can further influence MSC differentiation along multiple lineages [19]. Previous studies have shown that short-term TGF-β1 exposure upregulated genes for specific

differentiation pathways; however, additional cues were required to induce mature phenotypes [20]. Analysis of our previous transcriptional results revealed a number of highly regulated genes that serve as early markers for lineage commitment; however, a distinctive pattern, indicating a specific type of differentiation could not be identified (Table 1). Thus, we hypothesized that short term TGF-β1 exposure could prime the cells to differentiate into multiple lineages in the presence of pathway specific supplements. To test this hypothesis, the effects of TGF-β1 pretreatment on differentiation along adipogenic, osteogenic and myogenic lineages were characterized. Pretreated MSCs exhibited enhanced and more mature phenotypes along all three lineages.

Since, TGF-β1 pretreated cells exhibited enhanced adhesion and differentiation, we wanted to examine if the persistent altered phenotype can lead to increased wound healing *in vivo*. We found that TGF-β1 pretreated MSCs contributed to the closure of the wound and invaded the wound bed more efficiently (2.5 fold increase in directed migration towards the center of the wound). TGF-β1 pretreated MSCs maintained an increased surface β1 integrin expression which has been correlated with enhanced migration both *in vivo* and *in vitro* [21,22] and can be critical for the observed changes in migration. Additionally, pretreated MSCs displayed a more elongated phenotype,that had been associated with enhanced migration through smaller pores (Figure 3-10). Therefore, injected cells could invade wound tissue more efficiently leading to increased distribution . Previously, microarray data revealed upregulation of genes related to cytokines and ECM remodeling proteins (chapter 6, Appendix C) that can aid in the wound regeneration process. Other studies with pretreated MSCs have reported enhanced therapeutic efficacy in the inflammatory niche of myocardial infarction [23,24]. Taken together with the

presented results, pretreatment of MSCs can be critical for developing efficient cell-based therapeutics for inflammatory niches *in vivo*.

7.5. CONCLUSIONS

The function of *ex-vivo* expanded MSC based therapeutics has been shown to be limited after reintroduction *in vivo*. To understand and improve MSC functions, we have previously characterized the mechanical and chemical response of MSCs to soluble factors *in vitro*. In brief, studies with soluble factor TGF-β1 provided enhanced mechanical response with cytoskeletal remodeling and stiffening (Chapter 4) that contributed to directional migration of MSCs. TGF-β1 treated cells also provided molecular response to indicate adhesive strengthening, ECM remodeling and differentiation (Chapter 5 and 6). This study illustrates that pretreatment of MSCs with TGF-β1 resulted in sustained improvement in migration, adhesion and differentiation even after removal of the stimulus *in vitro*. Subsequently, these pretreated cells enhanced the *in vivo* wound healing process, which may lead to improved therapeutic efficacy. Future studies with site specific factors will be used to guide new strategies for microenvironment specific MSC based therapy.

7.6. REFERENCES

1. Guo S and LA DiPietro. (2010). Factors affecting wound healing. Journal of dental research 89:219-229.

2. Diegelmann RF and MC Evans. (2004). Wound healing: an overview of acute, fibrotic and delayed healing. Front Biosci 9:283-289.

3. Gillitzer R and M Goebeler. (2001). Chemokines in cutaneous wound healing. Journal of Leukocyte Biology 69:513-521.

4. Werner S and R Grose. (2003). Regulation of wound healing by growth factors and cytokines. Physiological reviews 83:835-870.

5. Wu Y, L Chen, PG Scott and EE Tredget. (2007). Mesenchymal stem cells enhance wound healing through differentiation and angiogenesis. Stem Cells 25:2648-59.

6. Falanga V. Wound healing and its impairment in the diabetic foot. The Lancet 366:1736-1743.

7. Brem H and M Tomic-Canic. (2007). Cellular and molecular basis of wound healing in diabetes. The Journal of Clinical Investigation 117:1219-1222.

8. Gosain A and LA DiPietro. (2004). Aging and wound healing. World journal of surgery 28:321-326.

9. Wu Y, J Wang, PG Scott and EE Tredget. (2007). Bone marrow-derived stem cells in wound healing: a review. Wound Repair Regen 15 Suppl 1:S18-26.

10. Tse JR and AJ Engler. (2001). Preparation of Hydrogel Substrates with Tunable Mechanical Properties. In: *Current Protocols in Cell Biology*. John Wiley & Sons, Inc.

11. Su Z-y, Y Li, X-l Zhao and M Zhang. (2010). All-trans retinoic acid promotes smooth muscle cell differentiation of rabbit bone marrow-derived mesenchymal stem cells. Journal of Zhejiang University SCIENCE B 11:489-496.

12. Adult stem cells from bone marrow (MSCs) isolated from different strains of inbred mice vary in surface epitopes, rates of proliferation, and differentiation potential. (2004).

13. Kean TJ, P Lin, AI Caplan and JE Dennis. (2013). MSCs: Delivery Routes and Engraftment, Cell-Targeting Strategies, and Immune Modulation. Stem Cells International 2013:13.

14. Greer N, N Foman, T Wilt, J Dorrian, P Fitzgerald, R MacDonald and I Rutks. (2012). Advanced Wound Care Therapies for Non-Healing Diabetic, Venous, and Arterial Ulcers: A Systematic Review.

15. Jackson WM, LJ Nesti and RS Tuan. (2012). Concise review: clinical translation of wound healing therapies based on mesenchymal stem cells. Stem cells translational medicine 1:44-50.

16. Yolanda M, A Maria, F Amaia, P Marcos and P Silvia. (2014). Adult Stem Cell Therapy in Chronic Wound Healing. J Stem Cell Res Ther 4:2.

17. Discher DE, DJ Mooney and PW Zandstra. (2009). Growth factors, matrices, and forces combine and control stem cells. Science 324:1673-1677.

18. Sasaki M, R Abe, Y Fujita, S Ando, D Inokuma and H Shimizu. (2008). Mesenchymal stem cells are recruited into wounded skin and contribute to wound repair by transdifferentiation into multiple skin cell type. the Journal of immunology 180:2581-2587.

19. Wang M-K, H-Q Sun, Y-C Xiang, F Jiang, Y-P Su and Z-M Zou. (2012). Different roles of TGF-β in the multi-lineage differentiation of stem cells. World journal of stem cells 4:28.

20. Kurpinski K, H Lam, J Chu, A Wang, A Kim, E Tsay, S Agrawal, DV Schaffer and S Li. (2010). Transforming Growth Factor-β and Notch Signaling Mediate Stem Cell Differentiation into Smooth Muscle Cells. Stem Cells 28:734-742.

21. Ip JE, Y Wu, J Huang, L Zhang, RE Pratt and VJ Dzau. (2007). Mesenchymal stem cells use integrin β1 not CXC chemokine receptor 4 for myocardial migration and engraftment. Molecular biology of the cell 18:2873-2882.

22. Zou C, G Song, Q Luo, L Yuan and L Yang. (2011). Mesenchymal stem cells require integrin β1 for directed migration induced by osteopontin *in vitro*. *In vitro* Cellular & Developmental Biology-Animal 47:241-250.

23. Hahn J-Y, H-J Cho, H-J Kang, T-S Kim, M-H Kim, J-H Chung, J-W Bae, B-H Oh, Y-B Park and H-S Kim. (2008). Pre-treatment of mesenchymal stem cells with a combination of growth factors enhances gap junction formation, cytoprotective effect on cardiomyocytes, and therapeutic efficacy for myocardial infarction. Journal of the American College of Cardiology 51:933-943.

24. Bartunek J, JD Croissant, W Wijns, S Gofflot, A De Lavareille, M Vanderheyden, Y Kaluzhny, N Mazouz, P Willemsen and M Penicka. (2007). Pretreatment of adult bone marrow mesenchymal stem cells with cardiomyogenic growth factors and repair of the chronically infarcted myocardium. American Journal of Physiology-Heart and Circulatory Physiology 292:H1095-H1104.

CHAPTER 8: CONCLUSIONS AND RECOMMENDATIONS

8.1. CONCLUSIONS

Mesenchymal stem cells (MSCs) hold great promise as a source of donor cells for tissue engineering and regenerative medicine applications [1-3]. For this promise to be fully realized these cells must be expanded and manipulated *ex vivo*. However, fundamental changes in isolated MSCs during *ex vivo* expansion result in altered differentiation potential as well as loss of native homing ability [4-6]. We found that MSCs uniquely altered their mechanical phenotype to migrate more efficiently in response to tumor condition media compared to fibroblasts, suggesting that the rheological property can be used as a biomarker for more successful MSC homing to target tissues. However, tumor condition media cannot be used for mechanical characterization of MSCs for clinical purposes. We have identified that soluble factor transforming growth factor-β1 (TGF-β1) induced similar mechanical response from MSCs, and can be potentially used to characterize expanded *ex vivo* population. Interestingly, PDGF, a mitogenic growth factor, contributed significantly to stiffening response when combined with TGF-β1 and the inhibition of the PDGF signaling pathway led to complete reversal of the stiffening response (Table 8-1). Thus PDGF signaling pathway provides a viable target for disruption of abnormal TGF-β1 signaling mediated pathological conditions.

MSCs displayed upregulated gene expression for both soluble and insoluble factors such as extracellular matrix molecules that can actively help in the tissue regeneration and remodeling process. Additionally, we have shown that TGF-β1

pretreated cells displayed enhanced differentiation and adhesion profile leading to increased *in vivo* wound healing. MSCs pretreated with TGF-β1 differentiated more efficiently to soft adipocytes, contractile smooth muscle phenotype and highly stiff osteoblasts, suggesting that pretreatment method can be universally adopted for a range of mechanically diverse tissue regeneration sites. Pretreated MSCs with enhanced differentiation potential can be beneficial for application in regenerative niches where multiple cell types are required for successful restoration of tissue functions (example: osteo-chondral cell lineages in arthritis).

8.2. RECOMMENDATIONS FOR FUTURE WORK

This document outlines a detailed mechanical and molecular characterization of the interactions between MSCs and inflammatory site specific soluble factors that can be used to design new strategies for microenvironment specific MSC based therapy. Future efforts in the development of MSC based therapy will require further evaluation of MSC characteristics both *in vitro and in vivo*. Four potential areas of advancement are listed below:

1. ***Effect of soluble factors on MSC mechanics and functions on substrates with different rigidities:*** In recent years biophysical cues such as matrix rigidity in concert with soluble factors has been shown to affect stem cell migration, proliferation and differentiation [7-10]. Future directions should include cells cultured on different matrix rigidities to further our understanding of MSC response to soluble factors.
2. ***Genetic modification of ABPs to manipulate cell mechanics:*** Although, TGF-β1 treated cells display dramatically different mechanical phenotype, it is also coupled with transcriptional changes in chemical and secretory properties of the cell. To study

the importance of cell mechanics in regulating key cell functions, it is essential to identify key signal transduction elements that can singularly modify mechanical properties of cells minimizing its effect on other aspects. MSCs can be genetically modified to express tailored proteins to enhance specific functions without inducing malignant transformation. For example, MSCs can be engineered to express α-actinin to manipulate its mechanical properties and characterize its effect on migration, adhesion and differentiation. The list of actin-binding proteins obtained from microarray analysis should be screened more rigorously to identify candidates similar to α-actinin.

3. ***Effect of preconditioning on long term fate of MSCs***: Mesenchymal stem cells contribute to wound healing via angiogenesis and differentiate into specific skin cell type [11]. MSCs secrete soluble factors to recruit host of other native cells and these paracrine effects of MSCs have been attributed to neovascularization *in vivo* [12]. Despite possessing the potential to form smooth muscle cells that stabilizes blood vessels [13, 14], MSCs have not been detected to actively participate in angiogenesis during wound healing. *In vitro* co-culture of pretreated MSCs with endothelial cells can provide new insights to enhance the incorporation of stem cells in blood vessel formation. Additionally, long term fate of topically delivered MSCs in wound bed is not well established. The survival rate and phenotypical fate of injected MSCs (pretreated vs untreated) should be characterized in more detail.
4. ***Characterizing global potential of pretreated MSCs in vivo:*** MSCs pretreated with TGF-β1 displayed enrichment in multiple functional networks that can be beneficial for different niches *in vivo.* Characterizing the functional behavior of pretreated

MSCs in these niches can provide new insights into the role of mechanical and chemical properties of MSCs in homing, engraftment, survival, migration and differentiation. Studies should be designed to address each aspect of the MSC function to improve the overall design. For example, pretreated MSCs should be infused in tumor carrying mice to evaluate homing and accumulation; whereas, to determine cell integration in mechanical environment, pretreated MSCs should be used *in vivo* model of myocardial infarction.

Table 8-1: Summary of effect of soluble factor treatment with or without small molecule signaling inhibitors on elastic (G') and viscous (G") moduli of Balb/C MSCs at frequency ($\omega=1s^{-1}$).

Condition	Elastic Modulus ($dyne/cm^2$)	Viscous Modulus ($dyne/cm^2$)
Control MSC	**1.42**	**5.1**
MSC treated with TGF-β1	**12.7**	**3.4**
MSC treated with PDGF	**1.77**	**3.75**
MSC treated with PDGF and TGF-β1	**142.64**	**3.75**
MSC treated with TGF-β1 and TGFβRI inhibitor	**2.20**	**6.00**
MSC treated with PDGF, TGF-β1 and TGFβRI inhibitor	**1.78**	**4.83**
MSC treated with TGF-β1 and PDGFR inhibitor	**1.33**	**3.50**
MSC treated with PDGF, TGF-β1 and PDGFR inhibitor	**1.20**	**5.19**
Tumor condition media from 4T1	**212.8**	**52.23**

8.3. REFERENCES

1. Caplan AI. (2007). Adult mesenchymal stem cells for tissue engineering versus regenerative medicine. Journal of cellular physiology 213:341-347.

2. Caplan Arnold I and D Correa. (2011). The MSC: An Injury Drugstore. Cell Stem Cell 9:11-15.

3. da Silva Meirelles L, AM Fontes, DT Covas and AI Caplan. (2009). Mechanisms involved in the therapeutic properties of mesenchymal stem cells. Cytokine & growth factor reviews 20:419-427.

4. Daley GQ. (2012). The promise and perils of stem cell therapeutics. Cell stem cell 10:740-749.

5. Chamberlain G, J Fox, B Ashton and J Middleton. (2007). Concise review: mesenchymal stem cells: their phenotype, differentiation capacity, immunological features, and potential for homing. Stem cells 25:2739-2749.

6. Ankrum J and JM Karp. (2010). Mesenchymal stem cell therapy: Two steps forward, one step back. Trends in molecular medicine 16:203-209.

7. Discher DE, P Janmey and Y-l Wang. (2005). Tissue cells feel and respond to the stiffness of their substrate. Science 310:1139-1143.

8. Lo C-M, H-B Wang, M Dembo and Y-l Wang. (2000). Cell movement is guided by the rigidity of the substrate. Biophysical journal 79:144-152.

9. Isenberg BC, PA DiMilla, M Walker, S Kim and JY Wong. (2009). Vascular smooth muscle cell durotaxis depends on substrate stiffness gradient strength. Biophysical journal 97:1313-1322.

10. Discher DE, DJ Mooney and PW Zandstra. (2009). Growth factors, matrices, and forces combine and control stem cells. Science 324:1673-1677.

11. Brem H and M Tomic-Canic. (2007). Cellular and molecular basis of wound healing in diabetes. The Journal of Clinical Investigation 117:1219-1222.

12. Hocking AM and NS Gibran. (2010). Mesenchymal stem cells: paracrine signaling and differentiation during cutaneous wound repair. Experimental cell research 316:2213-2219.

13. Hellstrom M, P Lindahl, A Abramsson and C Betsholtz. (1999). Role of PDGF-B and PDGFR-beta in recruitment of vascular smooth muscle cells and pericytes

during embryonic blood vessel formation in the mouse. Development 126:3047-3055.

14. Su Z-y, Y Li, X-l Zhao and M Zhang. (2010). All-trans retinoic acid promotes smooth muscle cell differentiation of rabbit bone marrow-derived mesenchymal stem cells. Journal of Zhejiang University SCIENCE B 11:489-496.

APPENDIX A

Table A-1: List of Primers

Gene name		Sequence	Amplicon size (B.P.)
Ezrin (*Ezr*)	Forward (5'-3')	CAA TCA ACG TCC GGG TGA C	104
	Reverse(5'-3')	GCC AAT CGT CTT TAC CAC CTG A	104
Moesin (*Msn*)	Forward(5'-3')	TCT TAT GCC GTC CAG TCT AAG T	121
	Reverse(5'-3')	GGT CCT TGT TGA GTT TGT GCT	121
α-actinin-1 (*Actn1*)	Forward(5'-3')	AGA AAT CCA GCT CCT AGC ACG	147
	Reverse(5'-3')	CTG TGA ACG TCT TCC TCT GCT	147
Tensin-1 (*Tns1*)	Forward(5'-3')	TCA CAG CCT ACC AGT CTC TCT	166
	Reverse(5'-3')	ACA TCT GAG CCA CTT CAC GG	166
PDGF-B (*Pdgfb*)	Forward(5'-3')	TCC GTA GAT GAA GAT GGG GCT	163
	Reverse(5'-3')	TCT GGA ACA CCT CTG TGC G	163
Troponin T2, cardiac (*Tnnt2*)	Forward(5'-3')	CCC GAT GGA GAG AGA GTG GA	155
	Reverse(5'-3')	CGA CGC TTT TCG ATC CTG TC	155
18s rRNA	Forward(5'-3')	CTT AGA GGG ACA AGT GGC G	107
	Reverse(5'-3')	ACG CTG AGC CAG TCA GTG TA	107
Cdc42	Forward (5'-3')	CCCATCGGAATATGTACCAACTG	78
	Reverse (5'-3')	CCAAGAGTGTATGGCTCTCCAC	78
RhoA	Forward (5'-3')	AGCTTGTGGTAAGACATGCTTG	138
	Reverse (5'-3')	GTGTCCCATAAAGCCAACTCTAC	138
Rac1	Forward (5'-3')	GAGACGGAGCTGTTGGTAAAA	138
	Reverse (5'-3')	ATAGGCCCAGATTCACTGGTT	138
GAPDH	Forward (5'-3')	AGGTCGGTGTGAACGGATTT	123
	Reverse (5'-3')	TGTAGACCATGTAGTTGAGGTCA	123

APPENDIX B

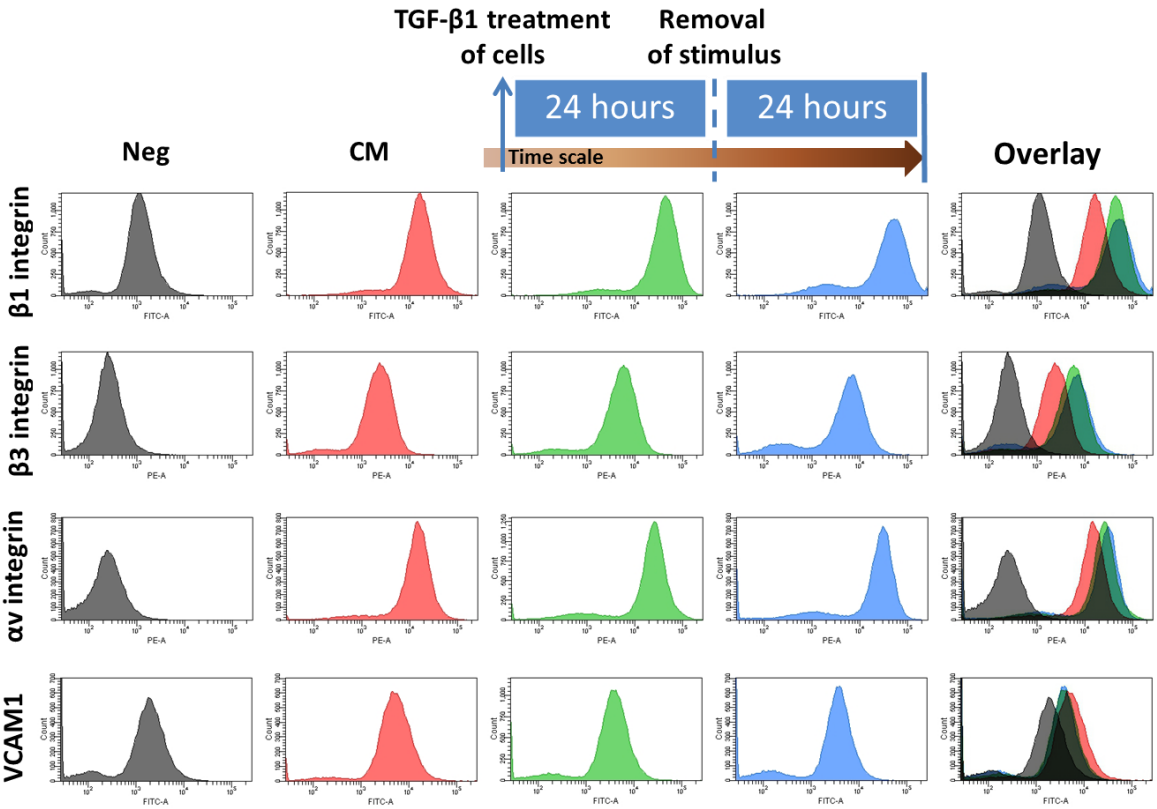

Figure B-1: Comparison of cell surface integrin expression between TGF-β1 treated MSCs at 24 hours and 48hours (additional 24 hours after removal of TGF-β1).

APPENDIX C

Table C-1: Regulation of critical genes related to defined functional groups.

Probe ID	Gene	PDGF vs Control	TGF vs Control	PDGF+TGF *vs* control
Growth Factors				
1422912_at	*Bmp4*	1.22	-1.96	-3.17
1415931_at	*Igf2*	0.69	-2.8	-3.01
1415854_at	*Kitl*	0.6	-2.54	-3
1450759_at	*Bmp6*	0.02	-2.92	-2.94
1438953_at	*Figf*	-0.18	-2.04	-1.86
1422243_at	*Fgf7*	-0.28	-1.93	-1.65
1418471_at	*Pgf*	0.02	-1.17	-1.19
1419139_at	*Gdf5*	-0.37	-1.51	-1.14
1420653_at	*Tgfb1*	0.14	1.21	1.06
1419417_at	*Vegfc*	-0.26	1.06	1.29
1426858_at	*Inhbb*	-0.52	0.79	1.31
1449826_a_at	*Fgf2*	-0.21	1.23	1.44
1432032_a_at	*Artn*	0.1	1.61	1.5
1420909_at	*Vegfa*	-0.23	1.4	1.58
1426238_at	*Bmp1*	-0.1	1.58	1.7
1419519_at	*Igf1*	0.6	2.52	1.99
1421207_at	*Lif*	-0.36	1.9	2.25
1418711_at	*Pdgfa*	-0.33	2.28	2.6
1423635_at	*Bmp2*	-0.75	3.35	4.1
Cytokines and Chemokines				
1419728_at	*Cxcl5*	-0.09	-6.69	-6.6
1423017_a_at	*Il1rn*	0.16	-4.47	-4.63
1422651_at	*Adipoq*	0.23	-4.23	-4.45
1419209_at	*Cxcl1*	-0.32	-3.92	-3.61
1422912_at	*Bmp4*	1.22	-1.96	-3.17
1417574_at	*Cxcl12*	0.45	-2.65	-3.11
1420380_at	*Ccl2*	0.12	-2.95	-3.07
1450759_at	*Bmp6*	0.02	-2.92	-2.94
1418126_at	*Ccl5*	0.32	-2.51	-2.83
1419083_at	*Tnfsf11*	0.08	-2.21	-2.3
1421228_at	*Ccl7*	0.26	-1.48	-1.75
1418219_at	*Il15*	0.73	-0.96	-1.69
1415803_at	*Cx3cl1*	0.3	-1.1	-1.4
1422080_at	*Il7*	0.25	-1.22	-1.15
1450297_at	*Il6*	0.1	-0.97	-1.07
1449982_at	*Il11*	0.96	-1.11	2.08
Extracellular matrix and adhesion				
1429072_at	*Col6a4*	-0.57	-4.37	-4.42
1415989_at	*Vcam1*	-3.1	0.5	-3.32
1450798_at	*Tnxb*	-0.27	-2.94	-3.28

Probe ID	Gene	PDGF vs Control	TGF vs Control	PDGF+TGF *vs* control
Extracellular matrix and adhesion (continued)				
1449563_at	*Cntn1*	-2.46	0.27	-2.56
1420484_a_at	*Vtn*	0.45	-2.67	-2.33
1439713_at	*Itga1*	-1.61	-1.62	-2.24
1435386_at	*Vwf*	-0.01	-1.29	-1.79
1420860_at	*Itga9*	-1.86	-1.92	-1.48
1427009_at	*Lama5*	1.12	1.02	-1.45
1450567_a_at	*Col2a1*	-1.09	-1.09	-1.39
1421997_s_at	*Itga3*	-0.73	0.76	-1.27
1426285_at	*Lama2*	-0.38	-0.1	-1.1
1447541_s_at	*Itgae*	1.07	0.09	1.03
1450501_at	*Itga2*	0.35	0.54	1.06
1417812_a_at	*Lamb3*	-1.94	0.5	1.18
1425815_a_at	*Hmmr*	-1.1	0.53	1.33
1423760_at	*Cd44*	1.36	0.15	1.37
1420853_at	*Sdc3*	0.38	1.09	1.37
1416623_at	*Thbs3*	1.18	-0.23	1.41
1423110_at	*Col1a2*	0.22	0.95	1.42
1421006_at	*Col4a6*	1.67	1.17	1.42
1426918_at	*Itgb1*	1.28	-0.07	1.48
1427883_a_at	*Col3a1*	1.37	-0.09	1.67
1419703_at	*Col5a3*	1.37	1.28	1.77
1426642_at	*Fn1*	1.25	-0.05	1.77
1418599_at	*Col11a1*	0.33	1.42	1.89
1427512_a_at	*Lama3*	0.61	1.05	2.02
1416740_at	*Col5a1*	2.22	0.16	2.07
1419088_at	*Timp3*	2.09	0.13	2.08
1420450_at	*Mmp10*	1.62	-0.49	2.11
1416740_at	*Col5a1*	0.27	2.31	2.14
1424807_at	*Lama4*	1.32	1.2	2.25
1421511_at	*Itgb3*	1.11	1.83	2.42
1442140_at	*Tnn*	1.13	2.76	3.48
1416342_at	*Tnc*	0.34	5.43	7.18
Transcription factors and signaling molecules				
1423259_at	*Id4*	-1.17	-3.4	-3.25
1416630_at	*Id3*	-0.11	-2.16	-2.45
1422537_a_at	*Id2*	-1.27	-1.43	-2.36
1425895_a_at	*Id1*	-0.75	-2.55	-2.14
1450782_at	*Wnt4*	-0.3	-1.37	-2.06
1422771_at	*Smad6*	-0.59	-1.31	-1.56
1422019_at	*Tgfbr2*	0.95	1.45	1.2
1417621_at	*Nfatc1*	0.9	2.33	2.6
1425377_at	*Wnt1*	0.25	2.05	3.05
1421341_at	*Axin2*	-0.13	4	4.21
1425901_at	*Nfatc2*	-0.83	3.76	4.32
1420891_at	*Wnt7b*	-0.31	4.6	5.15

Table C-2: Top 15 up- and down-regulated genes in PDGF treated cells compared to control

PDGF vs SF	Gene	Gene description	Log_2 ratio
1422651_at	Adipoq	adiponectin, C1Q and collagen domain containing	-1.95
1441313_x_at	Lhx9	LIM homeobox protein 9	-1.76
1449280_at	Esm1	endothelial cell-specific molecule 1	-1.74
1448162_at	Vcam1	vascular cell adhesion molecule 1	-1.72
1455251_at	Itga1	integrin alpha 1	-1.57
1421172_at	Adam12	a disintegrin and metallopeptidase domain 12 (meltrin alpha)	-1.54
1423555_a_at	Ifi44	interferon-induced protein 44	-1.51
1436739_at	Agtr1a	angiotensin II receptor, type 1a	-1.43
1448700_at	G0s2	G0/G1 switch gene 2	-1.43
1443170_at	Cnnm1	cyclin M1	-1.39
1418294_at	Epb4.1l4b	erythrocyte protein band 4.1-like 4b	-1.38
1455114_at	Ccno	cyclin O	-1.30
1448152_at	Igf2	insulin-like growth factor 2	-1.19
1419301_at	Fzd4	frizzled homolog 4 (Drosophila)	-1.14
1450928_at	Id4	inhibitor of DNA binding 4	-1.08
1427747_a_at	Lcn2	lipocalin 2	3.38
1424733_at	P2ry14	purinergic receptor P2Y, G-protein coupled, 14	3.18
1454783_at	Il13ra1	interleukin 13 receptor, alpha 1	3.03
1417625_s_at	Cxcr7	chemokine (C-X-C motif) receptor 7	2.83
1418945_at	Mmp3	matrix metallopeptidase 3	2.62
1418133_at	Bcl3	B-cell leukemia/lymphoma 3	2.50
1417290_at	Lrg1	leucine-rich alpha-2-glycoprotein 1	2.38
1418021_at	C4b	complement component 4B (Childo blood group)	2.28
1460469_at	Tnfrsf9	tumor necrosis factor receptor superfamily, member 9	2.19
1449199_at	Muc1	mucin 1, transmembrane	2.18
1416576_at	Socs3	suppressor of cytokine signaling 3	2.13
1418675_at	Osmr	oncostatin M receptor	2.03
1448326_a_at	Crabp1	cellular retinoic acid binding protein I	1.90
1419684_at	Ccl8	chemokine (C-C motif) ligand 8	1.64
1420512_at	Dkk2	dickkopf homolog 2 (Xenopus laevis)	1.44

Table C-3: Top 15 up- and down-regulated genes in TGF-β1 treated cells compared to control

TGF vs SF	Gene	Gene description	Log_2 ratio
1419728_at	Cxcl5	chemokine (C-X-C motif) ligand 5	-6.69
1457871_at	Colec10	collectin sub-family member 10	-6.35
1449280_at	Esm1	endothelial cell-specific molecule 1	-5.78
1451798_at	Il1rn	interleukin 1 receptor antagonist	-4.83
1459636_at	Angpt2	angiopoietin 2	-4.53
1422651_at	Adipoq	adiponectin, C1Q and collagen domain containing	-4.23
1448152_at	Igf2	insulin-like growth factor 2	-4.22
1437932_a_at	Cldn1	claudin 1	-4.04
1448162_at	Vcam1	vascular cell adhesion molecule 1	-3.93
1419209_at	Cxcl1	chemokine (C-X-C motif) ligand 1	-3.92
1450928_at	Id4	inhibitor of DNA binding 4	-2.99
1426152_a_at	Kitl	kit ligand	-2.95
1420380_at	Ccl2	chemokine (C-C motif) ligand 2	-2.95
1450759_at	Bmp6	bone morphogenetic protein 6	-2.92
1418294_at	Epb4.1l4b	erythrocyte protein band 4.1-like 4b	-2.89
1423606_at	Postn	periostin, osteoblast specific factor	6.72
1415978_at	Tubb3	tubulin, beta 3	6.05
1449169_at	Has2	hyaluronan synthase 2	5.47
1459994_x_at	Trfr2	transferrin receptor 2	4.91
1439604_at	Adamts16	a disintegrin-like and metallopeptidase with thrombospondin type 1 motif, 16	4.44
1416342_at	Tnc	Tenascin C	4.36
1421385_a_at	Myo7a	myosin VIIA	4.26
1436978_at	Wnt9a	wingless-type MMTV integration site 9A	4.24
1452968_at	Cthrc1	collagen triple helix repeat containing 1	4.22
1422812_at	Cxcr6	chemokine (C-X-C motif) receptor 6	4.22
1419613_at	Col7a1	collagen, type VII, alpha 1	4.08
1422125_at	Htr2b	5-hydroxytryptamine (serotonin) receptor 2B	4.00
1418350_at	Hbegf	heparin-binding EGF-like growth factor	3.96
1425789_s_at	Anxa8	annexin A8	3.93
1435994_at	Kcnh1	potassium voltage-gated channel, subfamily H (eag-related), member 1	3.77

Table C-4: Top 15 up- and down-regulated genes in combination of PDGF and TGF-β1 treated cells compared to control

PDGF+TGF vs SF	Gene	Gene description	Log_2 ratio
1457871_at	Colec10	collectin sub-family member 10	-7.12
1419728_at	Cxcl5	chemokine (C-X-C motif) ligand 5	-6.60
1449280_at	Esm1	endothelial cell-specific molecule 1	-5.15
1448152_at	Igf2	insulin-like growth factor 2	-4.91
1423017_a_at	Il1rn	interleukin 1 receptor antagonist	-4.63
1423954_at	C3	complement component 3	-4.56
1459636_at	Angpt2	angiopoietin 2	-4.51
1422651_at	Adipoq	adiponectin, C1Q and collagen domain containing	-4.45
1448162_at	Vcam1	vascular cell adhesion molecule 1	-4.43
1425663_at	Il1rn	interleukin 1 receptor antagonist	-4.41
1427313_at	Ptgir	prostaglandin I receptor (IP)	-4.19
1437932_a_at	Cldn1	claudin 1	-4.08
1420693_at	Myom1	myomesin 1	-4.03
1418745_at	Omd	osteomodulin	-3.89
1457644_s_at	Cxcl1	chemokine (C-X-C motif) ligand 1	-3.72
1423606_at	Postn	periostin, osteoblast specific factor	6.58
1415978_at	Tubb3	tubulin, beta 3	6.51
1449169_at	Has2	hyaluronan synthase 2	6.47
1416342_at	Tnc	Tenascin C	4.91
1422812_at	Cxcr6	chemokine (C-X-C motif) receptor 6	4.86
1459994_x_at	Trfr2	transferrin receptor 2	4.55
1422125_at	Htr2b	5-hydroxytryptamine (serotonin) receptor 2B	4.53
1421385_a_at	Myo7a	myosin VIIA	4.46
1452968_at	Cthrc1	collagen triple helix repeat containing 1	4.37
1436978_at	Wnt9a	wingless-type MMTV integration site 9A	4.28
1419613_at	Col7a1	collagen, type VII, alpha 1	4.26
1418350_at	Hbegf	heparin-binding EGF-like growth factor	4.21
1423635_at	Bmp2	bone morphogenetic protein 2	4.10
1425789_s_at	Anxa8	annexin A8	4.08
1449824_at	Prg4	proteoglycan 4 (megakaryocyte stimulating factor, articular superficial zone protein)	4.07

APPENDIX D

Permissions

1. *Nature Publishing Group (Figure 2-1)*

This is a License Agreement between Deepraj Ghosh ("You") and Nature Publishing Group ("Nature Publishing Group") provided by Copyright Clearance Center ("CCC"). The license consists of your order details, the terms and conditions provided by Nature Publishing Group, and the payment terms and conditions.

All payments must be made in full to CCC. For payment instructions, please see information listed at the bottom of this form.

License Number	3419060257630
License date	Jun 30, 2014
Licensed content publisher	Nature Publishing Group
Licensed content publication	Nature Reviews Immunology
Licensed content title	Mesenchymal stem cells in health and disease
Licensed content author	Antonio Uccelli, Lorenzo Moretta and Vito Pistoia
Licensed content date	Sep 1, 2008
Volume number	8
Issue number	9
Type of Use	reuse in a dissertation / thesis
Requestor type	academic/educational
Format	print and electronic
Portion	figures/tables/illustrations
Number of figures/tables/illustrations	1
High-res required	no
Figures	Figure 1

Author of this NPG article	no
Your reference number	None
Title of your thesis / dissertation	THERAPEUTIC EFFECT OF SOLUBLE FACTOR MEDIATED MECHANICAL RESPONSE OF MESENCHYMAL STEM CELLS
Expected completion date	Jul 2014
Estimated size (number of pages)	180
Total	0.00 USD

2. *Springer (Figure 2-2)*

This is a License Agreement between Deepraj Ghosh ("You") and Springer ("Springer") provided by Copyright Clearance Center ("CCC"). The license consists of your order details, the terms and conditions provided by Springer, and the payment terms and conditions.

All payments must be made in full to CCC. For payment instructions, please see information listed at the bottom of this form.

License Number	3406390625688
License date	Jun 12, 2014
Licensed content publisher	Springer
Licensed content publication	Springer eBook
Licensed content title	Smad4/TGF-β Signaling Pathways in Pancreatic Cancer Pathogenesis
Licensed content author	Alixanna Norris
Licensed content date	Jan 1, 2010
Type of Use	Thesis/Dissertation
Portion	Figures
Author of this Springer article	No
Order reference number	None

Original figure numbers	Figure 17-4
Title of your thesis / dissertation	THERAPEUTIC EFFECT OF SOLUBLE FACTOR MEDIATED MECHANICAL RESPONSE OF MESENCHYMAL STEM CELLS
Expected completion date	Jul 2014
Estimated size(pages)	180
Total	0.00 USD

3. *Company of Biologists Ltd. (Figure 2-4)*

Order Detail ID: 65119595
Journal of cell science by COMPANY OF BIOLOGISTS Reproduced with permission of Company of Biologists Ltd. in the format Republish in a thesis/dissertation via Copyright Clearance Center.
ISSN:0021-9533
Publication Type:Journal
Volume:
Issue:
Start page:
Publisher: Company of Biologists Ltd.
Author/Editor: COMPANY OF BIOLOGISTS
Permission Status: Granted Granted
Permission type: Republish or display content
Type of use: Republish in a thesis/dissertation
Order License Id: 3405640378638
Requestor type Academic institution
Format Print, Electronic
Portion chart/graph/table/figure
Number of charts/graphs/tables/figures 1
Title or numeric reference of the portion(s) Actin-binding proteins, Figure
Title of the article or chapter the portion is from N/A
Editor of portion(s) N/A
Author of portion(s) N/A
Volume of serial or monograph N/A
Page range of portion 1
Publication date of portion February 15, 2005
Rights for Main product
Duration of use Life of current edition
Creation of copies for the disabled no
With minor editing privileges no

For distribution to United States
In the following language(s) Original language of publication
With incidental promotional use no
Lifetime unit quantity of new product 0 to 499
Made available in the following markets Education
The requesting person/organization Deepraj Ghosh/Georgia Institute of technology
Order reference number None
Author/Editor Steven J. Winder
The standard identifier Dissertation/Thesis
Title Actin-binding proteins
Publisher Journal of cell science
Expected publication date Jul 2014
Estimated size (pages)200